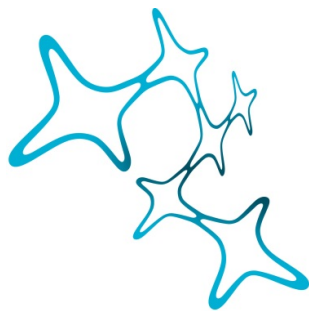


# Investigation of neuronal activity in a murine model of Alzheimer's disease using *in vivo* two-photon calcium imaging

Viktorija Korzhova



Graduate School of  
Systemic Neurosciences

LMU Munich



Dissertation

der Graduate School of Systemic Neurosciences  
der Ludwig-Maximilians-Universität München

30 May 2019

Supervisor

Prof. Dr. Jochen Herms

DZNE-Munich

Translational Brain Research

Feodor-Lynen-Strasse 17

D-81377 München

First Reviewer: Prof. Dr. Jochen Herms

Second Reviewer: Dr. Dr. Sabine Liebscher

External Reviewer Prof. Dr. Albrecht Stroh

Date of Defense: 11 September 2019

**Thesis Advisory Committee (TAC)**

Prof. Dr. Jochen Herms

Dr. Dr. Sabine Liebscher

Prof. Dr. Armin Giese

Prof. Dr. Stefan Lichtenthaler



# Summary

Alzheimer's disease (AD) is one of the biggest challenges for biomedical research nowadays as with the growth of life span more and more people are affected by this disorder. Etiology of AD is unknown, yet growing evidence identifies alterations in neuronal activity as of the great importance for pathology. Although several significant studies of neuronal activity alteration in AD were done during the last decade, none of them addressed the question of the time course of these changes over the disease progression.

Alzheimer's disease (AD) is characterized by impairments of brain neurons that are responsible for the storage and processing of information. Studies have revealed decrease in the activity of neurons (Silverman *et al.*, 2001; Prvulovic *et al.*, 2005) and it was proposed that generalized hypoactivity and silencing of brain circuits takes place as formulated in the synaptic failure hypothesis (Selkoe, 2002). However, more recent studies also reported opposite effects – hyperexcitability and hyperactivity of neurons in the AD models (Busche *et al.*, 2008; Sanchez *et al.*, 2012; Liebscher *et al.*, 2016). It still remains unclear if these are two sides of the same coin or if these are two stages, that follow each other. Moreover, it is not clear if observed neuronal activity alterations are caused by the dysfunction of individual neurons or if overall circuitry is disturbed because the crucial “activity controllers” (most probably - inhibitory neurons) alter their activity.

This project aimed to examine spontaneous neuronal activity in the murine model of AD at the early stages of disease progression using chronic *in vivo* imaging to address the character and the stability of neuronal activity alterations as well relation of the activity alterations to amyloid plaque proximity. Compared to earlier studies the approach of *in vivo* awake calcium imaging used in the current study has many benefits for brain research. The main advantage is that brain activity can

be measured without artifacts generated by anesthesia, which can exaggerate or mitigate experimental readouts.

In this project, I used genetically encoded calcium indicator GCaMP6 that enables prolonged repetitive imaging of the same neurons in an intact environment. Recording of calcium transients in cell bodies of neurons was accompanied by *in vivo* imaging of A $\beta$  plaques and followed by immunohistochemical staining of GCaMP6-expressing neurons to investigate how activity changes are correlated with proximity to the plaque. All the experiments were done in awake mice to ensure the absence of anesthesia-derived impact on spontaneous neuronal activity.

My results support previously published reports of the increased proportion of hyperactive excitatory neurons in the AD mouse model. Importantly, my results also demonstrate that this increased activity is present in the awake state, is stable over a longer period of time (one month) and does not depend on the distance to the closest plaque. These findings support the hypothesis of permanent network alterations driving aberrant activity patterns that appear early in the disease progression, resulting in a chronic excitation/inhibition disbalance.

Another important finding of my project is that individual neurons do not stay in the silent state and most of them remain functional demonstrating normal activity at the later time points. This finding requires further research as it has important implication for the development of the AD treatment, as in case many neurons remain functional and their normal neuronal activity can be recovered by addressing the cause of the circuit dysfunction with treatment.

To summarize, the study presented in this PhD thesis is the first longitudinal study of neuronal activity changes in an AD mouse model, and while it provides important insight into pathology, it also emphasizes the importance of chronic *in vivo* studies to investigate neuronal activity and its role in the disease progression.

# Content

Summary .....	iv
Content .....	vi
Figures .....	viii
Abbreviations .....	x
<b>1 Introduction .....</b>	<b>1</b>
1.1 Alzheimer's disease.....	1
1.1.1 Amyloid- $\beta$ and the amyloid hypothesis.....	6
1.1.2 The onset of pathology and clinical symptoms .....	13
1.1.3 Mouse models of amyloid-associated AD pathology .....	15
1.2 <i>In vivo</i> two-photon imaging in AD .....	18
1.2.1 <i>In vivo</i> two-photon microscopy.....	18
1.2.2 <i>In vivo</i> imaging of neuronal activity .....	21
1.2.3 <i>In vivo</i> microscopy in AD.....	28
1.3 Neuronal activity in AD .....	32
1.3.1 Synaptic dysfunction .....	32
1.3.2 Neuronal activity and circuit dysfunction.....	35
1.3.3 Role of amyloid plaques in neuronal dysfunction in AD .....	42
<b>2 Objectives.....</b>	<b>46</b>
<b>3 Material and Methods.....</b>	<b>47</b>
3.1 Animals .....	47
3.2 Genotyping.....	48

3.3	Cranial window .....	49
3.4	Longitudinal awake in vivo two-photon imaging.....	49
3.5	Tissue preparation, immunohistochemistry, and confocal microscopy.....	52
3.5.1	Transcardial perfusion of mice.....	52
3.5.2	Immunohistochemical identification of inhibitory neurons .....	53
3.6	Imaging data processing and analysis .....	53
3.6.1	Calcium imaging data pre-processing.....	54
3.6.2	Analysis of spontaneous calcium activity.....	54
3.6.3	Plaque distance analysis .....	55
3.7	Statistics.....	56
<b>4</b>	<b>Results.....</b>	<b>58</b>
4.1	Method establishment.....	58
4.2	Identity of the imaged neurons .....	64
4.3	Frontal cortex neurons in the AD transgenic mice have increased activity .....	65
4.4	Aberrant activity of neurons in the AD mouse model represents a stable pattern 67	
4.5	Only 5% of neurons stay hypoactive in the AD mouse model.....	68
4.6	Influence of plaque distance on neuronal activity.....	70
<b>5</b>	<b>Discussion.....</b>	<b>74</b>
5.1	Chronic awake calcium imaging as a tool to further investigate AD pathology.....	76
5.2	AD model mice demonstrate neuronal hyperactivity .....	77
5.3	The altered pattern of neuronal activity is stable.....	80
5.4	Hypoactive neurons might still be functional .....	81
5.5	Distance to the plaques does not affect aberrant neuronal activity.....	83
	References .....	85
	Acknowledgment .....	117
	Curriculum Vitae.....	119
	List of Publications .....	121
	Eidesstattliche Versicherung .....	122
	Declaration of Author Contributions .....	123

# Figures

Figure 1. Microscopic preparations of brain tissue of the first AD case.....	2
Figure 2. Amyloid plaques and neurofibrillary tangles are the hallmarks of AD.....	3
Figure 3. Progressive amyloid- $\beta$ accumulation in the brain of AD patients observed with PET. .....	4
Figure 4. Production of amyloid- $\beta$ . .....	7
Figure 5. Pathways leading to plaques and tangles form the basis of the amyloid- $\beta$ theory of Alzheimer's disease. ....	10
Figure 6. Age-related amyloid deposition in APPPS1 mice. ....	18
Figure 7. Comparison of scattering in confocal microscopy and two-photon microscopy. 20	
Figure 8. Calcium in the neuron. ....	22
Figure 9. Structure of GCaMP6m monomer in a cartoon scheme.....	24
Figure 10. Two-photon in vivo imaging of structural alterations in AD model mice. .	31
Figure 11. Model of molecular mechanisms involved in spine pathology in Alzheimer's disease. .....	35
Figure 12. Proposed by Busche and Konnerth (Busche and Konnerth, 2015) model of the sequence of events that may underlie the progression of neuronal dysfunction in Alzheimer's disease.	38
Figure 13. Neural circuits and synapses during the progression of AD – possible time course of events. ....	38
Figure 14. Types of amyloid plaques.....	43
Figure 15. Time line of the in vivo imaging experiments. ....	50

Figure 16. Preparation of experimental animals to in vivo two-photon imaging. ....	50
Figure 17. Measurements of plaque to neuron distances in 3D space. ....	56
Figure 18. Improvement of the head-fixation bar. ....	59
Figure 19. Exemplary traces of neuronal activity of individual neurons recorded with in vivo two-photon imaging.....	60
Figure 20. Active periods distinguished by the whiskers movements are not influencing activity of neurons in the recorded areas. ....	61
Figure 21. Color-coded neuronal activity of individual neurons (ROI) over time in each of the individual experiments (fov - field of view).....	64
Figure 22. Immunostaining of Ruby-expressing neurons against GAD67 to identify inhibitory neurons. ....	65
Figure 23. Three neuronal activity types in transgenic and non-transgenic mice. ....	67
Figure 24. The activity of individual neurons over time.....	68
Figure 25. The activity of individual neurons over time according to three activity categories. ....	69
Figure 26. Distribution of plaque to neuron distances at three different imaging time points. ....	70
Figure 27. The fraction of hyperactive and silent neurons in APPPS1 mice for close and distant neurons in individual experiments. Horizontal line denotes the mean. ....	71
Figure 28. Changes in neuronal activity with respect to plaque proximity. ....	72
Figure 29. Distribution of plaques distances. ....	72
Figure 30. Cumulative distribution of the change in neuronal activity for neurons in different plaque-distance bins.....	73

# Abbreviations

2P imaging/microscopy	two-photon imaging/microscopy
ADAM9 and ADAM10	A Disintegrin And Metalloproteinase domain-containing proteins 9 and 10
AAV	adeno-associated virus
AMPA	$\alpha$ -amino-3-hydroxy-5-methyl-4-isoxazolepropionic acid
APLP1/2	amyloid-like protein 1/2
Apo $\epsilon$ 4	apolipoprotein $\epsilon$ 4
APP	amyloid precursor protein
AICD	APP intracellular domain
A $\beta$	amyloid-beta
BACE	beta-secretase
BAPTA	1,2-bis(o-aminophenoxy)ethane-N,N,N',N'-tetraacetic acid
CCD camera	charge-coupled device camera
CAA	cerebral amyloid angiopathy
CMRO2	cerebral metabolic rate of oxygen

CSF	cerebrospinal fluid
CT	computed tomography
CTF	C-terminal fragment
CX3CR1	CX3C chemokine receptor 1
DMN	default mode network
DIAN	Dominantly Inherited Alzheimer Network
EEG	electroencephalogram
EGTA	ethylene glycol-bis( $\beta$ -aminoethyl ether)-N,N,N',N'-tetraacetic acid
FAD	familial AD
FDG-PET	fludeoxyglucose F 18 - positron emission tomography
fMRI	functional magnetic resonance imaging
GABA	$\gamma$ -aminobutyric acid
GAD67	glutamic acid decarboxylase 67
GCaMP6s, GCaMP6f	type of genetically encoded calcium indicator, created from a fusion of green fluorescent protein (GFP), Calmodulin, and M13; s and f indicate variants of GCaMP6 (slow and fast, respectively) that have different calcium-binding kinetics
GECIs	genetically encoded calcium indicators
GWAS	genome-wide association studies
GFP	green fluorescent protein
Iba1	ionized calcium binding adaptor molecule 1
LTP	long-term potentiation
MRI	magnetic resonance imaging
mGluR	metabotropic glutamate receptor
MCI	mild cognitive impairment
SCN1A	Nav1.1 sodium channel subunit

NDMA	N-Nitrosodimethylamine
NPY	neuropeptide Y
NFTs	neurofibrillary tangles
NA	numerical aperture
OGB-1	Oregon Green BAPTA-1
PET	positron emission tomography
PFA	paraformaldehyde
PMT	photomultiplier tubes
PS or PSEN	presenilin
ROI	region of interest
sAD	sporadic form
TACE	TNF alpha converting enzyme
TBOA	threo- $\beta$ -benzyloxyaspartate
WT	wild type

1

# Introduction

Alzheimer's disease (AD) has become an extremely important healthcare problem in the last decades as with the increase in lifespan the number of people suffering from AD is growing. In the century that passed since Alois Alzheimer discovered the disease, scientists have made remarkable advancement in understanding the illness. Nevertheless, despite tremendous investments in basic and clinical research, no cure or preventive treatment for AD exists, because the underlying pathological mechanisms remain elusive. Therefore, it is of great importance to investigate the pathology further. Changes in neuronal activity are thought to be among the first steps of cognitive decline in affected humans; however, it is still unclear what is the degree and the time course of these changes.

The aim of this thesis was to investigate the activity of the cortical neurons in the AD mouse model using the *in vivo* two-photon microscopy. The specific focus of this study was to follow neuronal activity over time: from early stages of the disease to the stage where amyloid plaque load is high and advanced axonal pathology is present.

The introduction chapter provides background information that was the basis of the study, and that is helpful to present the results described in chapter 3. Introduction is divided into three sections. Section 1.1 introduces the necessary basics of Alzheimer's disease pathology. Section 1.2 describes *in vivo* two-photon microscopy and its applications to AD research. Finally, section 1.3 gives an overview of the up-to-date research on the neuronal activity in the AD.

## 1.1 Alzheimer's disease

On November 3, 1906, Alois Alzheimer presented at the Meeting of the Psychiatrists of South West Germany and described the case of one of his patients, Auguste Deter, who had died of a dementing illness at the age of 55 (Alzheimer, 1907; Hardy, 2006a). He shortly discussed clinical

features of the case and described the pathological features he observed in her brain (Figure 1). These included the presence of plaques (miliary foci) and tangles (fibrils). Alzheimer was not the first to describe the clinical features of dementia (they have been documented in the elderly patients since the ancient times), as well as he was not the first to describe the plaques (Redlich, 1898). However, he was the first to describe the tangles (Perusini, 1991). Detection of the tangles was made possible due to the histological advances in the development of silver stains (Bielschowsky, 1902). The disease was named after Alois Alzheimer later by his senior colleague Emil Kraepelin (Kraepelin, 1910). For a while, the term was only used for the cases with a presenile onset age (with the onset at the age less than 65 years). The modern era of Alzheimer's research started with the finding that the majority of cases with senile dementia had Alzheimer's pathology, which meant Alzheimer's disease was not a rare neurological curiosity but a major research priority (Hardy, 2006a). An important step in this direction was made by Blessed, Tomlinson, and Roth in a series of papers, in which they reported that the majority of cases of "senile dementia" also had the plaque and tangle pathology of Alzheimer's disease and thus can be seen as the same disease as presenile dementia (Blessed, Tomlinson and Roth, 1968).

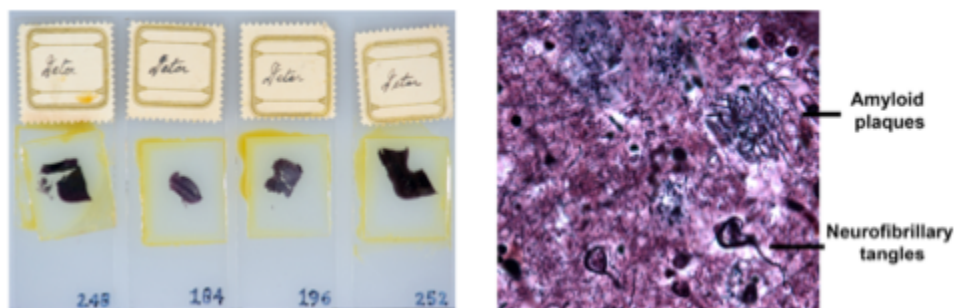


Figure 1. Microscopic preparations of brain tissue of the first AD case.

Preparations are done from brain autopsies of Auguste D. by Alois Alzheimer (left). Characteristic hallmarks of the AD, amyloid plaques and neurofibrillary tangles, are well visible in the slices (right). Source: Archives of Center of Neuropathology and Prion Research, LMU Munich.

Nowadays Alzheimer's disease is known to be the most common form of dementia in elderly with AD patients suffering from a progressive decline in memory and cognition (Blennow, de Leon and Zetterberg, 2006). In 2010, a meta-analysis, which combined data from multiple studies, estimated 35.6 million dementia cases worldwide (Prince *et al.*, 2013), including 21–25 millions of AD cases (60–70% of dementia cases are classified as AD). The study also implied an annual growth in prevalence of 1½ million, which thus creates a growing burden to the society. In the USA, where more than 5 million people live with AD, Alzheimer's and other dementias cost the nation \$259 billion. By 2050, these costs could rise as high as \$1.1 trillion (<http://www.alz.org>). In Germany,

approximately 1.5 million people are affected by AD, and the number is increasing by 40 000 each year ([www.deutsche-alzheimer.de](http://www.deutsche-alzheimer.de)).

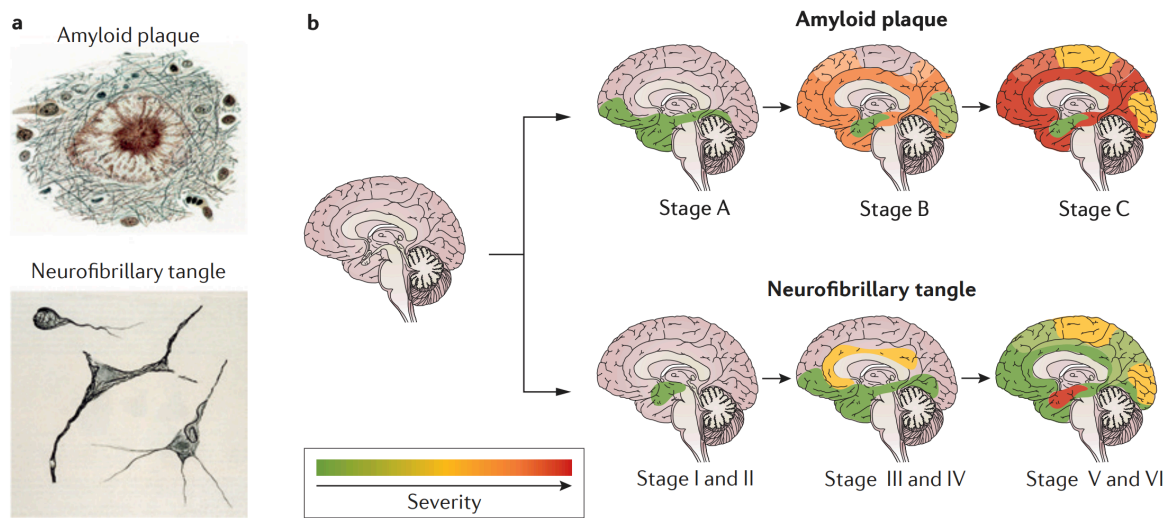


Figure 2. Amyloid plaques and neurofibrillary tangles are the hallmarks of AD.

A. Images on A are from Spielmeyer's classic textbook 'Histopathologie des Nervensystems' using the Bielschowsky method of silver impregnation to visualize amyloid plaques and neurofibrillary tangles (Spielmeyer, 1922). B. In typical cases of Alzheimer's disease, amyloid- $\beta$  deposition precedes neurofibrillary and neuritic changes starting from the frontal and temporal lobes, hippocampus and limbic system (top row). Less commonly, the disease seems to emerge from other regions of the cerebral neocortex (parietal and occipital lobes) with relative sparing of the hippocampus. The neurofibrillary tangles and neuritic degeneration start in the medial temporal lobes and hippocampus and progressively spread to other areas of the neocortex (bottom row). With the advent of molecular imaging techniques for A $\beta$  and tau, the longitudinal dispersal of pathological changes will become amenable to real-time in vivo study and will not be reliant on post-mortem reconstructions as depicted here. A $\beta$  deposition (stages A, B, and C) and neurofibrillary tangles (stages I–VI) are adapted from Braak and Braak (Ball et al., 1997). Reprinted from (Masters et al., 2015).

Unfortunately, current treatments provide only symptomatic relief and are only effective in a subset of AD patients and for a limited period of time (Golde, Schneider and Koo, 2011). The reason behind treatment difficulties is that even though AD is associated with clear pathological hallmarks, there is still no clear understanding of how and why the pathology develops, neither there are means of early diagnosis. The hallmarks of AD pathology are the generation of amyloid plaques, consisting of the amyloid- $\beta$  peptide (A $\beta$ ), and formation of neurofibrillary tangles by the accumulation of hyperphosphorylated microtubule-associated protein Tau (Figure 2). Structural changes in the AD brain were classified into two categories – “positive” lesions (plaques, tangles, neuropil threads, dystrophic neurites, cerebral amyloid angiopathy (CAA)) and “negative” lesions (massive atrophy of the brain tissue due to neuron loss, degeneration of neurites and synapses) (Serrano-Pozo, Frosch, et al., 2011). Each of these lesions is present in a characteristic pattern in AD, providing a clue that there is a relationship between the lesions and disease progression. Neuronal loss and synapse loss in most cases appear in parallel to tangle formation, although

whether tangles are the cause of neuronal and synaptic loss remains uncertain (Gómez-Isla *et al.*, 1997; Iqbal and Grundke-Iqbal, 2002; Bussire *et al.*, 2003; Hof *et al.*, 2003; Yoshiyama *et al.*, 2007; de Calignon *et al.*, 2009; De Calignon *et al.*, 2010).

Amyloid- $\beta$  lesions will be discussed in more details later as they are currently seen as a main pathogenic agent, while the role of Tau aggregates stays cryptic. Tau pathology can manifest within neuronal somata, referred to as tangles, or within neurites, called neuropil threads (Serrano-Pozo, Frosch, *et al.*, 2011). Tangles emerge in a spatiotemporal manner, allowing for categorization into Braak stages (I-VI) (Braak and Braak, 1991). The hierarchical pattern of neurofibrillary degeneration among brain regions is so consistent that a staging scheme is well accepted as part of the 1997 NIA-Reagan diagnostic criteria (Ball *et al.*, 1997). This scheme implies early lesions in the entorhinal/ perirhinal cortex, then hippocampal subfields, then association cortex, and finally primary neocortex (Figure 3).

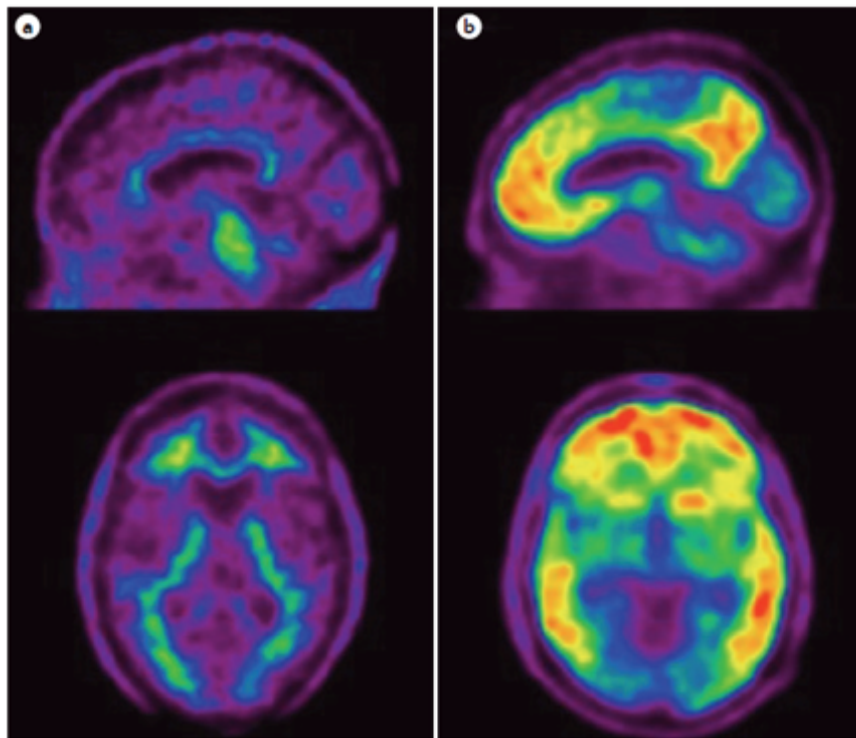


Figure 3. Progressive amyloid- $\beta$  accumulation in the brain of AD patients observed with PET.

PET scans for amyloid- $\beta$  using  $^{18}\text{F}$ -NAV4694 PET in two patients with mild cognitive impairment. The scan showed normal, nonspecific white matter binding, and the patient remained stable >4.5 years after the scan (part a). The second patient's scan showed extensive binding to  $A\beta$  plaques in the frontal, parietal, lateral temporal, posterior cingulate cortex and striatum as typically seen in patients with Alzheimer's disease. The patient progressed to dementia due to Alzheimer's disease three years after the scan (part b). Reprinted from (Masters *et al.*, 2015).

Clinical symptoms of AD are characterized by a progressive decline in memory function and cognition that can be classified into three distinct yet continuous stages: preclinical AD, mild cognitive impairment (MCI) and dementia due to Alzheimer's disease (Albert *et al.*, 2011; McKhann *et al.*, 2011; Sperling *et al.*, 2011). AD patients in Braak stages II and III typically demonstrate cognitive impairments in different domains, such as memory (in particular episodic memory), executive function, attention, language or visuospatial skills, all of which can be assessed by clinical tests (Albert *et al.*, 2011). The inability to pursue common daily activities marks the conversion from MCI to dementia (McKhann *et al.*, 2011). The terminal phase is characterized by a complete dependence on caregiving and eventual death occurring on average 4-8 years after diagnosis (Brookmeyer *et al.*, 2002; Larson *et al.*, 2004; Helzner *et al.*, 2008), most commonly caused by pneumonia or dehydration (Ganguli *et al.*, 2005). Conclusive AD diagnosis, however, can only be made upon neuropathological examination (Hyman and Trojanowski, 1997; McKhann *et al.*, 2011).

As mentioned earlier, the pathological events leading to the development of AD remain largely unknown. Hereditary familial AD (FAD) only accounts for approx. 1 % of all cases (Mayeux and Stern, 2012). Most AD cases occur in a sporadic form (sAD) without a clear cause for pathology. There are many environmental and genetic factors that have been shown to increase the risk for AD, but understanding the interplay between these risk factors and their contribution to the etiology of AD is an ongoing process (Bertram and Tanzi, 2012; Dong Hee *et al.*, 2014). Genome-wide association studies (GWAS) have identified over 20 loci that are connected to increased risk for sAD, including genes involved in innate immunity, cholesterol metabolism, and synaptic/neuronal membrane function, suggesting that the pathogenesis of sAD is quite heterogeneous (Davis *et al.*, 2004; Guerreiro and Hardy, 2014; Karch and Goate, 2015).

Overall, there are over 250 genetic alterations that have been linked to FAD. Those alterations that have been tested for effects on APP metabolism increase the overall production of amyloid- $\beta$  or the amyloid- $\beta$ <sub>1–42</sub>/amyloid- $\beta$ <sub>1–40</sub> ratio (Gómez-Isla *et al.*, 1999; Steiner and Haass, 2000; Jankowsky *et al.*, 2004; Karch, Cruchaga and Goate, 2014), or promote the accumulation of pathogenic amyloid- $\beta$  assemblies (Nilsberth *et al.*, 2001; Tsubuki, Takaki and Saido, 2003; Shimada *et al.*, 2011). But still, the only well-established mutation associated with the late-onset form of AD (between 60 and 80 years of age) is the genetic variant encoding apolipoprotein (Apo)  $\epsilon$ 4. A recent study suggested a possible mechanism of this risk factor involvement by demonstrating that ApoE secreted by glia stimulates neuronal A $\beta$  production with an ApoE4 > ApoE3 > ApoE2 potency rank order (Huang *et al.*, 2017). Interestingly, whole-genome data from almost 1800 Icelanders also revealed a protective APP mutation (A673T) that reduces the  $\beta$ -secretase-mediated cleavage of

APP and, consequently, amyloid- $\beta$  levels and thus decreases the risk of late-onset sporadic AD (Jonsson *et al.*, 2012; Maloney *et al.*, 2014).

Less than 1% of familial cases of AD are represented by the families with the autosomal dominant inheritance of AD, when disease develops between the ages of 30 and 50 years. Approximately half of those cases are results of mutations in genes encoding amyloid precursor protein (APP) and proteins involved in APP processing – presenilins 1 and 2 (PS1 and PS2). Mutations in those genes lead to an increased generation and further aggregation of A $\beta$ , which predisposes to the formation of plaques (Mayeux and Stern, 2012). These discoveries are in line with the decades-old observation that AD neuropathology almost invariably develops in patients with trisomy 21 (Down's syndrome), in which the extra copy of APP leads to increases in the expression of APP and in the deposition of A $\beta$  (Wisniewski *et al.*, 1985).

Basic research advances in recent years have furthered our understanding of the natural history of Alzheimer's disease; a body of data was gathered to describe the pathology and underlying mechanisms. There are however two main difficult questions in the AD research nowadays. The first one is the exact mechanism of pathology and its association with A $\beta$  aggregates. The second one is poor correlation of clinical symptoms of cognitive decline with the onset of brain pathology, that apparently starts decades earlier. These two points will be discussed in the following subchapters.

### **1.1.1 Amyloid- $\beta$ and the amyloid hypothesis**

The senile plaques, characteristically found in patients with AD, consist of A $\beta$  peptides and thus A $\beta$  have been a natural starting point for the research attempting to understand the disease. The two major genetic risks of FAD, presenilin and APP, are main players in the production of A $\beta$  and thus support the leading role of A $\beta$  in AD and the dominating paradigm of AD, the amyloid cascade hypothesis (Hardy, 2006b; Rosenblum, 2014). A $\beta$  is produced from the membrane-bound protein amyloid precursor protein (APP) upon protein cleavage by  $\beta$ - and  $\gamma$ -secretases (Vassar *et al.*, 1999; Wolfe, 2012). And presenilin is the catalytic unit of the  $\gamma$ -secretase complex that cuts APP to produce A $\beta$  (De Strooper *et al.*, 1998).

#### **1.1.1.1 APP and A $\beta$ in normal physiology**

Amyloid precursor protein is type I transmembrane glycoprotein with a single membrane-spanning domain, a large extracellular glycosylated N-terminus and a small intracellular C-terminus (Dyrks *et al.*, 1988). APP is located at the cell surface (alternatively – on the luminal side of endoplasmic reticulum or Golgi membranes) and part of the peptide is embedded in the membrane. It is widely

expressed in cells in various tissues of the body with different levels at different developmental and physiological states. The APP gene is localized on chromosome 21 in humans, and its expression produces three major isoforms (APP695, APP751, APP770; all around 170 kDa) generated via alternative splicing. APP695 is the predominant isoform of APP in neurons (Robakis *et al.*, 1987; Yoshikai *et al.*, 1990).

Full-length APP can be processed by  $\alpha$ -,  $\beta$ -,  $\eta$ -, and  $\gamma$ -secretases in three different pathways starting.  $\eta$ -secretase cleavage releases the soluble APPs $\eta$ , while CTF $\eta$  remains embedded in the membrane (Figure 4). CTF $\eta$  is further processed by  $\alpha$ - or  $\beta$ -secretase at the extracellular side generating A $\eta$ - $\alpha$  or A $\eta$ - $\beta$ . Cleavage of CTF $\eta$  within the transmembrane domain by  $\gamma$ -secretase produces the APP intracellular domain (AICD) containing the highly conserved interaction motif (YENPTY) and one of the two – the short extracellular peptides A $\beta$  in the amyloidogenic pathway or p3 peptide within the non-amyloidogenic pathway. The non-amyloidogenic pathway is driven by the  $\alpha$ -secretase liberating APPs $\alpha$  in the extracellular space (for review see Selkoe and Schenk, 2003). In the majority of cases, the  $\gamma$ -cleavage produces A $\beta$ 40, although it also generates a more toxic variant, A $\beta$ 42 (De Strooper, Vassar and Golde, 2010).

The identity of  $\alpha$ -secretase remains unclear although TACE (an enzyme responsible for cleavage of the TNF receptor family proteins at the cell surface) and ADAM9 and ADAM10 are candidates (Buxbaum *et al.*, 1998; Asai *et al.*, 2003).

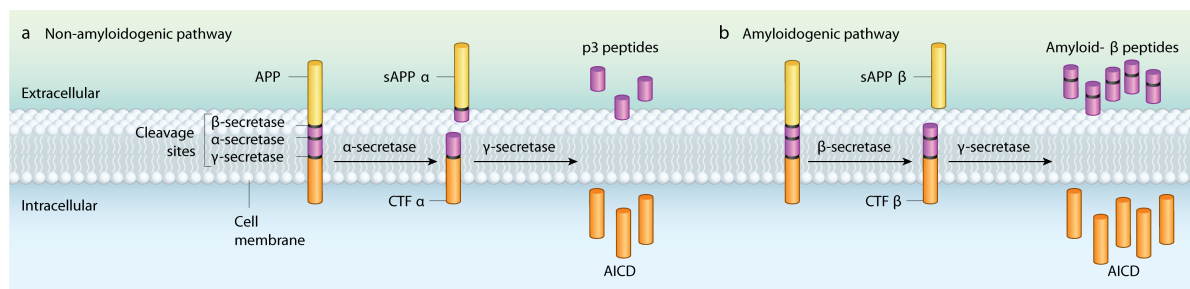


Figure 4. Production of amyloid- $\beta$ .

*Amyloid- $\beta$  peptides result from the sequential cleavage of APP, a type I integral membrane glycoprotein. The structure of APP includes an amyloid- $\beta$  domain (purple) with cleavage sites for secretase enzymes. Two pathways compete for the APP substrate, which leads to either amyloidogenic or non-amyloidogenic processing of the protein. Reprinted from (Canter, Penney and Tsai, 2016).*

The physiological role of APP, its various proteolytic products and the two other members of the protein family - amyloid precursor-like proteins 1 and 2 (APLP1/2) - are still not fully clarified.

Research shows that learning and memory processes manifested by functional and structural changes at synapses are altered in different APP and APLP1/2 mouse mutants (Fanutza *et al.*, 2015;

Hick *et al.*, 2015). Among those, it is known that APP and its fragments are implicated in regulating synaptic strength. Interestingly, while APLP2 and APP are functionally redundant, APLP1 exclusively expressed in CNS, might have distinctive roles within the synaptic network, but these functions still remain to be elucidated. Several mechanisms by which APP could modulate spine plasticity were proposed. Firstly, structural properties of the full-length protein may help to stabilize synapses, while binding of ligands to the extracellular part may trigger intracellular cascades, as in case of the classical receptor molecules. Additionally, recent findings revealed that APP play a role in modulating astrocytic D-serine homeostasis, while D-serine is an important component of synaptic function modulation due to its interactions with NMDA receptors. Lastly, it is possible that APP fragments trigger or alleviate the pathophysiological mechanisms involved in neurodegenerative diseases. Taken together, APP seems to regulate synaptic plasticity at several levels (Zou *et al.*, 2016, for review see Montagna, Dorostkar and Herms, 2017).

Interestingly, APPs $\alpha$ , one of the proteolytic products of non-amyloidogenic APP processing, was found to be a neurotrophic peptide that facilitates long-term potentiation (LTP) and restores impairments occurring with age. At the same time, the newly discovered  $\eta$ -secretase cleavage product, A $\eta$ - $\alpha$  acts in the opposite direction, namely decreasing LTP (Willem *et al.*, 2015; for the review see Ludewig and Korte, 2016). Another recent study demonstrates that even A $\beta$  can be “good” for the organism, as it can function as an antimicrobial peptide, and additional data show that bacteria and yeast can seed A $\beta$  into amyloid depositions. These data suggest a complex interplay between the normal function of A $\beta$ , its accumulation in the brain, and host immune defense (for the review see Golde, 2016; Kumar *et al.*, 2016).

A $\beta$  is a small hydrophobic peptide that occurs, as mentioned above, in two principal lengths: A $\beta$ 40 and A $\beta$ 42. The A $\beta$  region of APP includes first 12–14 residues of the transmembrane domain and the 28 residues outside the transmembrane domain (for review see Selkoe and Schenk, 2003). Looking at this constitution, A $\beta$  was originally assumed to arise only under pathological circumstances, as it was thought that the second cleavage should require prior membrane disruption to allow access of  $\gamma$ -secretase to the intramembranous region. This hypothesis was disproved in 1992 when A $\beta$  was shown to be constitutively secreted by different mammalian cells throughout life and it was proven that A $\beta$  occurs normally in plasma and cerebrospinal fluid (CSF) (Haass *et al.*, 1992; Seubert *et al.*, 1992; Shoji *et al.*, 1992). This discovery enabled studies of A $\beta$  production in cell culture and animal models, as well as high-throughput screenings on cultured cells to identify A $\beta$ -lowering compounds and determine their mechanism.

### 1.1.1.2 Amyloid cascade hypothesis

A $\beta$  molecules tend to aggregate to form oligomers, protofibrils, and mature fibrils. The early experiments demonstrating that synthetic fragments of A $\beta$  can kill cultured neurons (Yankner, Duffy and Kirschner, 1990), led to a series of further studies that have revealed the effects of A $\beta$  on the synaptic dysfunction and death of neurons in AD.

According to these studies, A $\beta$  may be most toxic in the form of soluble oligomers at the earliest stages of aggregation (Lambert *et al.*, 1998; Kaye *et al.*, 2003). Synapses are particularly susceptible to the adverse effects of aggregated forms of A $\beta$  as it was found that A $\beta$  can impair synaptic ion and glucose transporters, and electrophysiological studies demonstrated that A $\beta$  impairs synaptic plasticity (Mattson, 1997; Chapman *et al.*, 1999). Moreover, A $\beta$  can damage neurons by inducing oxidative stress and disrupting cellular calcium homeostasis (Mattson, 1997). Additionally, lack of sAPP $\alpha$  may contribute to the death of neurons: sAPP $\alpha$  is known to increase the resistance of neurons to oxidative and metabolic insults and coincident with the increased production of A $\beta$  in AD here is a decrease in the amount of sAPP $\alpha$  produced (Mattson, 1997). In APP transgenic mice memory deficits become apparent early in the process of A $\beta$  deposition, consistent with the timeline of neurotoxic effects of A $\beta$  occurring during the formation of oligomers (Koistinaho *et al.*, 2001).

Further evidence that A $\beta$  deposition seems to be a crucial event in AD is the remarkable finding that immunization of APP mutant mice with human A $\beta$ 42 results in the removal of A $\beta$  deposits from the brain (Schenk *et al.*, 1999) which may lead even to recovery of cognitive deficits (Morgan *et al.*, 2000). Based on the above-mentioned genetic evidence, biochemical data, and animal models, A $\beta$  has been suggested to be responsible for the pathogenesis of AD. This suggestion was called the amyloid hypothesis of AD.

The most common version of the amyloid hypothesis often referred to as the amyloid cascade hypothesis (Hardy and Higgins, 1992; Hardy, 2006b), asserted that toxic A $\beta$  overload is the cause of AD (Figure 5). One possible explanation of this overload is the impaired A $\beta$  clearance. Vascular transport of A $\beta$  across the blood-brain barrier can control A $\beta$  brain levels, and the A $\beta$  clearance is indeed shown to be impaired upon aging (Shibata *et al.*, 2000; Deane *et al.*, 2003; Deane and Zlokovic, 2007) and in AD (Mawuenyega *et al.*, 2010). This impairment is thought to gradually increase steady-state levels of toxic A $\beta$  leading to the build-up of plaques (Hardy, 2006b). This version of the hypothesis was a quantitative gain of toxic function (or “toxic by degree”) mechanism. The amount of A $\beta$  was seen as a defining cause of disease. This hypothesis has support

from a recent finding that  $A\beta$  is cleared from the brain during sleep and disturbed sleep leads to a pathological build-up of the amyloid (L. Xie *et al.*, 2013).

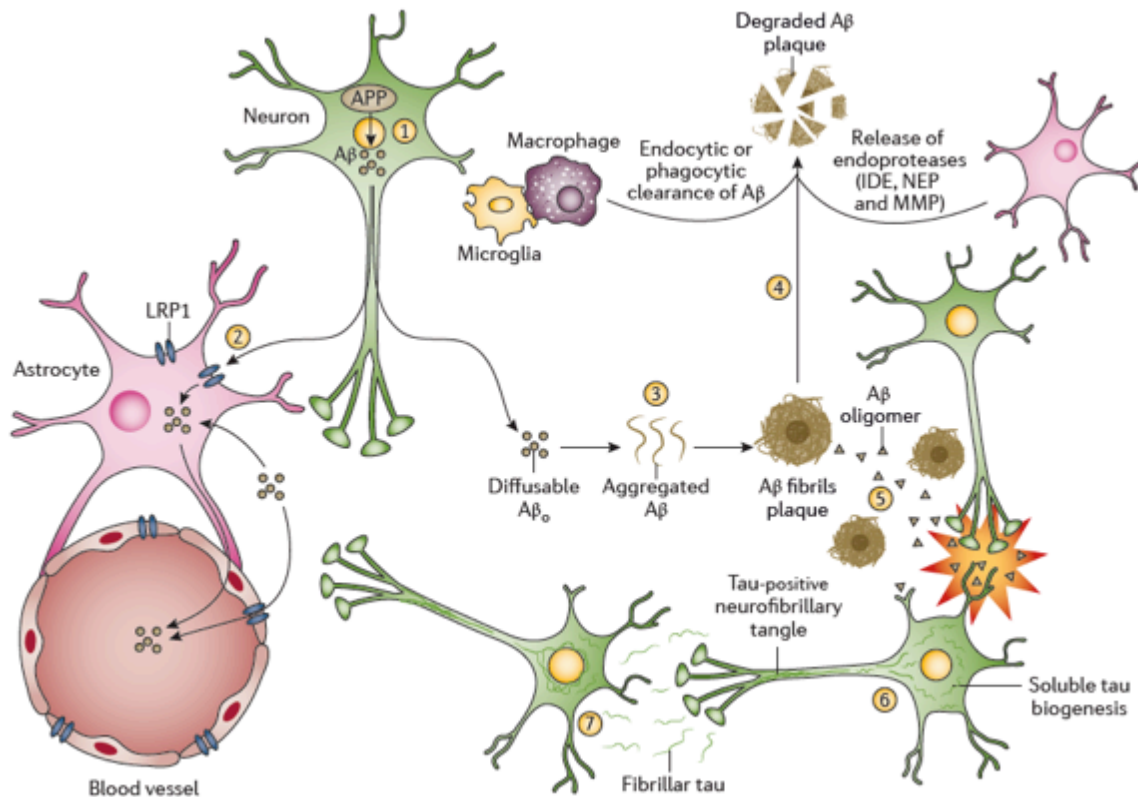


Figure 5. Pathways leading to plaques and tangles form the basis of the amyloid- $\beta$  theory of Alzheimer's disease.

*Amyloid- $\beta$  ( $A\beta$ ) is cleaved from amyloid precursor protein (APP; step 1) and is released into the extracellular milieu as diffusible oligomers ( $A\beta_o$ ).  $A\beta_o$  can be cleared by mechanisms that involve APOE or can be taken up by astrocytes via low-density lipoprotein receptor-related protein 1 (LRP1; step 2).  $A\beta_o$  can also aggregate in the intercellular space to form fibrillary constructs, which in turn assemble into plaques (step 3).  $A\beta$  plaques can be cleared from the brain via degradation by endocytic or phagocytic clearance (in macrophages and microglia), or by endoproteases from astrocytes (such as an insulin-degrading enzyme (IDE), neprilysin (NEP) and matrix metalloproteinase (MMP); step 4). However, some conformational oligomers that dissociate from  $A\beta$  fibrils and plaques may not be cleared and are toxic to adjacent synapses (step 5), and induce tau aggregation. Tau damage occurs in neurons and is mediated by the development of tau-positive neurofibrillary tangles (which extend into the dendrites; step 6). Fibrillar tau can be released and taken up by healthy neurons, triggering tau damage in the uptaking cell (step 7). Reprinted from (Masters *et al.*, 2015).*

There are several infirmities in the amyloid hypothesis of AD. Firstly, recent neuropathological studies did not find correlation between amyloid plaque density in the brain and the severity of dementia (Teich and Arancio, 2012; Sorrentino *et al.*, 2014). Moreover, 20–40% of non-demented elderly subjects have amyloid plaques in the brain in post-mortem examination; strikingly, in some cases, plaque density in non-demented individuals is comparable to that of AD patients (Lippa and Morris, 2006; Aizenstein *et al.*, 2008).

Secondly, most of anti-amyloid based therapeutic strategies researched so far failed to show clinically relevant results in improving cognitive performance or in halting the clinical progression of dementia in humans, even though they were effective in mice models (Cummings, 2006; Lippa and Morris, 2006).

Thirdly, the cellular and animal models of AD are based mostly on the genetic mutation associated with the early-onset AD. Nevertheless, as described earlier FAD accounts for the minority of the cases of AD dementia, whereas late-onset AD is far more common and is not associated with the mutations characteristic to the cases of FAD. On the opposite, sporadic AD has a complex etiology, involving multiple genetic polymorphisms with minor risk-effects and other pathological mechanisms. Surprisingly, many FAD-causing mutations in PS1 do not generally increase A $\beta$  production but often lower it (Chávez-Gutiérrez *et al.*, 2012; Wolfe, 2012).

These findings led to modification of the amyloid paradigm to imply that not the total A $\beta$  levels, but the ratio between long and short forms of A $\beta$  (mostly A $\beta$ 42/A $\beta$ 40) are molecular determinants of disease (Jan *et al.*, 2008; Karran, Mercken and Strooper, 2011); A $\beta$ 42 is well-established to be more toxic than A $\beta$ 40 (Hardy and Selkoe, 2002; Tiwari and Kepp, 2016), so this argument had support. Soluble oligomers of A $\beta$ , as first reported by Yankner *et al.* (Yankner *et al.*, 1989), are currently seen as more cytotoxic than the fibrils making up the major A $\beta$  plaques (Kayed *et al.*, 2003; Lesné *et al.*, 2006) (for review see Ono, 2017).

The toxic mechanism of A $\beta$ 42-enriched oligomers supposedly causing AD remains highly debated, and several toxic modes of action have been suggested (Götz *et al.*, 2011): oligomers may lead to impairment of long-term potentiation (Walsh *et al.*, 2002), permeabilization of cell membranes (Glabe, 2006; Sciacca *et al.*, 2012), oxidative stress (Lecanu, Greeson and Papadopoulos, 2005), and calcium dyshomeostasis (Arispe, Rojas and Pollard, 1993; Bhatia, Lin and Lal, 2000). A $\beta$  has a hydrophilic and a hydrophobic part well-suited for membrane interaction, and multiple studies have documented interaction with membranes (Quist *et al.*, 2005; Glabe, 2006; Sciacca *et al.*, 2012) and disruption of prion-protein interaction with NMDA receptors (You *et al.*, 2012) and of the respiratory chains of mitochondria (Lustbader *et al.*, 2004; Caspersen *et al.*, 2005; Manczak *et al.*, 2006).

However, the assignment of a single pathogenic form of A $\beta$  remains elusive (Haass and Selkoe, 2007; Balch *et al.*, 2008). Many researchers even started to doubt if the A $\beta$ -related effects are the cause of AD, suggesting alternative mechanisms of the pathology.

Alternatives to the amyloid hypothesis include consideration of other APP cleaving products and even versions that see amyloid plaques as a consequence rather than a reason for AD pathology. Uncertainties in this area also arise from the unknown physiological function of APP and its cleavage fragments that are produced and released under physiological conditions as discussed earlier. Some studies suggest loss of normal A $\beta$  function as a main cause of AD, as oligomerization implies a depletion of the pool of potentially functional A $\beta$  monomers. This etiology centers on the identification of the normal physiological function of the APP/A $\beta$  system and PSEN all related to maintaining relative metal ion levels within the neuron (for the review see Kepp, 2016).

Other hypotheses are based on the findings, that not only plaques are characteristic to AD pathology. Other biomolecular changes were found to be present during the progression of AD. These have led to several the suggestion of other causes of AD, focusing on the protein tau (Ballatore, Lee and Trojanowski, 2007; Ittner and Götz, 2011; Fu *et al.*, 2017), metal ion metabolism (for review see Mathys and White, 2017; Adlard and Bush, 2018), cholinergic dysfunction (for review see Hampel *et al.*, 2017), and oxidative stress (for review see Tönnies and Trushina, 2017; Tramutola *et al.*, 2017) hypotheses. Another hypothesis proposes that chronic inflammatory conditions cause dysregulation of mechanisms normally clearing misfolded or damaged neuronal proteins and this leads to accumulation of tau and tau-associated impairments of axonal integrity and transport (for review see Brunden *et al.*, 2017). This has several neuropathological consequences: induction of axonal swelling and leakage, followed by disruption of synaptic contacts; accumulation of mitochondria, resulting in metabolic impairments; deposition of APP in swollen neurites, and generation of aggregation-prone peptides of A $\beta$ ; further tau hyperphosphorylation, ultimately resulting in neurofibrillary tangle formation and neuronal death (for review see Krstic and Knuesel, 2013; Heppner, Ransohoff and Becher, 2015).

The amyloid hypothesis has recently been reviewed and arguments in its favor have been compiled by Selkoe and Hardy (Selkoe and Hardy, 2016). They concluded that that definitive proof of this controversial concept could only come from clinical trials that selectively target A $\beta$ . To prove the hypothesis this treatment in typical AD patients should produce slowing and ultimately suspension of cognitive decline. Indeed, recent trials of three different A $\beta$  antibodies (solanezumab, crenezumab, and aducanumab) have suggested a slowing of cognitive decline in subjects with mild AD in post hoc analyses (Cummings, Morstorf and Zhong, 2014; Doody *et al.*, 2014; Sevigny *et al.*, 2015). However, another antibody, Bapineuzumab, has been found not to improve cognition (Salloway *et al.*, 2014) and produce adverse effects (Castellani and Perry, 2012) even though it does lower A $\beta$  levels (Blennow *et al.*, 2012). Clearly, scientists need to understand better these different

outcomes, specifically how the various antibodies bind and modify the conformations and properties of A $\beta$ , as the various conformations of A $\beta$  that are targeted affect pathology differently (Rosenblum, 2014; Somavarapu and Kepp, 2015). In many of these cases, the human clinical data were substantially less encouraging than the mouse and cell data used to research new treatments (Karran and Hardy, 2014; De Strooper and Chávez Gutiérrez, 2015). This troubling finding is, nevertheless, consistent with the poor correlations between human and cell and mouse data from the meta-analysis (Tiwari and Kepp, 2016).

Amyloid cascade hypothesis is still the leading hypothesis of AD pathology nowadays. Despite many contradictions raised by the experimental observations it still holds its place as A $\beta$  is still considered a leading cause of pathological events. However, unsuccessful so far therapy trials point out that more research should be done in order to better understand the initial steps of pathology.

### **1.1.2 The onset of pathology and clinical symptoms**

It is becoming increasingly obvious that the pathogenic events in AD begin decades before the first clinical symptoms become evident (Jansen *et al.*, 2015; Ossenkoppele *et al.*, 2015). For example, in people at high risk of AD abnormal accumulation of A $\beta$  and amyloid deposition, measured by A $\beta$  levels in CFS and amyloid-PET, were detected 25 years before symptoms onset (Bateman *et al.*, 2012). Moreover, the Dominantly Inherited Alzheimer Network (DIAN) consortium found that pathophysiological brain changes, including changes in cerebrospinal fluid (CSF) biomarkers, cerebral amyloid deposition and brain metabolism, in people carrying autosomal dominant FAD mutations begin at least two decades before the predicted onset of clinical symptoms (Bateman *et al.*, 2012). Studies on the patients with genetic risk for AD (Bookheimer *et al.*, 2000; Quiroz *et al.*, 2010; Machulda *et al.*, 2011), cognitively normal individuals with evidence for A $\beta$  accumulation (Hedden *et al.*, 2009; Sperling *et al.*, 2009; Sheline *et al.*, 2010) and people with early AD (Dickerson *et al.*, 2005; Sorg *et al.*, 2007; Bakker *et al.*, 2012) reveal neural circuit impairments – hippocampal hyperactivation and impaired deactivation of the default-mode network during memory encoding. At the same time, the elderly without dementia or those clinically diagnosed with MCI can harbor AD pathology that may be quite indistinguishable from that of persons with dementia (Rentz *et al.*, 2010).

The fact that it takes many years for AD to develop may explain varying degrees of pathological alterations that appear before subjects start to present clinical symptoms, especially if we take into account that different factors, including environmental, may interfere with the development of the

disease. This becomes particularly evident in the overlap of neuropathological alterations in patients who are still regarded as MCI and patients with diagnosed AD dementia.

Data from CSF and molecular imaging studies add to the body of evidence that the accumulation of A $\beta$  in the brain precedes the onset of functional and structural pathological changes characteristic of AD (Fellgiebel *et al.*, 2004; Bouwman *et al.*, 2007; Mattsson *et al.*, 2009; Petersen *et al.*, 2009). These observations lead to the assumption of a hypothetical cascade of biological events of the pathology events. It begins by the production and accumulation of A $\beta$ 42 (in the brain revealed by reduced CSF A $\beta$ 42 and increased amyloid tracer Pittsburgh compound B retention), this triggers secondary events culminating in synaptic dysfunction and regional hypometabolism (found in FDG-PET studies), neurodegeneration (i.e., increased CSF Tau and phospho-Tau proteins) and structural changes (hippocampal and other regional atrophy). Finally, subjects start experiencing cognitive and functional difficulties, reaching the threshold for dementia diagnosis (Petersen *et al.*, 2009; Forlenza, Diniz and Gattaz, 2010). However, other studies suggest that neuronal activity alteration is the earliest pathological event that leads to the accumulation of A $\beta$ 42 and synaptic dysfunction. This data will be discussed in more details in chapter 1.3.

Animal models are employed to investigate the relationship of the amyloid plaques and morphological and functional changes in AD-affected brain. However, the results of these studies did not provide a clear description of the chain of events. On the one hand, there is an evidence of the pathological influence of A $\beta$  oligomers on the neurons and their neurites; on the other hand, it is debated if direct vicinity to the plaque is required for the pathological effects to occur. It has been shown that A $\beta$  oligomer administration (Shankar *et al.*, 2007, 2008) and virally induced overexpression of mutated APP (Hsieh *et al.*, 2006; Wei *et al.*, 2010) led to a reduced dendritic spine density in hippocampal slice cultures. Research results demonstrated that a decline in the density of the synapses and dendritic spine density in the hippocampus can be already detected at a time, when only soluble A $\beta$  but no amyloid plaques were present (Hsia *et al.*, 1999; Mucke *et al.*, 2000; Lanz, Carter and Merchant, 2003; Jacobsen *et al.*, 2006).

On the other hand, studies of the cerebral cortex discovered that there is an instability of pre- and postsynaptic structures within the vicinity of amyloid plaques (Liebscher *et al.*, 2014) and spine loss occurs shortly but with a significant time delay, after the birth of new plaques, and persists in the vicinity of amyloid plaques over many months (Bittner *et al.*, 2012), but spine loss also occurs in areas apart from amyloid plaques (Bittner *et al.*, 2010). One possible explanation of these discrepancies is that several spatiotemporally independent events contribute to a net loss of dendritic spines. It was suggested that these events coincided either with the occurrence of

intracellular soluble or extracellular fibrillar A $\beta$  alone, or the combination of intracellular soluble A $\beta$  and hyperphosphorylated tau (Bittner *et al.*, 2010).

As for other pathological changes observed in the AD brain, some of them show a clear association with the plaque vicinity, while others do not. Neuritic changes and dystrophies are observed, and they are accompanied by dendritic spine loss in the peri-plaque region (Grutzendler *et al.*, 2007). The vast majority of axonal dystrophies, characteristic to AD brains, are associated with A $\beta$  plaques, and in all these cases the formation of dystrophies was observed after the appearance of the A $\beta$  plaques (Blazquez-Llorca *et al.*, 2017a). In early studies, plaques were associated with substantial inflammatory responses including activation of microglia and astrocytes (Lue *et al.*, 1996; for review see Thal *et al.*, 2006). However, other researchers observed no correlation of morphological microglia activation with plaque volume or plaque lifetime, suggesting that amyloid deposits by themselves are not sufficient to attract and activate microglia *in vivo* (Jung *et al.*, 2015).

The results of neuronal activity investigation in relation to plaque distances are also inconclusive. Early study by Busche *et al.*, that for the first time reported activity changes in the AD mice also reported that most of the affected neurons are located in the direct vicinity of the amyloid plaques, thus proposing that pathological conditions of the plaque surrounding are the main cause of the activity changes (Busche *et al.*, 2008). Nevertheless, some of the later studies did not find a correlation of neuronal activity changes with the vicinity of the plaque (Liebscher *et al.*, 2016).

There is strong evidence that pathological events leading to AD start decades before the clinical symptoms appear. However, it remains unclear which of these events are the cause rather than a consequence of excessive A $\beta$  generation. Even though amyloid plaques were long seen as one of the early disease hallmarks producing pathological environment, it remains unclear if their presence in the tissue leads to pathological events, or most of the other pathological signs develop independently of plaques. For this reason, more intensive research of the early phases of AD is needed, which nowadays can only be done in animal models of AD as early enough diagnosis is still lacking in humans.

### **1.1.3 Mouse models of amyloid-associated AD pathology**

As evident from the previous chapters there are many unresolved questions in the field of AD research, and long progression of the disease with a hidden onset presents researchers with additional challenges. That is why experimental models of AD are crucial for gaining a better understanding of pathogenesis and to explore the potential of novel therapeutic approaches. It is

especially important if we want to study the early stages of disease progression that are extremely difficult to diagnose in humans.

To date, the dominant majority of AD experimental models are animal models, represented by transgenic mouse lines that express human genes responsible for the formation of amyloid plaques (by expression of human APP alone or in combination with human PS1) and neurofibrillary tangles (by expression of human Tau protein) (Wisniewski and Sigurdsson, 2010; Boutajangout and Wisniewski, 2014; Dujardin, Colin and Buée, 2015; Puzzo *et al.*, 2015a). Other models include invertebrate animals such as *Drosophila melanogaster* and *Caenorhabditis elegans* and vertebrates such as zebrafish. The disadvantage of non-mouse models is distance of their physiology from human physiology, so they are less extensively used (Newman, Ebrahimie and Lardelli, 2014; Bouleau and Tricoire, 2015; Hannan *et al.*, 2016). Starting from the time of the development of the first transgenic mouse model with prominent A $\beta$  plaque pathology in 1995 (Games *et al.*, 1995), many more transgenic models were established, each with a different phenotype of AD-associated pathology (Wisniewski and Sigurdsson, 2010; Dujardin, Colin and Buée, 2015; Puzzo *et al.*, 2015b).

Expression of FAD-mutant human or humanized APP (with or without co-expression of FAD-mutant PSEN1 or PSEN2) in the neurons of transgenic mice simulates key aspects of AD following the amyloid hypothesis, including elevated levels of human amyloid- $\beta$ , amyloid plaques, neuritic dystrophy, synaptodendritic impairments, astrogliosis, microgliosis, vasculopathy, network dysfunction, cognitive deficits and behavioural alterations (Ashe and Zahs, 2010). Unfortunately, none of the models can completely recapitulate AD in its entirety, and this could explain very high failure rate of clinical trials of AD therapeutics (of ~99.6%), many of which were successful in preclinical testing employing these animal models (Cummings, Morstorf and Zhong, 2014; Schneider *et al.*, 2014; Banik *et al.*, 2015). However, animal models still represent a valuable tool to closely study key aspects of AD, including the occurrence and growth of amyloid plaques, the onset, and progression of dendritic spine pathology, neuronal dysfunction and the induction of neuronal apoptosis (Radde *et al.*, 2008).

While animal models have been instrumental in studying the impact and mechanism of cerebral amyloidosis and in developing therapeutic strategies (Selkoe and Schenk, 2003), many of them have significant limitations such as the late onset of the pathology, gender differences in the pathology, effects of mixed genetic backgrounds, difficulties with breeding, and high variability in A $\beta$  levels. Therefore, researchers in the laboratory of Prof. M.Jucker developed a transgenic mouse model APPPS1 that addresses most of these issues. This was the model I used in my thesis due to several advantages that are discussed in the next chapter.

### 1.1.3.1 APPPS1 model

APPPS1 mice bear human transgenes for APP with the Swedish mutation and PS1 with an L166P mutation, both controlled by the Thy1 promoter. Expression of the human APP transgene in these mice is approximately 3-fold higher than the expression of endogenous murine APP. Human A $\beta$ 42 is generated preferentially compared to A $\beta$ 40, but levels of both increase peptides with age. In the brain, the A $\beta$ 42/A $\beta$ 40 ratio decreases with the onset of amyloid plaque deposition (Radde *et al.*, 2006; Maia *et al.*, 2013). This deposition starts in the neocortex at approximately six weeks of age (Figure 6. Age-related amyloid deposition in APPPS1 mice.), it then appears in the hippocampus at about 3-4 months, and in the striatum, thalamus, and brainstem at 4-5 months. The first paper characterizing this mouse model reported that mice exhibited impaired reversal learning of a food-rewarded four-arm spatial maze task at eight months of age (Radde *et al.*, 2006). Other publications reported also earlier observations of cognitive impairment, including deficits in the Morris Water maze at seven months of age (Serneels *et al.*, 2009). Impairments in hippocampal LTP in the CA1 region have also been reported to also start around the age of seven months (Gengler, Hamilton and Hölscher, 2010).

The APPPS1 mouse line combines several advantages of previous transgenic lines. (1) These mice have been created on a pure C57BL/6J background that is known to reduce the variability of A $\beta$  metabolism and deposition (Lehman *et al.*, 2003). (2) No gender effects in A $\beta$  level and amyloid deposition have been noted (Radde *et al.*, 2006). (3) It was shown that APPPS1 mice breed well, similar to wild-type C57BL/6J mice (Radde *et al.*, 2006). (4) The early onset of amyloid pathology has several advantages for research practice, including possibility for rapid readouts and testing of therapeutic amyloid-targeting strategies. Due to all these reasons, the APPPS1 mouse model presents a great tool to study pathological processes in chronic experiments. The fast pathology progression is especially handy for chronic *in vivo* microscopic imaging of the brain, as this can only be done within a timeframe of a few months – as long as the cranial window can remain clear and transparent allowing good imaging quality.

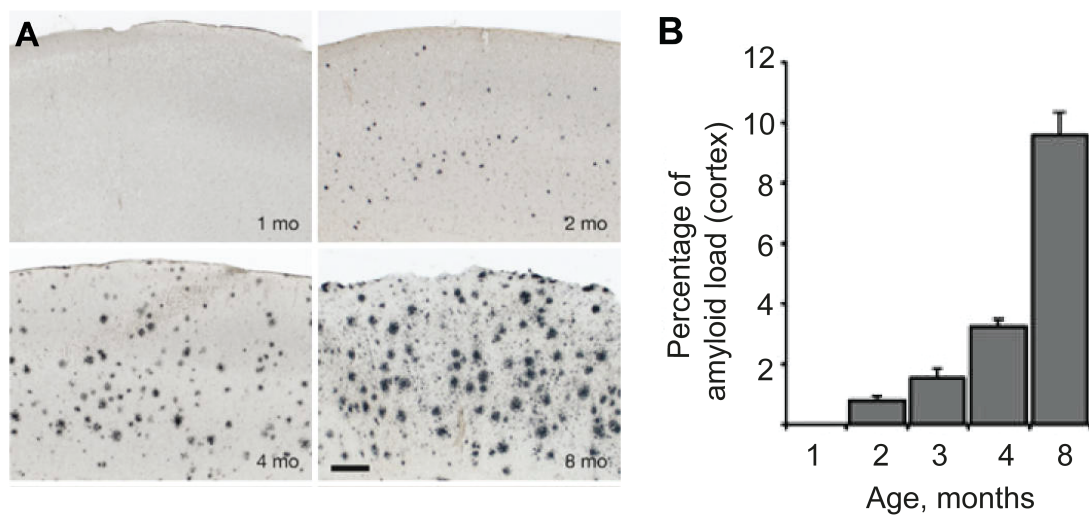


Figure 6. Age-related amyloid deposition in APPPS1 mice.

A.  $A\beta$  immunostaining in the frontal cortex of 1-, 2-, 4- and 8-month (mo)-old female transgenic mice. First amyloid aggregates start to appear at already two months of age. At eight months of age, amyloid deposits cover virtually the entire neocortex, are larger and are surrounded by diffuse amyloid. B. Results of the stereological analysis of amyloid load (%) show a significant increase from 1 to 8 months of age in the neocortex. SEM is shown.  $A\beta$ , amyloid  $\beta$ . Adapted from

## 1.2 *In vivo* two-photon imaging in AD

*In vivo* approaches have special value in disease research as they help scientists to better recapitulate main pathological features in the physiological environment of the organism and dynamics, while traditional histological analyses of affected brains only allow for a static assessment of pathology. Among different *in vivo* methods *in vivo* imaging has one of the leading roles, allowing less invasive and longitudinal experiments. The techniques used in this thesis, namely two-photon microscopy, has its advantages and limitations, which are discussed in more detail in the following subchapter. Also, the necessary background and settings of this experimental approach are explained.

### 1.2.1 *In vivo* two-photon microscopy

Classical fluorescence techniques, including confocal microscopy, cannot provide high-resolution deep imaging within the tissue which is especially important for *in vivo* experiments. Two-photon microscopy is able to overcome this limitation because of the special properties of two-photon excitation. Main advantages of two-photon microscopy are decreased scattering, good penetration into biological tissue and high contrast due to virtually excluded background fluorescence.

Two-photon excitation occurs when two near-infrared photons are simultaneously absorbed (typically within less than  $10^{-15}$  s) by a fluorophore. This promotes an electronic transition that would otherwise require a single photon of approximately twice the energy (Helmchen and Denk,

2005; Svoboda and Yasuda, 2006). Two-photon absorption occurs only with very high intensities of light (in general  $> 10^{17}$  W/m<sup>2</sup>), which provide a high density of photons (Denk and Svoboda, 1997). This high density can only be achieved by using a pulsed laser source with short high energy pulses emitted in a form of spatially focused laser beam passing through a high numerical aperture (NA) microscope lens. Lasers for two-photon microscopy provide laser pulses of about 100 fs width and with repetition rates of approximately 100 MHz. Mostly used type of laser is the Ti:sapphire laser with 700 – 1100 nm tunable output and high average power capability of 1 W.

Due to the longer wavelength, the excitation light is less susceptible to scattering and absorption in biological tissue. Thus, light can penetrate further in the tissue compared to other fluorescent microscopy methods. Moreover, in case of two-photon excitation fluorescence generation is confined to the focal region (as only here two photons have high chances to meet) and out-of-focus fluorescence is very low. As a consequence of this, two-photon microscopy has inherent optical sectioning without the need for a spatial filter, as the exact place of origin of fluorescence photons is well-defined at each point in time. Accordingly, all fluorescence photons (also scattered photons) that enter the objective and are passed by the detection filter are collected (Figure 7). Emitted photons are collected by photomultiplier tubes (PMT). PMTs rely on the photoelectric effect, meaning that when incoming photons reach a photocathode it releases an electron, which is then amplified by a set of dynodes. Eventually, electrons will reach the anode, and each of the incoming photons will be converted into a pulse of current.

Both the detection of scattered fluorescence and better penetration of the longer excitation wavelength light contribute to the capability of two-photon microscopy to provide high-resolution images from deep layers of living tissue (several hundred micrometers). Moreover, confining excitation to the focal region is not only important to allow for a significant increase in detection efficiency with increasing contrast but also it reduces photobleaching and damage in the out-of-focus tissue. These features make two-photon microscopy an invaluable tool for *in vivo* imaging applications.

Applying two-photon imaging in living mouse is only feasible after creating the optical access to the imaging tissue. To image the brain a so-called cranial window is used, which requires either open skull or thinned skull preparation. The open skull preparation (the technique of choice in this thesis project) is made by a circular craniotomy after which the exposed cortex is covered by a glass coverslip, and the window is sealed with dental acrylic (Holtmaat *et al.*, 2009). The alternative, thinned closed skull preparation can be performed by thinning the skull above the cortical region of interest (Yang *et al.*, 2010).

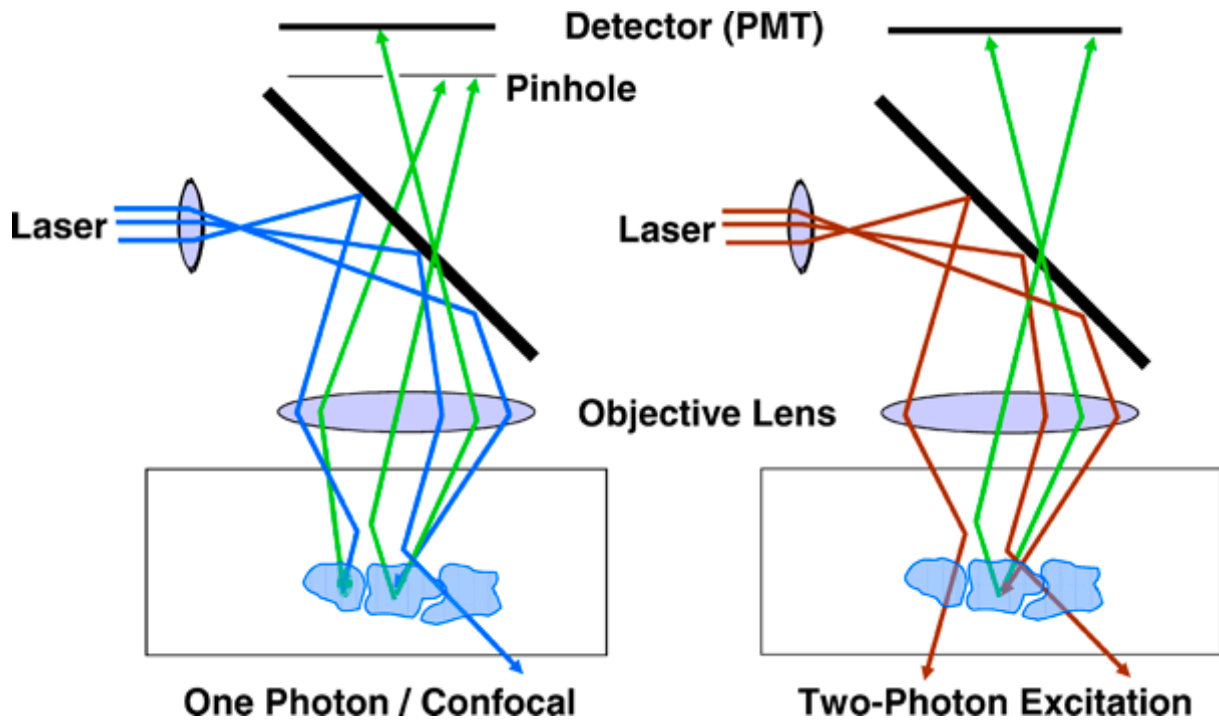


Figure 7. Comparison of scattering in confocal microscopy and two-photon microscopy.

In confocal microscopy (shown on the left), blue excitation light reaches the focus, and green fluorescence from the focus is collected and passes through a pinhole. In two-photon excitation microscopy (shown on the right), because no pinhole is needed, the scattered fluorescence photons can still be collected, thus increasing the collected signal. Further, the scattering of a single red excitation photon does not cause background (as the chance of two photons scattering to the same place at the same time is close to zero). Reprinted from (Piston, 2005).

Both techniques have their strong and weak sides. With skull thinning the area of the cortex accessible to imaging is very small, and thinning procedure needs to be executed repeatedly when long imaging intervals are planned, as the bone grows back. Re-thinning is time-consuming, it requires additional anesthesia and the resulting bone layer might vary in thickness, thereby altering imaging quality. In contrast, open skull preparations allow longitudinal imaging without additional interventions after the initial surgery. There is, however, a major concern regarding the open skull preparation, that is the induction of an inflammatory response. Accordingly, immunohistochemical analysis at different time points after window implantation revealed that within the window region there is an initial increase in the number of glial fibrillary acidic protein (GFAP) positive cells, representing activated astrocytes, which was normalized 30 days after implantation (Holtmaat *et al.*, 2009). However, open skull preparation remains the method of choice for longitudinal imaging as it enables stable preparation that can provide good imaging quality for over a year (Burgold *et al.*, 2014). As open skull preparation is also a well-established technique in our lab and as I was aiming at longer imaging period, for this thesis I implemented the open skull preparation with a four-week recovery period before imaging.

Two-photon imaging provides a possibility to study not only morphology but also functioning of the neurons *in vivo*. Conventional electrophysiological approaches to study the functional properties of neurons produce either a low spatial resolution (by recordings groups of neurons, e.g., in field recordings or EEG) or only for single-cell observations (e.g., patch clamp). Thus *in vivo* two-photon imaging using calcium indicators came about as an elegant way of analyzing the spatiotemporal dynamics of cell populations, with single cell resolution. Calcium indicators are based on the fact that the electrical activity of an excitable cell is tightly coupled to changes in intracellular calcium concentration (Tsien, 1981; Stosiek *et al.*, 2003).

### **1.2.2 *In vivo* imaging of neuronal activity**

*In vivo* imaging has become an irreplaceable tool in neuroscience research, as well as clinical trials, and medical practice. Consequently, in recent years it helped scientists to fundamentally increase our understanding of the morphological and functional changes in AD. Imaging techniques can be grouped by the type of energy used to obtain visual information (X-rays, positrons, photons or sound waves), the spatial resolution that is achieved (macroscopic or microscopic) or the type of information that is obtained (structural, functional, cellular or molecular) (Linden, 2012).

Macroscopic imaging methods include computed tomography scan (CT), magnetic resonance imaging (MRI) and positron emission tomography (PET), and they are currently in routine clinical and preclinical use. Microscopic imaging is used in clinical practice and in research to examine the structure and function of biological tissues with cellular and subcellular resolution. As discussed above, the microscopy techniques that use one-photon absorption processes are restricted for the use near the tissue surface for high-resolution imaging because at greater depths light scattering blurs the images (Helmchen and Denk, 2005; Kerr and Denk, 2008; Lichtman and Denk, 2011). The development of two-photon microscopy in combination with advances in fluorescence labeling techniques has allowed for *in vivo* imaging on the depth of several hundreds of micrometers in intact tissue with spatial resolution sufficient to distinguish individual neurons, dendrites, and even synapses. Combined with of transgenic animal models, two-photon imaging offers numerous possibilities in the investigation of the development, progression and potential treatment of brain diseases including AD research.

#### **1.2.2.1 *Calcium imaging***

Synaptic inputs and action potentials lead to the opening of voltage-sensitive calcium channels, release of calcium from internal stores or influx of it via glutamate receptors and thus create an increase in intraneuronal calcium concentrations (Figure 8) (reviewed by Higley and Sabatini, 2008).

This creates a basis for the development of calcium imaging, which involved two parallel processes: the development of calcium sensors, and the development and the implementation of the appropriate instrumentation, including experimental setups and data analysis approaches.

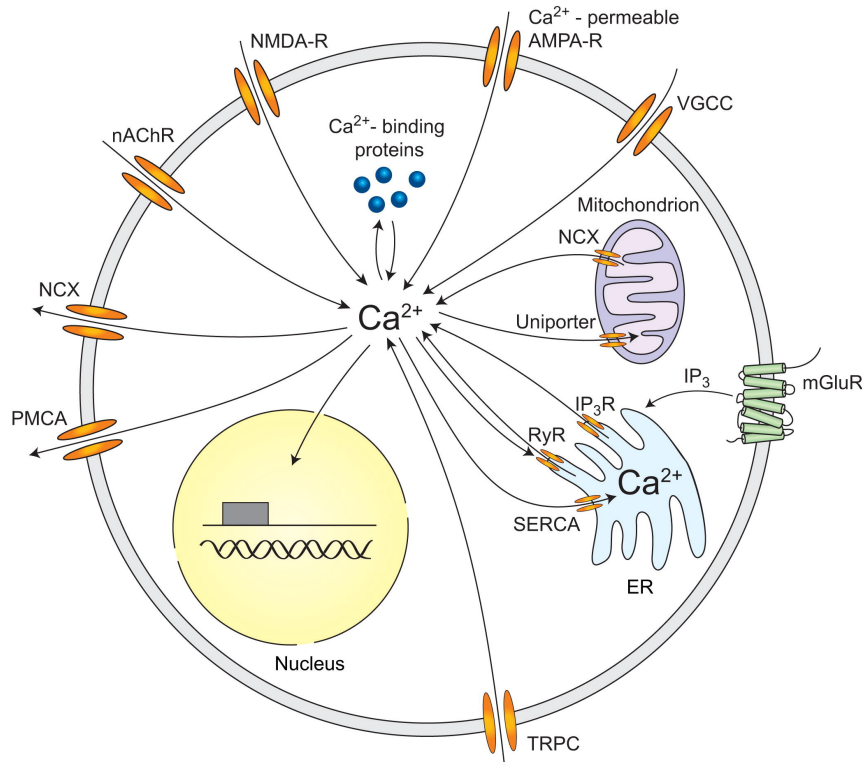


Figure 8. Calcium in the neuron.

Sources of calcium influx are calcium-permeable  $\alpha$ -amino-3-hydroxy-5-methyl-4-isoxazolepropionic acid (AMPA) and N-methyl-D-aspartate (NMDA) glutamate-type receptors, voltage-gated calcium channels (VGCC), nicotinic acetylcholine receptors (nAChR), and transient receptor potential type C (TRPC) channels. Calcium release from internal stores is mediated by inositol trisphosphate receptors (IP<sub>3</sub>R) and ryanodine receptors (RyR). Inositol trisphosphate can be generated by metabotropic glutamate receptors (mGluR). Calcium efflux is mediated by the plasma membrane calcium ATPase (PMCA), the sodium-calcium exchanger (NCX), and the sarco-/endoplasmic reticulum calcium ATPase (SERCA). Mitochondria are also important for neuronal calcium homeostasis. Reprinted from (Grienberger and Konnerth, 2012).

Among the first calcium indicators used for detection of the dynamics of calcium signaling in cells were bioluminescent calcium-binding photoproteins, such as aequorin (Shimomura, H. Johnson, and Saiga, 1962; Ashley and Ridgway, 1968). The next important step was the development of more sensitive and versatile fluorescent calcium indicators by Roger Tsien (Tsien, 1980). These indicators were created as the combination of highly calcium-selective chelators like EGTA or BAPTA with a fluorescent chromophore. The first generation of fluorescent calcium indicators included quin-2, fura-2, indo-1, and fluo-3. Out of dyes of that family fura-2 (Grynkiewicz, Poenie and Tsien, 1985) became very popular among neuroscientists, because it allowed for quantitative calcium measurements by the rationing of the signals obtained with alternating the excitation wavelengths (Neher, 1995). In the following years, many more calcium indicators have been

introduced, providing a wide range of excitation spectra and affinities for calcium. These include, among others, the Oregon Green BAPTA and fluo-4 dye families (Paredes *et al.*, 2008), which are widely used in neuroscience as they are easy to implement and at the same time they provide large signal-to-noise ratio. The major disadvantage of these chemical calcium indicator was the fact that they can only be used in acute experiments. So the next breakthrough, again from the laboratory of Roger Tsien (Miyawaki *et al.*, 1997), was the introduction of protein-based genetically encoded calcium indicators (GECIs), which now could be expressed in the cells of interest for longer periods of time and thus be used in chronic experiments. While the early types of GECIs had relatively limited areas of application due to their slow response kinetics and low signal-to-noise ratios there had been tremendous progress in recent years. GECIs will be described in more details in the next section.

The creation and development of the fluorescent indicators went along with the development of new imaging instrumentation. Among those – the implementation of video imaging (Smith and Augustine, 1988; Swandulla *et al.*, 1991), of CCD cameras (Connor, 1986; Lasser-Ross *et al.*, 1991), and high-speed confocal microscopy (Eilers *et al.*, 1995) for calcium imaging. The high signal strength of the fluorescent indicators in combination with these new technologies allowed for real-time fluorescence observations of biological processes at the single-cell level. A key advance was the introduction of above described two-photon microscopy by Winfried Denk and colleagues (Denk, Strickler and Webb, 1990) and its use for calcium imaging in the nervous system (Yuste and Denk, 1995). Two-photon imaging has revolutionized the field of calcium imaging (Helmchen and Denk, 2005; Svoboda and Yasuda, 2006) and is now used worldwide.

As an important additional tool during the last years powerful computational tools have been developed to derive spiking activity from calcium transients coming from calcium imaging (Greenberg, Houweling and Kerr, 2008; Mukamel, Nimmerjahn and Schnitzer, 2009; Vogelstein *et al.*, 2010; Cheng *et al.*, 2011; Goltstein, Montijn and Pennartz, 2015).

#### 1.2.2.1.1 Genetically encoded calcium indicators

A major advantage of GECIs compared to small molecule indicators is the possibility of performing long-term calcium imaging *in vivo*, and not only at the cellular level but also in specific subcellular compartments (Holtmaat and Svoboda, 2009; Holtmaat *et al.*, 2012). GECIs are based on autofluorescent proteins such as the green fluorescent protein (GFP) combined with calcium-sensitive proteins such as calmodulin or Troponin C (Mank and Griesbeck, 2008).

There are two commonly used classes of GECIs – the single-fluorophore GECIs GCaMP family and several families of Förster resonance energy transfer-based sensors (Miyawaki *et al.*, 1997; Nagai *et al.*, 2004; Palmer *et al.*, 2006; Mank *et al.*, 2008; Horikawa *et al.*, 2010). GCaMPs consist of a circularly permuted enhanced green fluorescent protein (cpEGFP), which is connected on one side to the calcium-binding protein calmodulin and the other side to the calmodulin-binding peptide M13 (Nakai, Ohkura and Imoto, 2001). In the presence of calcium, calmodulin-M13 interactions undergoes conformational changes in the fluorophore environment and it leads to an increase in the emitted fluorescence (Nakai, Ohkura and Imoto, 2001; Tian *et al.*, 2009). After characterization of the structure of the GCaMP2, GCaMP3 was developed by protein engineering with the improved signal-to-noise ratio, dynamic range, and response kinetics (Tian *et al.*, 2009; Yamada and Mikoshiba, 2012). However, GCaMP2 does not show reliable single action-potential-associated calcium signals. This was a major disadvantage of protein-based indicators for several years when comparing to sensitivity and speed of commonly used small molecule calcium indicators. However, recently a new class of genetically encoded indicators with greatly improved properties was developed (Chen *et al.*, 2013). Family of GCaMP6 (Figure 9) has higher sensitivity than commonly used synthetic calcium dyes (such as OGB1-AM) and detects individual action potentials with high reliability at reasonable microscope magnifications.

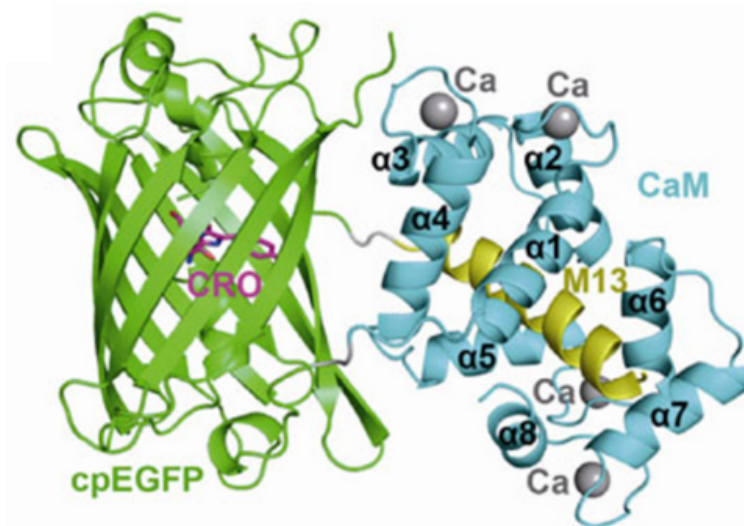


Figure 9. Structure of GCaMP6m monomer in a cartoon scheme.

Functional domains M13, cpEGFP and CaM are colored in yellow, green and cyan, respectively; the chromophore (CRO) is shown as stick models and colored in magentas; the four  $\text{Ca}^{2+}$  bound to the CaM are shown as grey spheres. Reprinted from (Ding *et al.*, 2014).

Three main variants of GCaMP6 (slow, medium, and fast) were developed, they have different calcium-binding kinetics and, thus, they temporally filter intracellular  $\text{Ca}^{2+}$  dynamics to different

degrees (Chen *et al.*, 2013). The slow variant, GCaMP6s, binds calcium more tightly than the fast variant, GCaMP6f. Because of this GCaMP6s has greater  $\text{Ca}^{2+}$  sensitivity, but lower signaling speed and lower ability to distinguish action potentials appearing as a quick sequence. For GCaMP6s, the fluorescence signals have a rise time constant of 180 msec and a decay time constant of 580 msec, whereas, for GCaMP6f, these values are 30 msec and 150 msec, respectively (Chen *et al.*, 2013). These sensors found widespread applications for diverse problems in brain research and calcium signaling, now GCaMP6 family is commonly used as a GECIs of choice. They can be used over multiple imaging sessions separated by months to image large groups of neurons as well as small synaptic compartments.

In contrast to the small molecule indicators GECIs cannot be directly applied to the tissue of interest. Instead, the genetic vector that codes for the indicator should be delivered into the cells of interest and the cellular transcription and translation machinery will produce the final protein. Vector in the form of DNA plasmids can be electroporated (commonly, *in utero*) into cells by application of brief electric pulses (Hires, Tian and Looger, 2008; Mank *et al.*, 2008). An alternative method of vector delivery that allows for much higher transfection rates is viral vector-mediated delivery (Lütcke, 2010). In recent years, viral transfection by adeno-associated virus (AAV) has become a method of choice for delivering the genetically encoded calcium indicators into the mouse brains in many laboratories. This is also a method implemented in the thesis project.

During the last 5 years several transgenic GECI mice have been developed, that possess certain advantages over viral delivery of GECIs (Hasan *et al.*, 2004; Díez-García *et al.*, 2005; Tallini *et al.*, 2006, 2007; Heim *et al.*, 2007; Atkin *et al.*, 2009; Drenth *et al.*, 2012; Zariwala *et al.*, 2012; Dana *et al.*, 2014). However, they also present limitation due to the nature of the transgenes, namely, in most cases lower expression levels compared to viral delivery, requiring higher laser power. Another possible drawback is that many transgenic lines are based on the use of Thy-1 promoter, that has mosaic expression and is not functional in inhibitory neurons.

As a final note on the method, it is important to point out that calcium indicators measure changes in the cytosolic free calcium concentration and that calcium indicators can influence calcium homeostasis of the cell. In normal state, calcium ions in the cytosol are in equilibrium with the calcium ions that are bound to endogenous calcium buffers (Baimbridge, Celio and Rogers, 1992). When calcium indicator is added in calcium imaging experiments, it behaves as exogenous calcium buffer and thereby it contributes to the total amount of cellular calcium buffer molecules (Helmchen, Imoto and Sakmann, 1996), and thus changes the intracellular calcium dynamics (Augustine and Neher, 1992). Therefore, choosing the appropriate indicator in the appropriate

concentration is crucial for the interpretation of the experimental results. For example, fluorescent signals observed with low-affinity indicators reflect more accurately the change in the free cytosolic calcium concentration, as these indicators add little buffer capacity to the cell (Helmchen, Borst and Sakmann, 1997). However, the use of such indicators is limited by the need for sufficient sensitivity, especially when imaging in the noisy *in vivo* condition or when imaging small structures, such as dendritic spines.

In this thesis, I used one of the latest GCaMP versions (GCaMP6s) available at the time the experiments were conducted. Delivery of the genetic construct into the cell of interest was achieved by virally mediated expression employing an AAV1-hSyn1-mRuby2-GCaMP6s- construct (for a detailed description of the construct see Material and Methods).

#### 1.2.2.2 *Awake imaging versus anaesthetized imaging*

Anesthesia is widely used in animal research to provide immobilization of animals and to conduct the procedures not possible in awake animals. For example, chemical calcium indicators can only be used in acute experiments and thus their use is restricted to working with anaesthetized animals. Even though very handy for researchers this approach has disadvantages - it does not allow for chronic studies of the same brain areas/neurons over prolonged periods. At the same time, chronic studies are especially important to study disease progression. Another disadvantage of anesthesia is even more important to note when implementing calcium imaging - it can significantly alter neuronal activity thus producing artifacts or hindering pathological activity alterations.

General anesthesia has multiple physiological effects as it induces pronounced changes in the receptor, ion channel, single neuron and network functions (Rudolph and Antkowiak, 2004; Franks, 2008). From the molecular level point of view, a common characteristic of most anesthetics is potentiation of GABAA receptor activity and inhibition of potassium channels and AMPA- and NMDA receptors (Vahle-Hinz *et al.*, 2001, 2006; Franks, 2008). One of the striking features of the neocortex under deep levels of anesthesia is the presence of slow rhythm of alternating depolarized (UP) and hyperpolarized (DOWN) states that take advantage of spontaneous action potential firing and result in strongly synchronized activity patterns (Steriade, Nuñez and Amzica, 1993; Ecker *et al.*, 2014).

Moreover, the local dynamics of cortical spontaneous activity have been shown to differ between the awake and anesthetized state (Steriade, Nuñez and Amzica, 1993; De Kock and Sakmann, 2008; Greenberg, Houweling and Kerr, 2008; Kreuzer *et al.*, 2010), even under light levels of anaesthesia, in the absence of clear-cut UP/DOWN states, correlations between spontaneous activity patterns

of individual neurons increase (Greenberg, Houweling and Kerr, 2008; Golshani *et al.*, 2009). During wakefulness, the inhibitory drive in the cortex is much higher compared to anesthesia (Haider, Häusser and Carandini, 2013), which makes the overall activity in the cortex very different between these two states. The study of the rat visual cortex showed ketamine anesthesia modulated population-wide synchronization and the relationship between firing rate and correlation at the same time decreasing firing rates and spike bursting (Greenberg, Houweling and Kerr, 2008). Similar results of increased correlations in spontaneous neuronal spiking activity under isoflurane anesthesia accompanied by reduced direction selectivity were observed in mice (Goltstein, Montijn and Pennartz, 2015).

Moreover, anesthesia changes the metabolism and oxygenation of the tissue. Comparison of the awake and anesthetized brains reveals that isoflurane induces arterial dilation, elevates blood flow, and reduced oxygen extraction fraction in a dose-dependent manner. As a result of the combined effects, the cerebral metabolic rate of oxygen (CMRO<sub>2</sub>) is reduced in the anesthetized brain under both normoxia and hypoxia (Cao *et al.*, 2017). These changes may differentially affect healthy and diseased brains, thus making it difficult to discriminate differences occurring due to the pathology from those occurring due to the anesthesia-related stress.

Another problem of the studies in anaesthetized animals is that the mode and deepness of anesthesia are rarely monitored and even if it was monitored it is very vaguely reported in the research papers. This not only makes it difficult to reproduce the study design in another lab and compare the results of different research groups but also rises the concerns that in some case animal is not adequately anaesthetized but rather just immobilized. The lack of the proper anesthesia level may reveal the effects of pain or other symptoms caused by the experimental set-up instead of answering the initial research question.

All in all, however, anesthesia is a powerful and sometimes inevitable research tool; it comes with many drawbacks. Luckily, in the area of calcium imaging, significant progress in the development of GECIs make the awake imaging available and more and more widely used.

Calcium imaging studies in awake rodents generally use one of two main types of optical instrumentation. One option is that the animal is head-fixed under the objective lens of a conventional upright two-photon fluorescence microscope (Dombeck *et al.*, 2007; Nimmerjahn, Mukamel and Schnitzer, 2009). This head-restrained imaging format is compatible with conventional two-photon microscopy and is also well suited for use with custom-designed fluorescence microscopy setups that provide novel imaging capabilities (Horton *et al.*, 2013; Heys,

Rangarajan and Dombeck, 2014; Lecoq *et al.*, 2014; Low, Gu and Tank, 2014; Quirin *et al.*, 2014; Stirman *et al.*, 2014; Bouchard *et al.*, 2015) or combine two-photon Ca<sup>2+</sup> imaging and two-photon optogenetic capabilities in behaving mammals (Packer *et al.*, 2012, 2015; Rickgauer, Deisseroth and Tank, 2014). An alternative approach is that the animal carries a miniature fluorescence microscope on its head, allowing calcium imaging studies during unconstrained animal behavior (Helmchen *et al.*, 2001; Flusberg *et al.*, 2008). Both these approaches allow long-term imaging over weeks (Komiyama *et al.*, 2010; Huber *et al.*, 2012; Ziv *et al.*, 2013; Peters, Chen and Komiyama, 2014).

Head fixation allows cellular level brain imaging using conventional optics while constraining and enhancing experimental control over the behavioral repertoire (Andermann, 2010). The head-fixed format for optical brain imaging allows the use of conventionally sized optical instrumentation, typically a two-photon microscope residing on a vibration-isolation table. Initial Ca<sup>2+</sup> imaging studies in awake head-restrained rodents involved relatively simple behaviours such as quiet wakefulness (Greenberg, Houweling and Kerr, 2008; Bathellier, Ushakova and Rumpel, 2012; Kato *et al.*, 2012) and grooming or locomotion (Dombeck *et al.*, 2007; Dombeck, Graziano and Tank, 2009; Nimmerjahn, Mukamel and Schnitzer, 2009). Behavioural assays have since progressed, making use of the head-fixed preparation suitability for controlled delivery of sensory stimuli (Verhagen *et al.*, 2007; Carey *et al.*, 2009; Andermann *et al.*, 2011; Blauvelt *et al.*, 2013; Patterson, Lagier and Carleton, 2013; Miller *et al.*, 2014). A key consideration is whether limiting an animal's range of behavior via head fixation will be a benefit or a drawback. To address many scientific questions, it is crucial to gather data from a large set of stereotyped trials, and the behavioral constraints imposed by head fixation can facilitate both the controlled delivery of sensory stimuli and behavioral stereotypy in an animal's responses.

To summarise, even though anaesthetized imaging has several advantages and sometimes is the only possible approach, awake imaging is certainly beneficial for brain research. The main advantage is that the brain activity can be measured in the intact state without artifacts generated by anesthesia which can exaggerate or mitigate experimental readouts, e.g., pathological signs when studying brain diseases. For this reason, anaesthetized imaging with head-fixation was the approach chosen in this thesis.

### **1.2.3 *In vivo* microscopy in AD**

Traditional histological analyses only allow for a static assessment of pathology. The appearance of two-photon microscopy (Denk, Strickler and Webb, 1990) has enabled *in vivo* long-term imaging studies (Holtmaat and Svoboda, 2009), from which the field of AD research has benefited

tremendously. *In vivo* imaging of transgenic mice through a cranial window not only allows to monitor general neuropathological features of AD-like lesions, but also to address questions regarding the kinetics and temporal sequence of pathological events and facilitates direct observation of the effects of new treatment approaches (Bacsikai *et al.*, 2001; Spires, 2005; Spires-Jones *et al.*, 2011).

### 1.2.3.1 Imaging of senile plaques

Amyloid- $\beta$  plaques have been studied extensively as one of the major hallmarks of AD, and as a consequence, many treatment studies are aimed at reducing the formation of plaques (Shah *et al.*, 2008; Chopra, Misra and Kuhad, 2011; Kurz and Perneczky, 2011). *In vivo* imaging of amyloid plaques is possible thanks to the existence of dyes binding to  $\beta$ -sheet protein structures. These dyes, such as Thioflavin S or Methoxy-XO4, are applied either topically or peripherally, as some of the dyes can cross the blood-brain-barrier (Christie *et al.*, 2001; Klunk *et al.*, 2002; Bacsikai *et al.*, 2003). As an addition to such dyes, which only allow for the visualization of the compact forms of plaques, fluorescently labeled antibodies against A $\beta$  additionally mark diffuse plaques.

Senile plaques were first studied in living animals by B. Hyman's group (Christie *et al.*, 2001). In this early study, the authors utilized *in vivo* two-photon imaging of the fluorescent plaque-binding substance Thioflavin S in the Tg2576 mouse model of AD (Hsiao *et al.*, 1996). Further work of this group identified additional fluorescent plaque markers, such as Thioflavin T, Thiazine Red, Pittsburgh compound B (PIB) (Bacsikai *et al.*, 2003; McLellan *et al.*, 2003), suitable for *in vivo* two-photon microscopy. Of great value was the introduction of Methoxy-XO4 by Klunk *et al.* (Klunk *et al.*, 2002) in 2002. This lipophilic Congo red derivative is capable of crossing the blood-brain barrier and, thus, allows easy staining of cerebrovascular as well as plaque-bound amyloid via intravenous or even intraperitoneal injection. During the last decade, Methoxy-XO4 has become a standard tool for *in vivo* visualization of the plaques. It is especially beneficial for longitudinal imaging experiments due to its easy administration (i.p.), brightness and efficient binding to plaques. However, while using plaque dyes in experiments, it should be bared in mind, that some of them possess certain anti-amyloidogenic properties by physically blocking amyloidogenic sites of the plaques (Cohen, Ikonovic, *et al.*, 2009; Pratim Bose *et al.*, 2010).

Two-photon microscopy allows for simultaneous imaging of multiple fluorescent markers as it is possible to separate different emitted wavelengths with filters on the detection side. This approach is beneficial for AD research, because it allows for simultaneous imaging of well-known pathological signs, such as plaque, in parallel to imaging something else in a different channel.

For example, viral transfer of GFP into cortical neurons in APP transgenic mice, that also received an injection of Methoxy-X04, enabled to image the detrimental effects of plaques on adjacent dendrites and spines (Spires, 2005). Another possible approach is to cross AD transgenic mice with mouse lines containing fluorescent markers (Brendza *et al.*, 2003; Tsai *et al.*, 2004; Meyer-Luehmann *et al.*, 2008). With this approach, it has been shown that anti-A $\beta$  antibody treatment leads to a decrease in the number of plaques and a rapid reduction in the number and size of dystrophic neurites in AD transgenic mice (Brendza *et al.*, 2005; Rozkalne *et al.*, 2009). Furthermore, by crossing transgenic Iba1-GFP (Bolmont *et al.*, 2008) or CX3CR1-GFP mice (Davalos *et al.*, 2005; Koenigsnecht-Talboo *et al.*, 2008) with AD transgenic mice the dynamic interaction between plaques and microglia have been imaged *in vivo*.

Crucial aspects addressed by longitudinal two-photon imaging are the process of *de novo* plaque formation as well as the kinetics of cerebral amyloidosis (Bittner *et al.*, 2012; Burgold *et al.*, 2014). In addition to plaque formation, the aggregation of A $\beta$  results in widespread cerebral amyloid angiopathy (CAA), which is the aggregation of A $\beta$  in cerebral vessel walls. Formation of CAA can lead to a loss of smooth muscle cells (Mandybur, 1975; Vinters, 1987), disruption of vessels (Greenberg, 2002), and even parenchymal hemorrhage (Kalyan-Raman and Kalyan-Raman, 1984; Mott and Hulette, 2005). The application of two-photon microscopy and plaque dyes helped to study the initiation and progression of methoxy-X04 labeled CAA in APP transgenic mice (Robbins *et al.*, 2006). Traditional methods that have previously examined histological sections from animals and humans at single time points were not able to monitor those sequential events during the formation of CAA, which are important for treatment development.

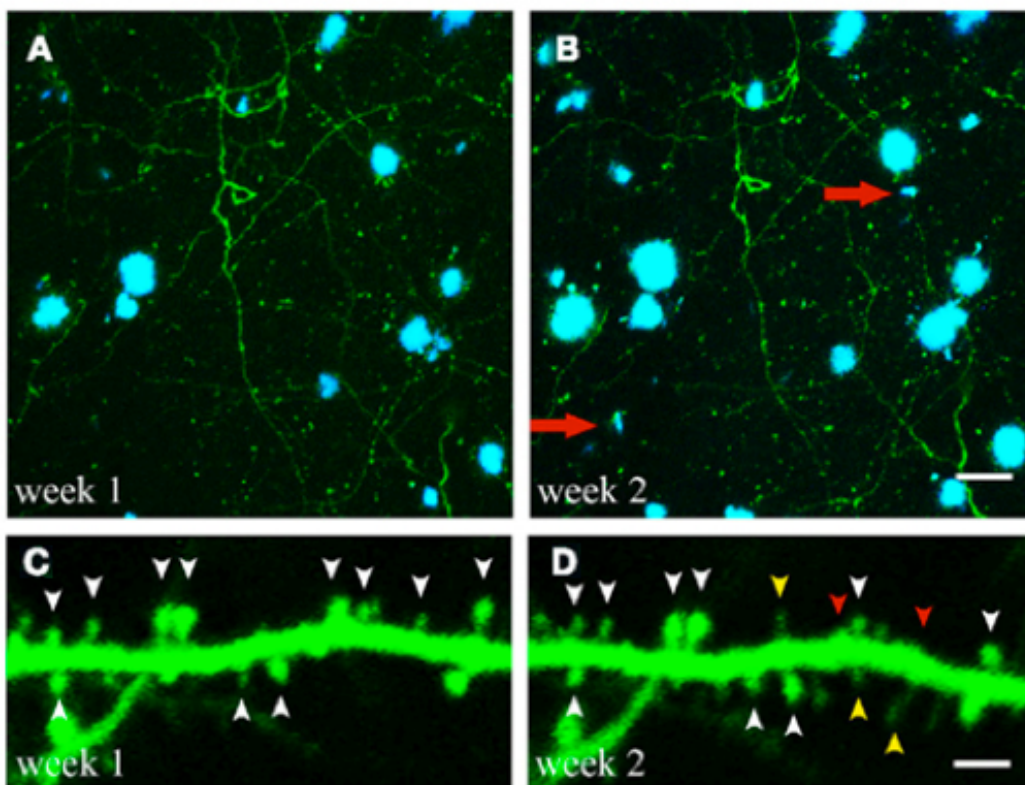


Figure 10. Two-photon *in vivo* imaging of structural alterations in AD model mice.

A, B. Maximum projections of  $z$ -stacks with GFP expressing neuronal structures and Metboxy-XO4 labeled amyloid plaques. Over the course of 1 week two new plaques emerged within the region analyzed (marked with red arrows). C, D. Spine dynamics of an apical dendritic tuft (layer V pyramidal neuron of GFP-M mouse). Spines present at both imaging time points are indicated by white arrowheads, spines lost over the course of 1 week are labeled with red arrowheads, spines newly formed during the same period are marked with yellow arrowheads. Scale bars represent 25  $\mu\text{m}$  (B), and 2  $\mu\text{m}$  (D), respectively. Reprinted from (Liebscher and Meyer-Luebmann, 2012).

Experiments with transcranial *in vivo* two-photon microscopy on transgenic mouse models of AD has shed some light on the temporal sequence and kinetics of AD hallmarks development and structural and functional alterations associated with them (Figure 10). *In vivo* imaging data supports amyloid cascade hypothesis, stressing the relevance of amyloid plaques as a focal source of neurotoxicity, because numerous pathological features, like the occurrence of dystrophic neurites, neurite breakage, spine loss are tightly spatially and temporally linked to plaque deposition. Furthermore, two-photon imaging can provide not only morphological but also functional insights into AD pathology.

Recently, researchers have begun to use two-photon microscopy in combination with calcium-sensitive fluorescent indicators to explore functioning of neurons and glia in AD transgenic mouse models *in vivo*. These studies have revealed significant functional impairments for both, that neuronal and astrocytic populations in plaque-depositing AD transgenic mice. Neuronal activity

aberrations will be discussed in more detail later. It was found that glial cells near amyloid plaques become hyperactive (that is, they exhibit an increased number of  $\text{Ca}^{2+}$ -transients) in response to  $\text{A}\beta$ -induced pathology, and this can have multiple effects (Delekate *et al.*, 2014). Since astrocytes can secrete gliotransmitters (e.g., adenosine triphosphate, glutamate, D-serine) in a calcium-dependent manner (Allen, 2014), hyperactive astrocytes may directly enhance neuronal activity. Furthermore, they may release proinflammatory factors and induce microglial activation, which may contribute further to neurotoxicity through excessive cytokine release (Chung *et al.*, 2015). Moreover, other functions of astrocytes, including buffering of extracellular potassium during neuronal activity and the uptake of neurotransmitters (e.g., glutamate, GABA) from the extracellular space may also be disturbed. Overall, these observations and considerations suggest that glial cells contribute significantly to various aspects of brain dysfunction in AD (Heneka *et al.*, 2015; De Strooper and Karran, 2016; Pekny *et al.*, 2016).

### **1.3 Neuronal activity in AD**

Alzheimer's disease (AD) is associated with functional impairments of brain neurons that are responsible for the storage and processing of information. Early studies revealed a massive decrease in the activity of neurons (Silverman *et al.*, 2001; Prvulovic *et al.*, 2005) and the idea of a generalized silencing of brain circuits found strong support in the synaptic failure hypothesis (Selkoe, 2002). However, more recent studies also reported opposite effects - hyperexcitability and hyperactivity of neurons in the AD models (Busche *et al.*, 2008, 2015; Sanchez *et al.*, 2012; Liebscher *et al.*, 2016). It remains unclear if these are two sides of the same coin or if these are two stages, that follow each other. While the final answer requires more research, the data acquired so far helps to specify several hypotheses to be tested. To give an overview of this current knowledge, the neuronal dysfunction observed both in AD patients and AD model animals is described in this chapter on several levels starting from the morphology of synapses through neuronal activity to wide-range circuit function.

#### **1.3.1 Synaptic dysfunction**

Amyloid- $\beta$  peptides can exert numerous adverse effects on different cells of the brain (De Strooper and Karran, 2016), including effects on the neurons and synapses. As a peptide species with acute toxicity, oligomeric amyloid- $\beta$  directly can induce neuronal apoptosis through interactions with cell-surface receptors. Moreover, longer-term accumulation of toxic amyloid- $\beta$  species in the parenchyma also leads to oxidative damage of DNA and proteins, to physical injury of cellular organelles and dysregulation of intracellular calcium levels, and each of those can provoke cell

death (Kayed and Lasagna-Reeves, 2012). Exposure to amyloid- $\beta$  under *in vitro* conditions can induce neuronal dysfunction and cause cell death within hours, but it takes years for amyloid accumulation to have detectable consequences *in vivo*. Despite these differences in timescale, the brains of people with AD show alterations similar to those seen in neurons *in vitro* and patient neuronal death accompanies the onset of cognitive decline (Jack *et al.*, 2009).

However, amyloid- $\beta$ -induced deficits in synaptic plasticity, circuit function, and cognition develop before cell loss occurs (Jorge J. Palop and Mucke, 2010). Neurons exposed to pathologically elevated levels of amyloid- $\beta$  *in vitro* or *in vivo* show signs of atrophy, including lower dendritic spine density and shorter dendrites (Spires and Hyman, 2004; Koffie *et al.*, 2009), alterations that can increase intrinsic cellular excitability (Šišková *et al.*, 2014) and may explain the hyperactivity of some excitatory neurons. In addition to the loss of spines, studies in mouse AD models also revealed various structural pathological changes in neurites, i.e., axons and dendrites (Bittner *et al.*, 2012; Zou *et al.*, 2016; Blazquez-Llorca *et al.*, 2017b). Neurites show curvature changes and are prone to develop dystrophies and to eventually break (D'Amore *et al.*, 2003; Tsai *et al.*, 2004; Spires, 2005; Garcia-Alloza *et al.*, 2006; Meyer-Luehmann *et al.*, 2008).

Synaptic loss can precede the existing neuronal loss within a particular cortical area. Moreover, the degree of region-specific synapse loss is a stronger correlate of cognitive decline in AD than counts of plaques, tangles and neuronal loss (DeKosky and Scheff, 1990; Terry *et al.*, 1991). The loss of the synapses has been shown to contribute to circuit dysfunction and cognitive decline in mouse models of AD (Palop *et al.*, 2007; Šišková *et al.*, 2014). Because of this remaining neurons become less well connected to their synaptic partners and likely this is why synaptic density is the best correlate of cognitive decline (DeKosky and Scheff, 1990; Scheff, DeKosky and Price, 1990; Scheff and Price, 1993; Scheff *et al.*, 2007). Worth noting, an inverse correlation has been observed between synaptic density and the size of the remaining synapses measured by the length of the postsynaptic density. This enlargement of remaining synapses has been interpreted as a compensatory response (DeKosky and Scheff, 1990; Scheff, DeKosky and Price, 1990; Scheff and Price, 1993).

The role of A- $\beta$  aggregates in the synaptic pathology is not entirely clear. However, several studies reported brain areas close to plaques to be the most affected. Using *in vivo* imaging, it was found that spine loss in the hippocampus and frontal cortex became apparent only after plaques were deposited, and was most pronounced in the vicinity of plaques (Bittner *et al.*, 2010, 2012). Also, other studies found that degenerative changes happen in close relationship to amyloid plaques further underlying a key role of plaques in AD pathology (Grutzendler *et al.*, 2007; Penzes *et al.*,

2011). Another recent study by Liebscher *et al.* revealed a pronounced instability of pre- and postsynaptic structures within the vicinity of amyloid plaques. Treatment with a  $\gamma$ -secretase inhibitor (GSI) attenuated the formation and growth of new plaques and led to a normalization of the dynamics of synaptic structures close to plaques (Liebscher *et al.*, 2014).

If the synapses are not lost, they are still likely to be affected by the pathological environment in the two main directions - neuronal hyperexcitability and synaptic depression.

The molecular changes on the synaptic level seem to cause hyperexcitability *in vitro* and *in vivo* (Palop *et al.*, 2007; Sanchez-Mejia *et al.*, 2008; Minkeviciene *et al.*, 2009; Harris *et al.*, 2010; Morris *et al.*, 2011; Um *et al.*, 2012; Busche *et al.*, 2012; A. Ittner *et al.*, 2014; Born *et al.*, 2014; Kurudenkandy *et al.*, 2014; Bezzina *et al.*, 2015). Acute amyloid- $\beta$  application initially and transiently (10–20 minutes) increases the levels of surface AMPA-type glutamate receptors and GluN2B-containing NMDA-type glutamate receptors (NMDARs) (Sanchez-Mejia *et al.*, 2008; Um *et al.*, 2012) and the frequency of spontaneous excitatory postsynaptic currents in primary neuronal cultures (Sanchez-Mejia *et al.*, 2008; Um *et al.*, 2012). In brain slices, the amyloid- $\beta$  application also acutely increases the rate of action potential firing by hippocampal pyramidal cells (Kurudenkandy *et al.*, 2014). In FAD mice (lines hAPP-J20, hAPP-J9, APP23xPS45 and APP/PSEN1dE9) both hyperactive and hypoactive neurons were discovered — observed in abnormally high or low rates of action potential-dependent calcium transients or levels of transcripts for the immediate early genes *Arc* and *Fos* — both before (Chin *et al.*, 2005; Palop *et al.*, 2007) and after (Busche *et al.*, 2008; Grienberger *et al.*, 2012; Rudinskiy *et al.*, 2012) amyloid deposition becomes detectable.

Amyloid- $\beta$  can also induce synaptic depression (Chapman *et al.*, 1999; Kamenetz *et al.*, 2003; Hsieh *et al.*, 2006; Shankar *et al.*, 2007; Jorge J. Palop and Mucke, 2010). For example, amyloid- $\beta$  blocks neuronal glutamate uptake at synapses, which could result in glutamate spillover around the synaptic cleft (Li *et al.*, 2009) and A $\beta$ 1–40 monomers and dimers were found to enhance the presynaptic release of glutamate (Fogel *et al.*, 2014). The rise in glutamate may desensitize synaptic NMDARs and aberrantly activate extra- or perisynaptic GluN2B-containing NMDARs and metabotropic glutamate receptors (mGluRs), and both GluN2B-containing NMDARs and mGluRs can promote long-term synaptic depression retraction (Liu *et al.*, 2004; Hsieh *et al.*, 2006; Li *et al.*, 2009). Amyloid- $\beta$ -induced NMDAR- and mGluR-dependent long-term depression can be prevented by lowering extracellular glutamate (Li *et al.*, 2009) and can be mimicked by application of the glutamate reuptake inhibitor threo- $\beta$ -benzyloxyaspartate (TBOA), which can also trigger epileptiform discharges in wild-type brain slices (Campbell, Hablitz and Olsen, 2014). These events,

leading to synaptic depression, might lead to network hypersynchrony, which was reported in AD mouse models (Roberson *et al.*, 2011).

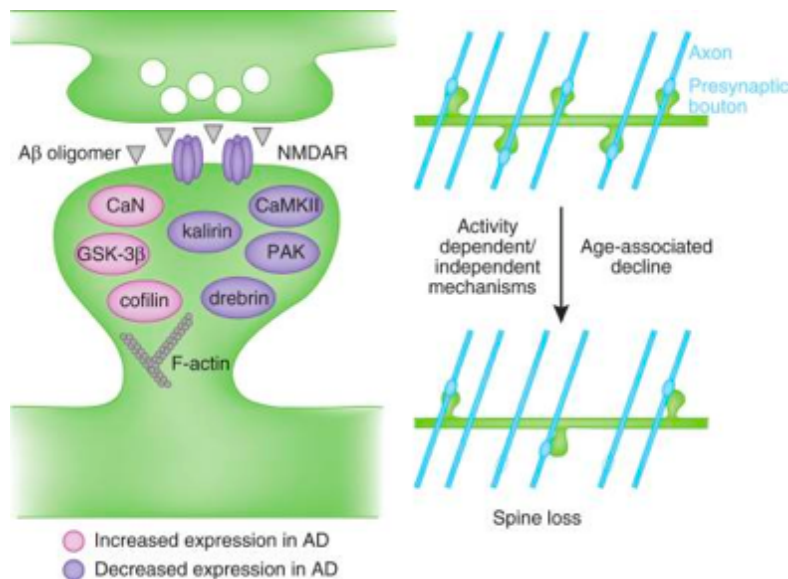


Figure 11. Model of molecular mechanisms involved in spine pathology in Alzheimer's disease.

*Aβ oligomers disrupt synaptic plasticity mechanisms and induce spine dysgenesis, likely by interfering with NMDAR-dependent regulation of the spine cytoskeleton, causing synapse loss and decreased connectivity with nearby axons (blue lines) later in life. Reprinted from (Penzes *et al.*, 2011).*

To summarise, AD is accompanied by a range of synaptic dysfunction signs, from synaptic depression and hyperexcitability to eventual synapse loss (Figure 11). Results obtained in various animal models of the disease show Aβ-mediated inhibition of synaptic currents (Hsia *et al.*, 1999; Kamenetz *et al.*, 2003; Chang *et al.*, 2006), disruption of synaptic plasticity (Walsh *et al.*, 2002; Jacobsen *et al.*, 2006), as well as endocytosis of glutamate receptors (Kamenetz *et al.*, 2003; Oddo *et al.*, 2003; Snyder *et al.*, 2005; Hsieh *et al.*, 2006; Shankar *et al.*, 2007; Nimmrich *et al.*, 2008). These findings are summarized in the synaptic failure hypothesis suggesting that “AD represents, at least initially, an attack on synapses” (Selkoe, 2002). At the same time, different dysfunctional states were observed in different experimental approaches, which makes it difficult to put these events together in one scheme and see their relationship. It is still an open question of how these low-level synaptic changes are connected to overall circuit dysfunction, which will be described in more details in the following subchapter.

### 1.3.2 Neuronal activity and circuit dysfunction

In general, it is difficult to extrapolate the pathology of synapses and neurons to the overall effects on the microcircuits and complex networks level. However, the structural changes, described in

the previous chapter, undoubtedly contribute to the brain circuit dysfunction in AD, which can be detected both in patients and AD mouse models.

Although AD is viewed as a heterogeneous, multicausal syndrome, its fMRI signature seems to be remarkably consistent, particularly during the early stages of the disease. The results from longitudinal human fMRI imaging show hyperactivation of the hippocampal region and increased medial temporal lobe activation during an associative memory paradigm. These symptoms are present even before the appearance of severe clinical AD symptoms and with time progress to a massive loss of hippocampal activity (Dickerson *et al.*, 2005; O'Brien *et al.*, 2010). Hippocampal hyperactivation and reduced deactivation of default-mode network (DMN) components during memory-encoding tasks have been also observed in cognitively normal individuals with cerebral amyloid deposits (Sperling *et al.*, 2009) (a potential trigger of AD), cognitively normal carriers of the APOE  $\epsilon$ 4 allele (Filippini *et al.*, 2009) (the major genetic risk factor for AD), presymptomatic carriers of FAD-causing mutations (Quiroz *et al.*, 2010; Sepulveda-Falla, Glatzel and Lopera, 2012) and patients with MCI (Dickerson *et al.*, 2005; Celone *et al.*, 2006; Bakker *et al.*, 2012), which often develops into AD. In later stages of AD, the hippocampal formation is hypo- active during memory encoding, whereas the reduced deactivation of the DMN persists (Celone *et al.*, 2006; Persson *et al.*, 2008; Sperling *et al.*, 2009). However, accumulating evidence suggests that this hyperactivation might be pathogenic and may impair learning and memory (Putcha *et al.*, 2011; Bakker *et al.*, 2012, 2015).

Also, evidence from human FDG-PET imaging indicates that increased glucose metabolism in brain regions with high amyloid plaque burden can precede a cognitive and metabolic decline in later disease stages (Cohen, Price, *et al.*, 2009; Johnson *et al.*, 2014; Oh *et al.*, 2014). Interestingly, FDG-PET in combination with 3D-microscopic autoradiography in an AD mouse model (the APP<sup>swe</sup>/ PS1M146L model) revealed that the glucose hypermetabolism is most pronounced in the direct vicinity of amyloid plaques (Poisnel *et al.*, 2012).

In FAD mice models researchers also found alterations of normal neuronal function and ability to adequately respond to the stimuli. Recent studies indicate that neurons of visual cortex experience functional impairments, represented by a progressive deterioration of neuronal tuning for the orientation of visual stimuli that occurs in parallel with the age-dependent increase of the amyloid- $\beta$  load (Grienberger *et al.*, 2012). In this study, deterioration was present only in neurons that are hyperactive during spontaneous activity. The impairment of visual cortical circuit function also correlates with pronounced deficits in visual-pattern discrimination. Another study revealed that sensorimotor signals in old AD mice are differentially affected (Liebscher *et al.*, 2016). Visually-

driven and motor-related signals are strongly reduced, but neuronal responses signaling a mismatch between expected and actual visual flow are selectively spared. Researchers also observed an increase in aberrant activity during quiet states. However, in this study, no correlation with plaque proximity was observed (Liebscher *et al.*, 2016). Jointly, results indicate a decline of sensory processing in the visual cortex. However, the role, played by amyloid aggregates in this process remains controversial. In both of these studies, the functional alterations came in hand with increased neuronal activity, appearing during quiet states (spontaneous activity).

In line with these observations in cortical neurons, hippocampal neuronal hyperactivity in pre-accumulating AD mouse brains was observed (Busche *et al.*, 2012) which was shown to be associated with a profound impairment of place cell function (Wilson *et al.*, 2005; Koh *et al.*, 2010; Mably *et al.*, 2017). As a specific reason, disturbed coordination of place cell firing by hippocampal rhythms in AD model mice was reported. Remarkably, these disturbances were observed at an age before detectable A $\beta$  pathology had developed (Mably *et al.*, 2017). Interestingly, fMRI imaging revealed that in humans at risk of AD (APOE4 allele carriers), hyperactivity of the hippocampus was associated with diminished grid-cell-like representations in the entorhinal cortex during a virtual reality spatial memory task (Kunz *et al.*, 2015).

Additionally, by employing large-scale calcium fluorescence imaging of the mouse cortical surface, it was revealed that the long-range coherence of slow-wave oscillations across neocortical areas was impaired in amyloid plaques-bearing APP23 and APP23 x PS45 mouse models when compared with wild-type littermates. This impairment could be restored by the normalization of the excitatory/inhibitory balance, through the application of a low dose of a benzodiazepine that enhances GABAergic inhibition. This restoration also resulted in the improvement of memory deficits of APP23 x PS45 mice (Busche *et al.*, 2015).

To summarise, there is abundant evidence that neuronal activity is disturbed under AD pathological conditions, which leads to disturbed neuronal circuit function. However, the details of these dysfunctions, as the specific role of A- $\beta$  aggregates in these dysfunctions, remain controversial and the underlying mechanism is not deciphered (Figure 12; Figure 13). To tackle this question more animal studies are being done aiming for better characterization of the neuronal activity dysfunction. An important consideration is also that according to the recent research not only A $\beta$  can influence the neuronal activity but also the other way around.

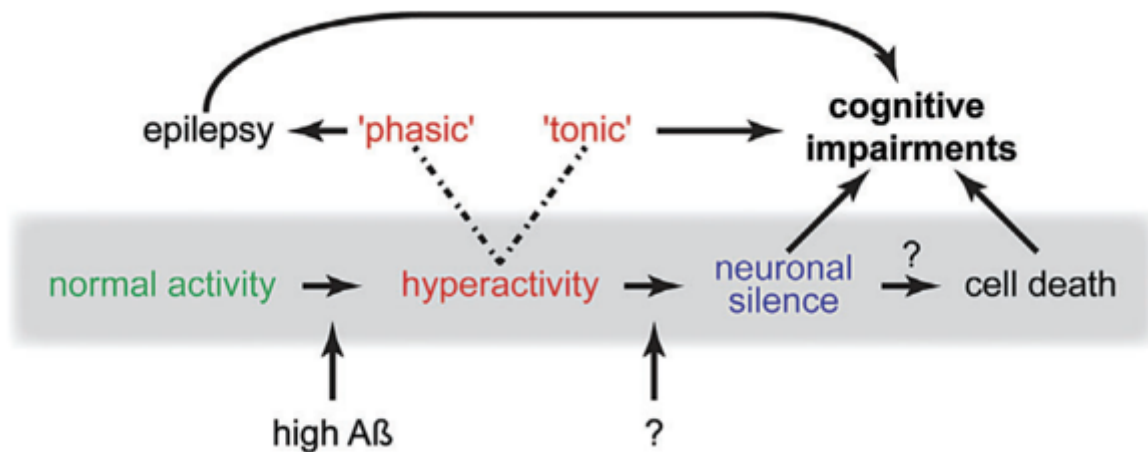


Figure 12. Proposed by Busche and Konnerth (Busche and Konnerth, 2015) model of the sequence of events that may underlie the progression of neuronal dysfunction in Alzheimer's disease.

According to this hypothesis, during early stages of AD, elevated levels of soluble amyloid- $\beta$  ( $A\beta$ ) promote the occurrence of hyperactivity. This is followed by progressive neuronal silencing and cell death through unknown mechanisms. Both tonic and phasic hyperactivity contribute to cognitive impairments seen in AD patients. Reprinted from (Busche and Konnerth, 2015).

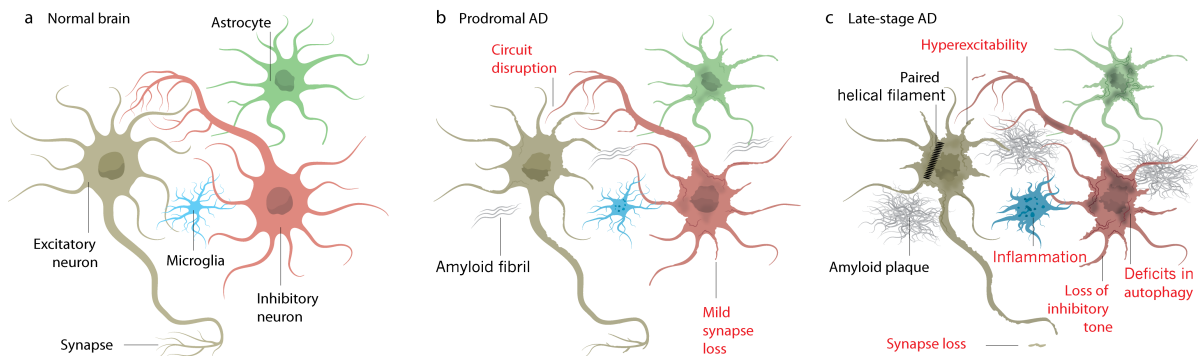


Figure 13. Neural circuits and synapses during the progression of AD – possible time course of events.

A. Subpopulations of neurons and glial cells form functional circuits through synaptic connections. B. In prodromal AD, amyloid- $\beta$  fibrils begin to form in the extracellular space, possibly contributing to early circuit dysfunction. C. In late-stage AD, amyloid- $\beta$  plaques grow and intracellular neurofibrillary tangles consisting of hyperphosphorylated tau protein form. The activation and proliferation of glial cells promote inflammation and can affect the circuit function in numerous ways. Several mechanisms affect GABAergic signaling and contribute to the loss of inhibitory tone. Despite the loss of synapses, excitatory neurons become hyperexcitable, compromising the fidelity of synaptic network connections for long-range communication. Reprinted from (Canter, Penney and Tsai, 2016).

It was observed that neural activity could regulate local concentrations of  $A\beta$  in the interstitial fluid that surrounds neurons (Cirrito *et al.*, 2005). Amyloid- $\beta$  levels are higher during wakefulness than during sleep (Kang *et al.*, 2009; Xie *et al.*, 2013). In mice, sleep promotes amyloid- $\beta$  clearance (Xie *et al.*, 2013), whereas sleep deprivation increases amyloid- $\beta$  levels and amyloid deposition (Kang *et al.*, 2009), suggesting that brain states can modulate amyloid deposition. In young FAD mice (line

Tg2576), interstitial levels of soluble amyloid- $\beta$  vary markedly in different regions and relate closely to regional differences in metabolic activity (Bero *et al.*, 2011). Higher levels of metabolic activity are associated with higher levels of soluble amyloid- $\beta$  and predict the regional amyloid burden in older mice. Thus, networks with higher metabolic rates may be more prone to amyloid deposition. Also, experimental increases in neuronal activity by chronic optogenetic activation promote amyloid deposition and trigger epileptiform activity in FAD mice (line APP-A7) (Yamamoto *et al.*, 2015).

Subsequently, the topography of neural connections was shown to direct the spread of tau, and A $\beta$  protein aggregates in mouse models of neurodegenerative disease (Pooler *et al.*, 2013; Brettschneider *et al.*, 2015). Additionally, circuit connectivity between the hippocampus and the cortex has been proposed to be a primary driver of the stepwise spread of intracellular tau aggregates between these brain regions in people with Alzheimer's (Yankner, Lu and Loerch, 2008). In a recent paper, Iaccarino and colleagues suggest that not only connectivity but also patterns of neural activity — in particular, gamma oscillations — play a part. According to their hypothesis, dysfunctional neural-network activity promotes the accumulation and spread of misfolded proteins that, in turn, cause further circuit disruption in a harmful positive feedback loop (Iaccarino *et al.*, 2016).

The possible high importance of neural activity changes to overall AD pathology is supported by the many-years notion, that there are signs of neuronal hyperactivity in AD patients and mouse models. The incidence of epileptic activity is increased in sporadic AD (Amatniek *et al.*, 2006) but is particularly high in humans with early-onset autosomal dominant AD (Snider *et al.*, 2005; Cabrejo *et al.*, 2006; Larner and Doran, 2006; Palop and Mucke, 2009). Mice overexpressing FAD-mutant genes have spontaneous epileptiform discharges (“spikes”) and/or seizures detectable by EEG recordings (Lalonde *et al.*, 2005; Palop *et al.*, 2007; Harris *et al.*, 2010; Roberson *et al.*, 2011; Vogt *et al.*, 2011; A. A. Ittner *et al.*, 2014; Born *et al.*, 2014; Bezzina *et al.*, 2015; Yamamoto *et al.*, 2015; Kam *et al.*, 2016). Furthermore, chronic video-EEG monitoring revealed that APP transgenic mice exhibited aberrant excitatory nonconvulsive seizure activity in cortex and hippocampus that was counteracted by a compensatory inhibitory response in the hippocampus, including altered levels of neuropeptide Y (NPY) receptors, ectopic NPY expression, GABAergic sprouting, and increased synaptic inhibition (Palop *et al.*, 2007; Minkeviciene *et al.*, 2009). People with AD who have seizures exhibit worse cognitive outcomes (Volicer, Smith and Volicer, 1995), and the cognition of individuals with mild cognitive impairment is restored temporarily when they are treated with the anti-epileptic drug levetiracetam to reduce abnormal activity (Bakker *et al.*, 2015). The correlation

between altered activity and cognitive performance suggests that these aberrant patterns of activity might be directly related to memory impairment. Counteracting hyperactivity in mouse models of AD not only rescues local circuit dynamics (Sanchez *et al.*, 2012) but also reestablish long-range network coherence to repair learning (Busche *et al.*, 2012).

However, until now the question of whether the hyperactivity is a consequence, or a cause of pathology remains open. On the one hand, A $\beta$  is known to disturb synaptic function which leads to neuronal activity changes. On the other hand, as described above, in AD patients and nondemented humans, amyloid deposits are predominantly distributed along with networks with aberrant neuronal activity (Buckner, 2005; Sperling *et al.*, 2009), suggesting activity-driven pathology (Bero *et al.*, 2011). It all shows, however, that network abnormalities leading to or induced by A $\beta$  accumulation may be a relatively early pathogenic event in AD (Sperling *et al.*, 2009).

The collective results from the last decade of research have led to two main hypothetical mechanisms by which neuronal pathology in AD develops. It is also likely that they jointly promote pathology. The one side of the coin is represented by the molecular and morphological changes that increase neuronal excitability and hyperactivity, the other side – by disruption of the inhibitory network, that should coordinate the normal circuit function.

Synaptic changes leading to neuronal hyperexcitability and synaptic depression are discussed in more details the previous section. Shortly, it was shown that A $\beta$  mediates hyperexcitability by disruption of synaptic plasticity and endocytosis of glutamate receptors (Palop *et al.*, 2007; Minkeviciene *et al.*, 2009; Roberson *et al.*, 2011; Sanchez *et al.*, 2012; Verret *et al.*, 2012). At the same time, A $\beta$  has an inhibitory impact on synaptic transmission by impairing long-term potentiation (Walsh *et al.*, 2002; Klyubin *et al.*, 2014) and enhancing long-term depression (Kim *et al.*, 2001; Hsieh *et al.*, 2006; Li *et al.*, 2009).

Loss of synaptic inhibition can occur through numerous pathways, including the downregulation of cell-surface voltage-gated sodium channels. Several laboratories have provided evidence for a potential contribution of reduced GABAergic inhibition, mainly via a functional impairment of inhibitory interneurons (Verret *et al.*, 2012) and a decline of GABAA currents (Limon, Reyes-Ruiz and Mileti, 2012). Reduced expression of the Nav1.1 sodium channel subunit (SCN1A) in a mouse model of AD hinders the propagation of action potentials through inhibitory parvalbumin-expressing interneurons, which results in a reduction of the primary inhibitory neurotransmitter, GABA ( $\gamma$ -aminobutyric acid), release and the loss of inhibition on excitatory neurons (Verret *et al.*, 2012) — restoring Nav1.1 levels in hAPP mice by Nav1.1-BAC expression increased inhibitory

synaptic activity and gamma oscillations and reduced hypersynchrony, memory deficits, and premature mortality (Sanchez *et al.*, 2012).

Long-term amyloid- $\beta$  accumulation, disinhibition of excitatory cells and synaptic loss add up to molecular reasons for hyperexcitability and lead to neuronal hyperactivity, which occurs in brain regions associated with learning and memory (such as the hippocampus) in some presymptomatic individuals (Vossel *et al.*, 2013). In time, this can lead to epileptiform activity. In a mouse model of AD-like amyloid- $\beta$  accumulation, such activity induces the compensatory sprouting of inhibitory axons that can impair learning processes (Palop *et al.*, 2007).

Important to note is that a disruption in the balance of excitation and inhibition may underlie both the functional impairment of local neuronal circuits as well as that of large-scale networks in the amyloid-depositing brain. Apparently, there is a mix of both hypoactivity and hyperactivity at the level of neurons, circuits and wider networks (Jorge J Palop and Mucke, 2010), even though some of the experimental results suggest that hyperactivity seen in AD mice is unrelated to increased intrinsic neuronal excitability (Busche *et al.*, 2008).

The relation between synaptic/neuronal activity and AD pathology is complex and of high interest for AD research, since it affects the homeostasis of APP, A $\beta$  and tau, and since functional alterations can be detected very early in subjects at risk for AD. Overall, the classic view that the structural damage by amyloid plaques and the loss of neurons underlies cognitive impairment in AD through a reduced cortical activity (synaptic failure hypothesis of AD) is challenged by recent findings from animal and human studies showing that, in fact, excess neuronal activity, hypersynchrony and altered brain oscillations are also key features of the disease. However, even though abundant, the data provided by different labs does not seem to come to a consensus, some pointing to the direction of hyperexcitability, others - impaired inhibitory networks. Most probably, synaptic depression and excess neuronal activity coexist in an unknown manner in AD transgenic mice as well as in humans with AD, leading to overall functional distortion of the circuits and networks.

Some researchers hypothesize that physiologic synaptic activation (without induction of epileptic seizure) might be protective for neuronal preservation, and persistence of normal cognitive functions during aging (Tampellini, 2015). In this case, the higher activity observed in preclinical or early MCI patients might be a compensatory response attempting to promote survival pathways, and preventing A $\beta$  accumulation within neurons by maintaining its degradation and physiological secretion. Indeed, one of the recent experimental findings supports this hypothesis by providing

evidence that optogenetic activation of excitatory cortical neurons restored slow oscillations by synchronizing neuronal activity, halted the accumulation of amyloid plaques and prevented calcium overload in neurons (Kastanenka *et al.*, 2017). Another recent study demonstrated that Nav1.1-overexpressing interneuron transplants enhance behavior-dependent gamma oscillatory activity, reduce network hypersynchrony, and improve cognitive functions in human amyloid precursor protein (hAPP)-transgenic mice (Martinez-Losa *et al.*, 2018), which again points out that normalization of the aberrant neuronal activity is beneficial for the AD symptoms.

While it is difficult to uncover what is the cause of the functional changes, even more, basic questions remain unanswered. It is entirely unclear what comes first, neuronal silencing or hyperactivity, and whether plaques or soluble A $\beta$  are directly involved in the initiation of neuronal dysfunction. From this point of view, studying the progress of the pathology on the early stages of the disease and the involvement of the amyloid aggregates is an important step to be done, before assessing the underlying cause of the disrupted activity.

### **1.3.3 Role of amyloid plaques in neuronal dysfunction in AD**

Senile plaques, described in detail by Alzheimer using Bielchowsky silver staining on brain sections from a patient with dementia, were determined in the early 1980s to be largely composed of the amyloid- $\beta$  peptide (Glennner and Wong, 1984; Masters and Selkoe, 2012). Neuritic, or dense-cored, plaques have a dense center of amyloid surrounded by a halo of silver positive neurites (Figure 14). After the sequencing of A $\beta$  and development of A $\beta$ -specific antibodies, it was discovered that A $\beta$  also aggregates in “diffuse” plaques of several different morphologies (Dickson and Vickers, 2001; Gomez-Isla *et al.*, 2008; Serrano-Pozo, Frosch, *et al.*, 2011). There is no conclusive link between observations of these different plaque morphologies and the cognitive symptoms (Hyman *et al.*, 2012).

Cross-sectional studies of postmortem human brain showed that senile plaque deposition occurs early in the disease progression, beginning in the neocortex and progressing slowly through the allocortex, then to the diencephalon, striatum, and basal forebrain cholinergic nuclei, followed by the development of depositions brainstem nuclei and finally in the cerebellum (Thal *et al.*, 2002). Watching plaques appear in real time in the brains of mice that overexpress AD-associated APP and PS1 mutations with *in vivo* multiphoton imaging revealed further details of plaque development. According to some of the recent studies plaques form within 24 hours, and the effects on surrounding neurites occur within days after plaque formation (Meyer-Luehmann *et al.*, 2008). This

observation is however heavily debated and more recent *in vivo* multiphoton studies show that the growth of plaques is slow and takes weeks to months (Burgold *et al.*, 2014; Peters *et al.*, 2018).

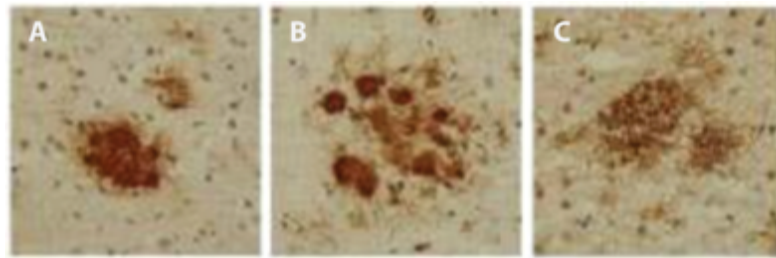


Figure 14. Types of amyloid plaques.

(A-B) Dense-core plaques and (C) diffuse plaques immunostained with anti-A $\beta$  antibody (4G8). Figure adapted from (Rak *et al.*, 2007).

It was reported that dense plaques are particularly toxic to the surrounding brain parenchyma, contributing to synapse dysfunction and loss. In many cases neurites surrounding plaques exhibit swollen, dystrophic morphologies and they often contain aggregates of phospho-tau and multiple cellular components that likely accumulate due to disrupted cellular transport (Woodhouse *et al.*, 2005; Serrano-Pozo, Frosch, *et al.*, 2011). The trajectories of axons and dendrites are usually fairly straight, in mouse models of AD are disrupted in the vicinity of amyloid plaques, and this may impact synaptic integration of signal (Le *et al.*, 2001; Urbanc *et al.*, 2002; Spiess, 2005). Moreover, gliosis and related oxidative stress were revealed around plaques, which are likely to contribute to synaptic changes (McLellan *et al.*, 2003; Ingelsson *et al.*, 2004; Serrano-Pozo, Mielke, *et al.*, 2011). However, the evidence cannot establish if there is a causative link between these plaques and surrounding pathology or if these events just go in parallel. These doubts are intensively investigated by animal AD research.

Due to the obvious neuropil disruption surrounding dense-core plaques, fibrillar A $\beta$  was long assumed to be the toxic kind of aggregates. However, results of studies obtained over the past decade strongly suggest that soluble forms of A $\beta$  which accumulate around dense plaques are more toxic than fibrils. Series of experiments by several groups over the late 1990s and 2000s revealed that soluble forms of A $\beta$  cause loss of dendritic spines in cultured neurons, while fibrils and monomers are comparatively inert (Lambert *et al.*, 1998; Klein, 2006). Further research demonstrated that oligomeric forms of A $\beta$  produced by cultured cells or extracted from human AD brain are toxic to synaptic function, including disrupting LTP in brain slices and impairing cognition when injected into healthy rodents *in vivo* (Walsh *et al.*, 2002; Cleary *et al.*, 2005; Walsh, 2005; Shankar *et al.*, 2007, 2008). There is also an association of dimers of A $\beta$  with dementia in the

human brain (Mc Donald *et al.*, 2010). *In vivo* imaging studies in plaque-bearing mice revealed a loss of dendritic spines around plaques due to altered structural plasticity (Spires, 2005; Spires-Jones *et al.*, 2009; Rozkalne, Hyman and Spires-Jones, 2011). Removing soluble A $\beta$  with topical application of antibody results in increased formation of dendritic spines *in vivo* and long-lasting increases in synaptic markers (Rozkalne *et al.*, 2009; Spires-Jones *et al.*, 2009), supporting the idea that soluble forms of A $\beta$  are toxic to synapses. These studies suggest that whereas the plaques themselves consist of inert A $\beta$  fibrils the surrounding environment of the plaque bears pathological A $\beta$  species and/or other abnormal biochemical substances (like proinflammatory proteins or enzymes, released from glia or distorted neurites), that can disrupt neuronal morphology and activity. In this case, pathology is mediated by soluble amyloid- $\beta$  and plaques are not an essential requirement.

Three papers recently addressed the relationship between amyloid plaques and either intracellular calcium concentration or spontaneous neuronal activity (Busche *et al.*, 2008, 2012; Kuchibhotla *et al.*, 2008). Busche and co-workers for the first time described aberrant neuronal activity in the immediate proximity of amyloid plaques in the cortex of APP23xPS45 mice while pre-depositing mice had no neurons with aberrant activity (Busche *et al.*, 2008). Consistent with these findings, a study using an adenoviral-based expression of the genetically encoded calcium indicator Yellow Cameleon 3.6 in combination with two-photon microscopy demonstrated that resting calcium levels in cortical dendrites of AD transgenic mice were abnormally increased in the area surrounding plaques (Kuchibhotla *et al.*, 2008). This calcium overload was associated with morphological neuritic alterations mediated, at least in part, by activation of the calcium/calmodulin-dependent phosphatase calcineurin. Furthermore, the study provided a link between structural and functional alterations, since more than half of the neurites with elevated calcium concentration were beaded, i.e., dystrophic (Kuchibhotla *et al.*, 2008). Surprisingly, there is also evidence that the changes in neuronal activity in the visual cortex are not correlated with plaque proximity (Liebscher *et al.*, 2016). Another study by Busche *et al.* revealed that in the hippocampus of APP transgenic mice increase in hyperactive neurons' fraction appears already before the formation of the plaques in contrast to cortical neurons that were normally active in pre-depositing brain in the earlier study (Busche *et al.*, 2012). This controversy is important to study in more details, since previous *in vitro* studies provided clear evidence that structural hippocampal abnormalities can occur at very early stages of the disease, long before the emergence of plaques (Hsia *et al.*, 1999; Moechars *et al.*, 1999; Mucke *et al.*, 2000). The controversial data could be explained by the different susceptibility of neurons and neuronal circuits in different brain areas or by different levels of

soluble A $\beta$  in different mouse AD models. However, experiments are to be done to favor one of these possibilities.

Some studies suggest that existence of plaques is not necessary for the activity alterations and, thus, that soluble A $\beta$ , rather than plaques themselves, may be causally related to the functional alterations of neurons and circuits. There is experimental evidence suggesting that soluble species of A $\beta$ , particularly oligomers, may be the disease-causing entity in AD (Shankar *et al.*, 2008). In the study by Busche *et al.* a single oral dose of a gamma-secretase inhibitor (GS-inhibitor), which significantly reduced the concentrations of soluble amyloid- $\beta$  (Abramowski *et al.*, 2008), was sufficient to rescue hyperactivity (Busche *et al.*, 2012). Also, local application of soluble amyloid- $\beta$  oligomers in the form of synthetic dimers mimicked hyperactivity of CA1 neurons and disrupt the slow-wave activity of the frontal and occipital cortex in wild-type mice (Busche *et al.*, 2012, 2015).

However, there is a possibility for another explanation of observed phenomena, suggesting that A $\beta$  aggregation is a consequence of altered neuronal activity, rather than a cause. This can explain both the appearance of activity alterations before plaque deposition and more obvious alterations of activity around the plaques that appear later. As also described in the previous section, in humans and mice, soluble amyloid- $\beta$  levels in the interstitial fluid of different brain regions fluctuate with the brain state and depend on the neuronal activity. Thus, the causal relationship might be exactly the opposite with increased activity being responsible for further plaque accumulation around hyperactive neurons and circuits. However, this can additionally add up to pathology and cause further circuit disruption in a harmful positive feedback loop (Iaccarino *et al.*, 2016).

To summarize, many evidences point out that the vicinity of the plaque creates the most pathological environment, that leads to neuronal activity alterations. However, it remains unclear whether these alterations appear due to the presence of the fibrillar A $\beta$ , direct effect of A $\beta$  oligomers or other factors such as proinflammatory substances released from activated microglia (Heneka *et al.*, 2012) and astrocytes (Kuchibhotla *et al.*, 2009), that surround the plaque.

To better understand the intricate relationship between neuronal activity changes and amyloid aggregate formation, more studies are needed, that will focus on longitudinal measurements of both parameters. Especially important is to move the focus from the late pronounced stages of the disease to the early and prodromal stages to catch the first pathological events. Observing the early stages of AD progression was exactly the motivation behind this PhD project, which will be presented in the further chapters.

## Objectives

Alzheimer's disease is associated with functional alterations of brain neurons, represented both as hyperactivity and hypoactivity (as reviewed in Introduction). Understanding activity alterations has important therapeutic implications since pathological changes of neuronal and network function is one of the very early events in a disease progression and it determines the level of cognitive impairment in patients. However, the nature, stability as well as the mechanisms driving these neuronal activity aberrations remain poorly understood.

This project aimed to examine spontaneous neuronal activity in the murine model of AD at the early stages of disease progression using chronic *in vivo* and by following single neurons over extended periods of time. This allowed to investigate the character and the stability of neuronal activity alterations as well relation of those changes to amyloid plaque proximity.

To achieve this, I for the first time longitudinally monitored the activity of individual neurons in layer 2/3 of the frontal cortex using calcium imaging in awake AD transgenic mice.

Specifically, the aims of this project were:

1. Examine neuronal activity of individual neurons in the frontal cortex of young AD transgenic mice over 4 weeks.
2. Analyze the stability of neuronal activity in the AD mouse model over the 4 weeks of amyloid pathology development.
3. Establish whether amyloid plaque proximity has influence on neuronal activity and its changes.

## Material and Methods

This chapter provides detailed information on the methodological aspects of the thesis. All experimental procedures complied with institutional animal welfare guidelines and were approved by the state government of Upper Bavaria, Germany (Regierung von Oberbayern).

### 3.1 Animals

The studies were carried out in accordance with an animal protocol approved by the Ludwig-Maximilians-University Munich and the government of Upper Bavaria (ref number GZ: 55.2-1-54-2532-163-13). The cranial window preparation was performed under anesthesia, and all efforts were made to minimize the suffering of the animals.

As an AD model, the double transgenic mouse line APPPS1 (Radde *et al.*, 2006) on a C57BL/6J genetic background was used. These mice coexpress mutated amyloid precursor protein (APP, Swedish double-mutation KM670/671NL) and mutated presenilin 1 (PS1, L166P) under the control of a neuron-specific Thy-1 promoter element. Cerebral amyloidosis in this mouse model starts at 6–8 weeks of age. The line is hemizygous for transgenes so as a control in all experiments the non-transgenic (wild type) littermates were used (referred to as WT), both male and female mice were used. In total, the data from 9 APPPS1 and 5 WT mice were included in the final dataset for analyses. The exclusion criteria were: deterioration of the cranial window quality or imaging artifacts (described in the Data analysis subchapter).

Mice were kept under a 14/10-hr light/dark cycle. Food and water were provided *ad libitum*. Before the cranial window implantation surgery mice were housed in groups of three to six individuals in

standard cages, with standard bedding and additional nesting material. After the surgery, mice were singly housed in standard cages.

### 3.2 Genotyping

A small section of the tail was removed from each mouse for genotyping. First, the DNA was extracted following instructions of the Invisorb® DNA Tissue HTS 96 Kit/C (Stratag molecular). The tissue was incubated in 400 µl Lysis Buffer G (inclusive Proteinase K) at 52°C under continuously shaking until lysis is completed and centrifuge at 1.700 x g (4.000 rpm) for 10 min and RT. The supernatant was carefully transferred into a 2 ml Collection Plate, and 200 µl Binding Buffer A was added to each well of the 2 ml Collection Plate and mixed it by pipetting up and down. The plate was centrifuged at 1.700 x g (4.000 rpm) for 5 min at RT. The filtrated was discarded and the plate air-dried. The pellet was re-suspended in 550 µl of Wash Buffer and centrifuged at 1.700 x g (4.000 rpm) for 5 min at RT followed by another centrifugation for at least 15 min at max. 1.700 x g (4.000 rpm). To finalize the DNA extraction, 100 µl prewarmed elution buffer (52°C) was added in each well and centrifuged for 5 min at 1.700 x g (4.000 rpm).

The extracted DNA was subjected to a polymerase chain reaction (PCR) to amplify PSEN1 gene - if present. The PCR solution consisted of: 12,5 µl OneTaq HotStart QuickLoad, 0,5 µl of each forward primer (CTA GGC CAC AGA ATT GAA AGA TCT; AAT AGA GAA CGG CAG GA), 0,5 µl of each reverse primer (GTA GGT GGA AAT TCT AGC ATC ATC C; GCC ATG AGG GCA CTA AT), 0,5 µl template DNA and 10 µl distilled water. This solution was placed in a thermocycler, and the following PCR program was used:

STEP	TEMPERATURE (°C)	TIME (SEC)	REPEAT
1	94	180	1x
2	94	30	} 27x
3	54	60	
4	68	40	
5	68	300	1x
6	4	∞	1x

The PCR samples were separated by gel electrophoresis using a 1,5% agarose containing SYBR® Gold Nucleic Acid Gel Stain in TAE buffer as the running buffer. Between 120-195 V was applied

for approximately 60-90 minutes and the gel imaged with a UV light source. A photograph was taken for documentation.

### **3.3 Cranial window**

For allow for *in vivo* two-photon imaging, a cranial window was implanted as described previously (Fuhrmann *et al.*, 2007; Holtmaat *et al.*, 2009) at the age of 3,5 months (Figure 15; Figure 16, A; B). Mice were anesthetized with an intraperitoneal injection of ketamine/xylazine mixture (14 mg/kg body weight; WDT/Bayer Health Care). Additionally, dexamethasone (6 mg/kg body weight; Sigma) was intraperitoneally administered immediately before surgery.

In the beginning, a round craniotomy of 3 mm in diameter was made above the right hemisphere frontal to bregma (coordinates of the center of the craniotomy: 1.5 mm anterior, 1.75mm lateral to bregma) using a dental drill (Schick-Technikmaster C1; Pluraden; Offenbach, Germany). Then the virus injection was performed approximately around the center of the craniotomy excluding areas of big blood vessels to prevent their damage.

The virus AAV2.1.hSyn1.mRuby2.GSG.P2A.GCaMP6s.WPRE.SV4 (Rose *et al.*, 2016; Cat.No 50942-AAV1 Penn Vector Core) was injected at 1:50 dilution of the original stock (final virus titer  $0.33 \times 10^{13}$  GC/ml). The injection was of a volume of 300  $\mu$ l and 3-5 injections at a depth of 0.8 mm were performed for each cranial window. Injection speed was set at 33 nl/min and was controlled by the NANOLITER 2010 Injector with Micro4 Controller (World Precision Instruments). Immediately, after all the injections were done, the cranial window was covered with a round coverslip (3mm, 0.16 - 0.19 mm thickness, World Precision Instruments). The coverslip was sealed using dental acrylic resin (Cyano-Veneer fast; Schein). A custom-made small metal bar was attached next to the coverslip to allow for a stable head fixation during training and awake imaging sessions. After surgery, mice received subcutaneous doses of the analgesic Carprofen (7.5 mg/kg; Pfizer) and the antibiotic Cefotaxime (5 mg/kg; Pharmore) and were daily monitored until recovery.

### **3.4 Longitudinal awake in vivo two-photon imaging**

*In vivo* two-photon imaging was performed in awake, head-fixed mice as described previously (Andermann, 2010). Mice were trained to accommodate head fixation for 14-21 days before imaging (adjusted individually to the pace of each mouse's habituation). On the first 2-3 days of the training, mice were handled to habituate to researcher and setup noise, and they were allowed to explore and habituate to the holder.

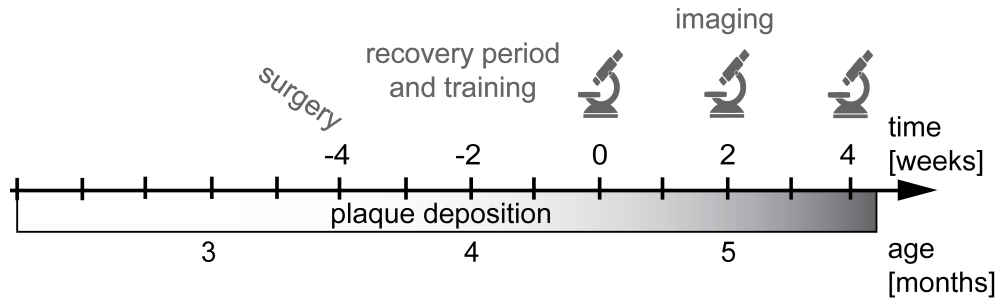


Figure 15. Time line of the *in vivo* imaging experiments.

The holder consists of a cardboard tube and metal frame (Figure 16, B, C). The metal bar connected to the mouse head can be fixed on the metal frame with the screw. Separate holding cardboard tube was assigned to each mouse.

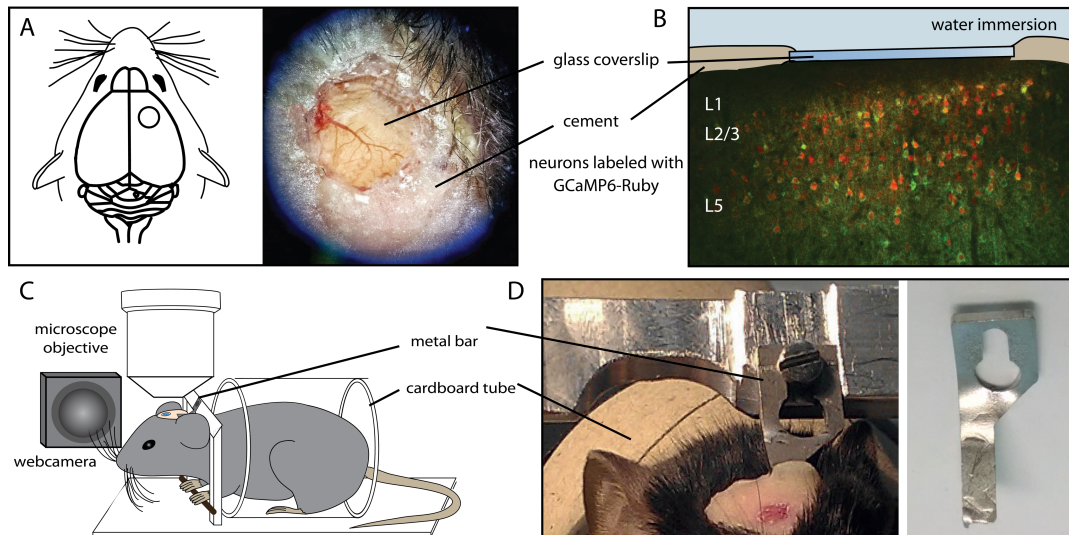


Figure 16. Preparation of experimental animals to *in vivo* two-photon imaging.

*A, B. Cranial window is implanted over mouse frontal cortex. B. Cortical neurons of layers 2/3 are labelled with expression of GCaMP6-Ruby construct. C. During the imaging session head-fixed mouse is sitting in the cardboard tube under the microscope objective. In addition to microscopic imaging whisking movements are monitored with the webcam. D. Custom-made metal bar is used to head-restrain the experimental animal during imaging sessions.*

After initial 2-3 days of training, mice were occasionally head-fixed after passing through the holding tube for a brief period (10s-30s) for the next two days. In the following days, periods of head fixation were gradually increased up to 1 hour at the end of the training. Care was taken that the mice feel comfortable in the holding tube and individual adjustments of the tube height and width were made for each mouse if necessary.

Weekly imaging sessions started at earliest four weeks after surgery to allow mice to recover and cranial windows to become transparent and not earlier than the mouse successfully underwent required training. If the mouse was not getting habituated to the setup and showed signs of distress during fixation after the training period, this animal was removed from the experimental group.

Around 5-15 hours before imaging, Methoxy-XO4 (Xcessbio, San Diego, CA, USA, 3.3% vol. of 10 mg/ml stock solution in DMSO (light-shielded), 6.66% vol. Cremophore EL (Sigma Aldrich) in 90% vol. PBS), a dye that readily crosses the blood-brain-barrier and binds to fibrillary A $\beta$ , was intraperitoneally injected to stain amyloid plaques (Klunk *et al.*, 2002).

Before each imaging session, mice were head-fixed and placed under the microscope for 5 min to habituate. Imaging was performed in the dark without any stimuli. In each mouse, two to six regions of the frontal cortex were imaged. The imaging regions were selected at a depth of 120 – 200  $\mu\text{m}$  below the pial surface (referring to the cortex layer 2/3). *In vivo*, time-lapse image series of GCaMP6 and mRuby2 fluorescence were acquired using the LaVision Trim Scope microscope equipped with two tunable Ti:sapphire two-photon lasers (Coherent Chameleon and Mai Tai Spectra Physics). The setup was controlled using LaVision Inspector software (LaVision Biotech, Germany). The imaging frequency was set up to the frame rate of 10 Hz

To enable simultaneous excitation of mRuby2 and GCaMP6s the Chameleon laser was tuned to 940nm. As an objective, A 25x, NA 1.05 water-immersion objective (Olympus) was used. There were two cohorts of experiments included in the data analysis. For the first cohort the imaging dimensions were  $173 \times 173$  pixels; corresponding to  $151 \mu\text{m} \times 151 \mu\text{m}$ , for the second cohort –  $223 \times 223$  pixels and  $220 \mu\text{m} \times 220 \mu\text{m}$ . At each of the weekly session, the same cells for each area of interest were imaged over 5000 frames (8.3 min of continuous imaging time).

To the analysis of the distances between the neurons and the amyloid plaques, z-stacks images of the surrounding tissue around the area with imaged neurons were acquired, with each z-stack covering 250-350  $\mu\text{m}$  in depth ( $520 \times 520$  pixels; x,y dimensions: 350  $\mu\text{m}$ , z increments 0.5 $\mu\text{m}$ ). The simultaneous excitation of Methoxy-XO4 and mRuby2 was achieved by the Mai Tai laser tuned to 750 nm. During the z-stack acquisition, mice were anesthetized by isoflurane (0.5 vol. %), this was done after the awake imaging session.

Emitted fluorescence light was split at 495 nm and 560nm, to separate the emitted light into three channels corresponding to the fluorescence from Methoxy-XO4, GCaMP6s, and mRuby2 and detected by photomultiplier tubes.

At all times laser power was kept under 80mW measured at the back-focal plane of the objective.

During head-fixation, mice typically showed long episodes of quiet wakefulness (quiet) interrupted by brief episodes of intensive whisking and movement (active). Therefore, we used the whisking movement monitored with the webcam as an indicator of behavioral state (quiet vs. active). A web camera was controlled by LaVison Inspector software which allowed synchronous recordings with the same frame rate for mouse whisking behavior (via web camera) and GCaMP6 and mRuby2 fluorescence (via microscope). Active epochs were not considered in the further analysis of neuronal activity.

Mice were imaged in repetitive weekly sessions for 3-10 weeks after the first imaging session. Only data sets from mice with more than five weeks of imaging span in total were further analyzed. Single imaging session would typically last around 60-80 min. In such period images from 2-6 areas of interest were acquired (~9 min per area, 50-150 cells per area) and in case of transgenic animals 2-6 z-stacks representing each of the imaged areas were additionally taken (~5 min per area).

### **3.5 Tissue preparation, immunohistochemistry, and confocal microscopy**

#### **3.5.1 Transcardial perfusion of mice**

After the final *in vivo* imaging session mice were sacrificed and perfused allowing for *post mortem* analysis of brain tissues.

For the transcardial perfusion mice were first lethally anesthetized with ketamine/xylazine mixture (14 mg/Kg body weight; WDT/Bayer Health Care), and fixed with the needles to Styrofoam plate. With the large medical scissors, two incisions were made parallel to the lower edge of the rib cage. Next, the abdominal wall was opened and incisions parallel to the rib cage to the vertebral column were performed. The diaphragm was cut open just below the xiphoid cartilage and then dissected off along its costal insertions. The right and left ribs were cut off the vertebral column, as close as possible to their insertions. Two cuts converged above the heart level to the *manubrium sterni*. The hypodermic needle attached to the perfusion pump tubing was later inserted into the left ventricle. The left ventricle comprises the cardiac apex and can be recognized by its lighter color (compared with the dark red of the right ventricle). Next, the right atrium was opened with spring scissors, and the perfusion pump was started (Ismatec, ISM796B). The animal was perfused with 1x PBS at ~5 mL/min for approximately 1 min (until the liver turned from dark red to clay-like brown). Then the pump was turned off, the tubing end was put in the tube with 4% PFA, and the perfusion was restarted with the same speed as above until the mouse was perfused with ~25 mL of 4% PFA. Then the brain was removed from the skull and postfixed in 4% PFA for 48h. After the post-

fixation period of 48h, the brain was rinsed with 1x PBS and stored in 0.01%  $\text{NaN}_3$  (#13412, Riedel de Häen) in 1x PBS.

### **3.5.2 Immunohistochemical identification of inhibitory neurons**

They PFA fixed brains were cut on the vibratome (Leica VT 1000S) into coronal sections of 50  $\mu\text{m}$  thickness. Immunohistochemistry was performed on free-floating sections.

Firstly, sections were incubated overnight in 2% Triton X-100 in PBS at room temperature to increase permeabilization. Secondly, they were blocked for 2 hours at room temperature with 3% I-Block™ Protein-Based Blocking Reagent (Thermo Fisher Scientific) containing 0,2% Triton X-100 in PBS. Then sections were incubated with the primary antibodies (mouse anti-GAD67 in 1:500 dilution (Millipore, catalogue number MAB5406B)) overnight. The following incubation with secondary antibodies (goat anti-mouse Alexa Fluor 647 1:500, Life Technologies, catalogue number A21236) lasted for two days at room temperature.

Next, confocal stacks (Zeiss LSM 780) were acquired. In the beginning, images were acquired at low magnification (10x objective) to allow for the identification of virus-transfected regions. Confocal stacks of re-identified transfected spots were then acquired with a 40x magnification.

Analysis of images was performed using ZEN software (Zeiss). For this, raw z-stacks were manually scrolled through and mRuby2- and GAD67-positive neurons were marked in respective frames.

### **3.6 Imaging data processing and analysis**

Collected two-photon images of GCaMP6 and mRuby2 combined with web camera images were processed and analyzed with the use of custom written codes in MATLAB (The MathWorks, Inc.) and semi-automatically in ImageJ (<http://rsb.info.nih.gov/ij/>). Standard recording consisted of three series of images. The first series of images, recorded by two-photon microscope on the red channel, represented cell bodies labeled with mRuby2 (calcium insensitive). The second series of images coming from the green channel was a representation of calcium concentration changes reported by changes in fluorescence of GCaMP6s in neuronal cytoplasm. The third series of images were recorded by the camera focused on the mouse whiskers and represented the behavioral time-series.

For the analysis, two-photon imaging series were aligned, then ROI was drawn around the neuronal cell bodies using MATLAB and at the next step corresponding traces of neuronal activity were

extracted and analyzed. Behavioral data of whiskers movement was used to identify quiet (no whisking) and active (movements of whiskers) phases.

### **3.6.1 Calcium imaging data pre-processing**

Image pre-processing for calcium imaging data was done using a custom-made script written by Dr. Pieter M. Goltstein (Goltstein, Montijn and Pennartz, 2015). Brief description of the image pre-processing is below.

A number of previous studies have shown that there is a strong correlation between  $\Delta F/F$ , relative fluorescence change over baseline, responses in somatic calcium recording (using OGB as fluorescent calcium indicator) and individual neurons spiking activity (Kerr, Greenberg and Helmchen, 2005; Ohki *et al.*, 2005; Greenberg, Houweling and Kerr, 2008). Thus, analysis of the  $\Delta F/F$  time series proved to reproduce several previously reported electrophysiological findings, which supports the validity of the calcium imaging approach that was used in this study.

Collected by the microscope and web camera images were processed and analyzed using custom-written codes in MATLAB and semi-automatically in ImageJ software. A typical neuronal recording consisted of two series of images recorded using two-photon microscopy. One series contained fluorescence in neuronal cell bodies labeled with mRuby2 (calcium-insensitive, red channel,  $>560\text{nm}$ ). The other series contained fluorescence of the cytoplasmic calcium indicator GCaMP6s (green channel,  $495\text{-}560\text{nm}$ ). The behavioral state was recorded by a camera focused at the whiskers and classified as active or quiet using custom-written MATLAB code.

Small movement artifacts in the x-y plane were corrected for by realigning the images (Guizar-Sicairos, Thurman and Fienup, 2008). Recordings with clear movement artifacts along the z-axis observed during manual check were excluded from further analysis. Then, regions of interest (ROIs) were outlined semi-automatically with the help of custom-made GUI based on a maximum projection of all frames for all neurons for each repetition block separately. Indicator-filled cells were identified visually as bright cells in the green (GCaMP6 fluorescent) channel that did not have nucleus visible during the neuronal activity calm phase. These indicator-filled neurons were excluded from the analysis.

### **3.6.2 Analysis of spontaneous calcium activity**

Further analysis was performed using custom-written MATLAB code kindly provided by Dr. Sabine Liebscher. As a first step individual images from each of the time series were aligned to each other in the x-y plane. Image alignment parameters (x/y shift) were estimated using a Fourier transform-based approach (Guizar-Sicairos, Thurman and Fienup, 2008) on image data from the

mRuby2 channel (Rose *et al.*, 2016) that represents stable fluorescent within cell bodies. Next, the same imaging alignment parameters were applied to the GCaMP6 recording and for each ROI a raw GCaMP6s fluorescence time series was constructed. For this, the pixel values were averaged within the region of interest for each imaging frame.

As the following step, a region surrounding the selected ROI was considered, and the average fluorescent intensity within that area was calculated for each frame to allow for the correction of possible neuropil contamination (Chen *et al.*, 2013). The corrected ROI signal was computed based on the equation (Chen *et al.*, 2013; Liebscher *et al.*, 2016):

$$F_{\text{ROI\_comp}} = F_{\text{ROI}} + 0.7 \times (\text{median}(F_{\text{neuropil}}) - F_{\text{neuropil}}),$$

$F_{\text{ROI\_comp}}$  is the actual signal within the selected ROI after compensating for neuropil contamination, while  $F_{\text{ROI}}$  reflects the signal within the initially selected ROI;

$F_{\text{neuropil}}$  represents the signal within the surrounding neuropil.

Traces representing neuronal activity were then low pass filtered at 5Hz. Slow fluctuations were removed by subtracting the 8th percentile within a window of  $\pm 15$  seconds (Dombeck *et al.*, 2007). For the estimation of  $F_0$  the 8th percentile was subtracted in a window of  $\pm 15$  seconds and the median of all values below the 60th percentile of this ‘noise band’ was then used as  $F_0$ . This approach allowed for detection of  $F_0$  for both highly active and silent cells.

In the end, traces were smoothed over five frames, and then transients were identified. To be considered individual transients peaks in the traces had to have a minimum distance of 15 frames (1.5 seconds) and a minimum height of 3x standard deviation of the noise band. The classification into activity groups was based on the frequency of transients according to earlier described groups (Busche *et al.*, 2008): silent and hypoactive neurons  $< 0.25$  transients/min; normoactive neurons 0.25 - 4 transients/min; hyperactive  $> 4$  transients/min.

### 3.6.3 Plaque distance analysis

Plaque distance analysis was carried out in MATLAB (MathWorks) using custom-written routines, kindly provided by Dr. Sabine Liebscher (Figure 17).

The position and size of the ROIs were projected into the 3D rendered overview stack semi-manually. The two channels carrying either the Ruby2 or the Methoxy-XO4 signal were background-subtracted. Subsequently, the GCaMP6m (green) channel was subtracted from the Methoxy-XO4 (blue) channel to remove slight bleed-through. Then, each frame of the Methoxy XO4 channel was median-filtered and binarized with the threshold being the background

fluorescence level plus 3x standard deviation. Distance between the neurons and the plaques was measured as the 3D Euclidean distance between the centroid of the respective neuronal ROI and the nearest Methoxy-XO4 positive voxel.

In parallel, all overview stacks were visually checked, and 3D rendered stacks were inspected for accurate neuron and plaque detection and assignment. This helped to rule out accidental measuring of the distances between neurons and voxels carrying signal from the dura. The distances from those incorrect assignments of plaque voxels were exchanged for the manually measured distances. Manual measurement was done with manual measurement tool in ImageJ (<http://rsb.info.nih.gov/ij/>), the distance between the centroid of the respective ROI and the nearest was measured Methoxy-positive voxel taking into account Pythagorean theorem in case the nearest plaque was not in the same plane as the ROI.

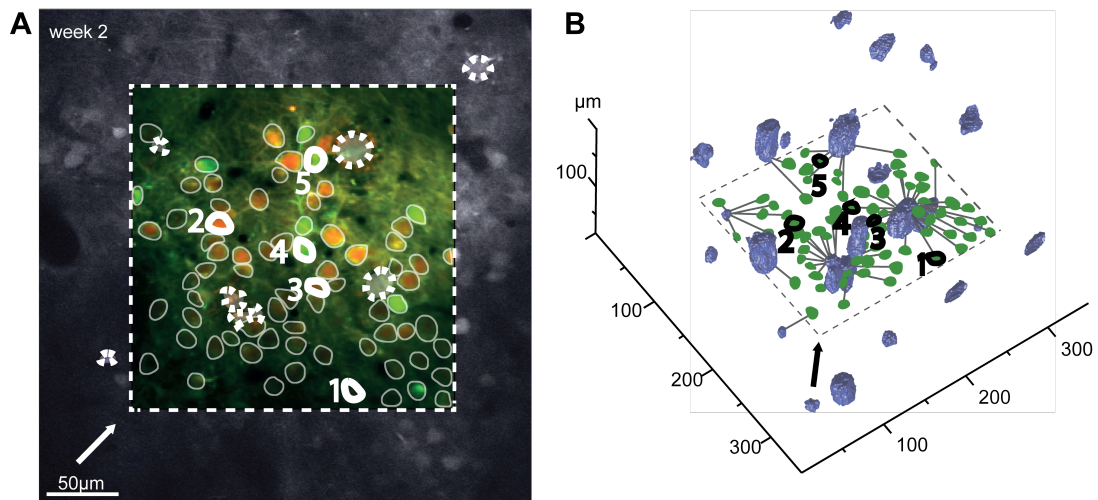


Figure 17. Measurements of plaque to neuron distances in 3D space.

*A. Representative in vivo two-photon image, showing the location of a  $Ca^{2+}$  imaging field of view (dashed rectangle) within the single plane of a  $z$ -stack (GCaMP6s green, mRuby2 red). Selected regions of interest (ROIs) and amyloid plaques are marked by solid and dashed lines, respectively. Example ROIs marked by numbers 1-5 correspond to neurons 1-5 in (B). The arrow indicates the viewing angle in (B).*

*B. 3D reconstruction of the  $z$ -stack of the imaged area shown in (A) with the location and distances between amyloid plaques (blue) and the selected ROIs (green). ROIs numbers correspond to the ones in (A). Lines connecting the ROIs and the plaques represent the shortest distance from a given neuron to its nearest plaque border.*

### 3.7 Statistics

Neuronal activity and fractions of different activity categories and their changes over time were compared using a two-way repeated measure ANOVA. Distributions of activity changes were

compared using a Kolmogorov-Smirnov (KS) test. P-values are reported as follows: \*P < 0.05, \*\*P < 0.01 and \*\*\*P < 0.001.

## 3

## Results

In order to characterize the activity of neurons in the frontal cortex of AD model mice, I performed longitudinally *in vivo* two-photon imaging in APPPS1 transgenic mice and their non-transgenic littermates at the age of 4-5 months. The establishment of the method and the results of the measurements are described in this chapter.

### 4.1 Method establishment

To investigate the neuronal activity of the neurons in the frontal cortex of the AD transgenic mice I used *in vivo* two-photon microscopy in awake animals. The technique was implemented in the chronic approach, allowing for repetitive measurements of the same set of neurons.

One of the major challenges of this thesis was that the method was not fully established in the lab at the beginning of the project. Therefore, together with Dr. Marinkovic, I invested significant time in the initial phase of the project to establish the methodology and adjust it to AD transgenic line. As first steps, we adjusted virus injection titre to avoid toxic effects, and further setup the imaging parameters to follow cells and plaques (found suitable laser power to avoid cell damage and bleaching). Next crucial step in the establishment of this method was working out the parameters for awake imaging, including habituation and suitable holder. Successful habituation helps provides stability of the visual plane which is necessary for the good quality recordings.

According to the literature reports at the beginning of the project habituation and training time was planned to be one week with daily trials. However, the APPPS1 mice proved to be more difficult to train compared to the other mouse lines used in our laboratory. After one-week training, the APPPS1 mice were still not ready and kept moving under the microscope, which

created too many artifacts in the imaging data. The imaging data for these mice thus had to be excluded. To solve the problem of artifacts in the following experiments, two solutions were implemented. The first one was a longer training period (up to three weeks), the second one – improved holder with a longer head-attached bar that provided stronger hold for the head-fixation.

The final settings for training were two- to three-week training with a very slow increase in the time of head-fixation. These settings proved to be appropriate for this mouse line and helped to reduce the amount of excluded trials in the following experiments.



*Figure 18. Improvement of the head-fixation bar.*

*Improved holder (on the right) has a longer head-attached bar that provides stronger hold for the head-fixation.*

Overall, in the final dataset, only the mice that had three imaging time points with the total span of 4 weeks were included. This represents 9 APPPS1 mice and 5 control non-transgenic littermates. In the following sections, the imaging time points will be referred to as time points 1, 2 and 3 (tp1, tp2, tp3) or weeks 0, 2, 4.

The microscopic imaging was accompanied by the imaging of the whiskers with the web camera to distinguish active awake and quiet awake behavioral states. The reasoning behind this discrimination was the hypothesis that different behavioral states could create different brain dynamics and thus drive neuronal activity in different directions. Additionally, monitoring the mouse with the web camera during the imaging session allowed me to make sure it does not fall asleep and does not express signs of distress.

The active states were defined as the periods, in which the mouse moves the whiskers. These periods lasted for 1-10 sec each and comprised 5-30% of the whole imaging session time. The rest of the imaging time, when the mouse did not actively move was defined as quiet time.

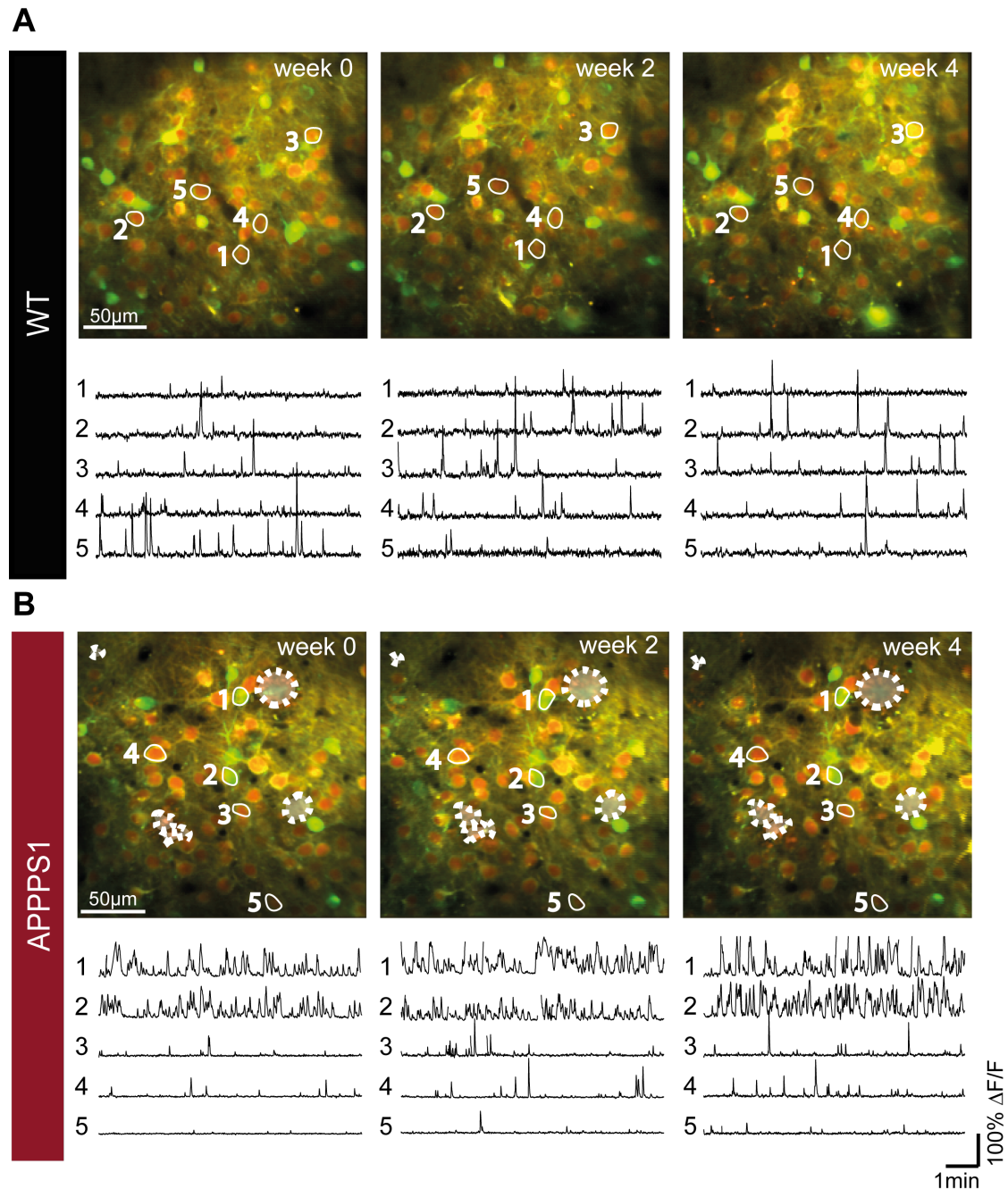


Figure 19. Exemplary traces of neuronal activity of individual neurons recorded with *in vivo* two-photon imaging.

A, B. Representative average projections of a recorded field of view (FOV) in the frontal cortex of both a WT (upper panel) and an APPPS1 (lower panel) mouse (*mRuby2* expression shown in red, *GCaMP6s* in green). Example traces of neurons labeled within the projections are shown below. Dashed lines denote the location of amyloid plaques.

However, contrary to my hypothesis I could not find any difference in neuronal activity in my areas of interest in active and quiet states. Neither there was any correlation between average neuronal activity and fraction of whisking time in the total imaging time (Figure 20, A; week 0: WT –  $p=0.72556$   $R=-0.13683$ , APPPS1 –  $p=0.63586$   $R=0.091778$ ; week 2: WT –  $p=0.077792$

$R=0.5816$ , APPPS1 –  $p=0.70965$   $R=0.072226$ ; week 4: WT –  $p=0.30385$   $R=-0.34161$ , APPPS1 –  $p=0.35949$   $R=-0.17658$ ), nor excluding the active state could change the overall activity distribution (Figure 20, B, C). Since during active state frequent imaging artifacts occur, for the further analysis only the data from the quiet state was included.

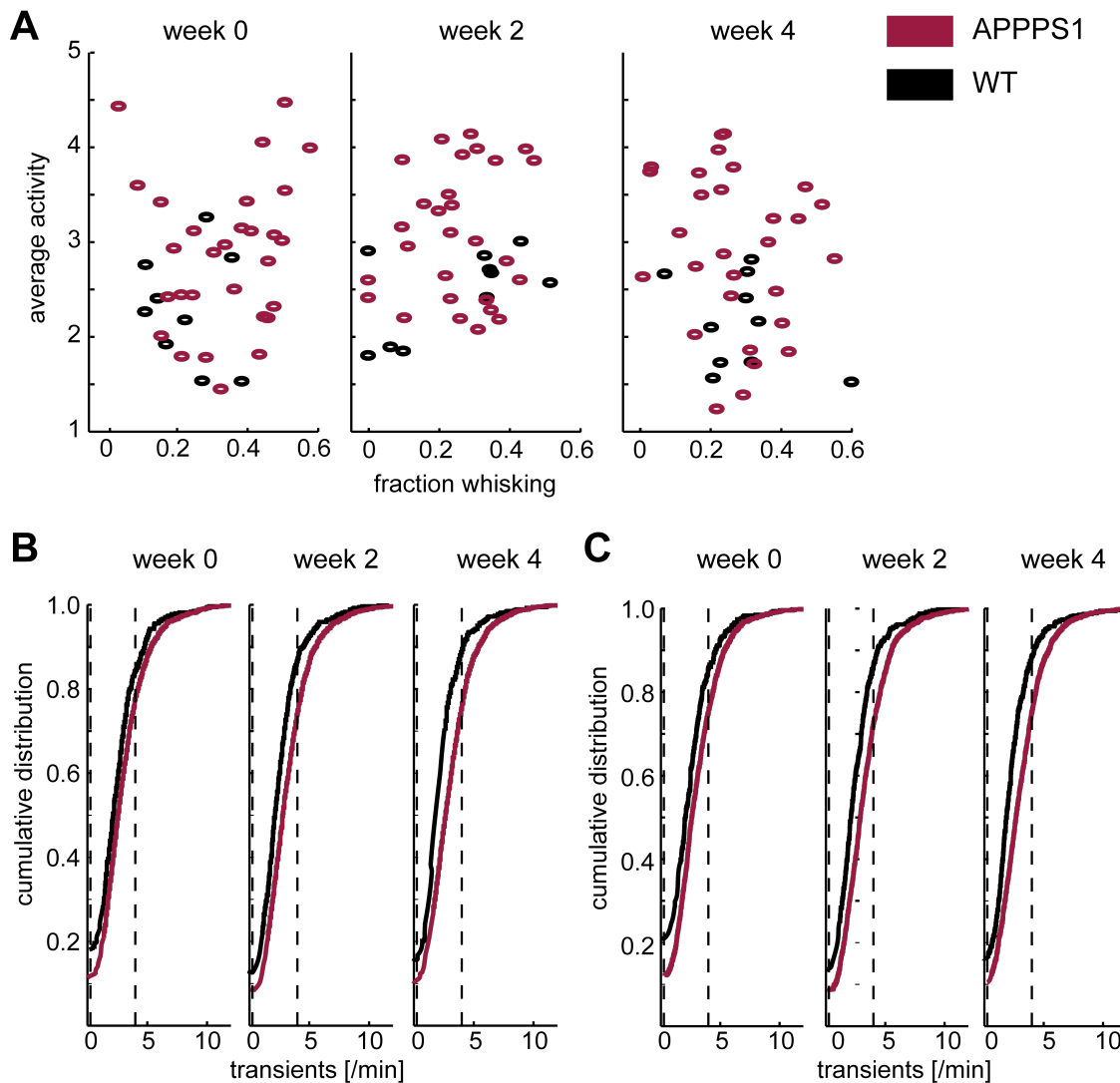


Figure 20. Active periods distinguished by the whiskers movements are not influencing activity of neurons in the recorded areas.

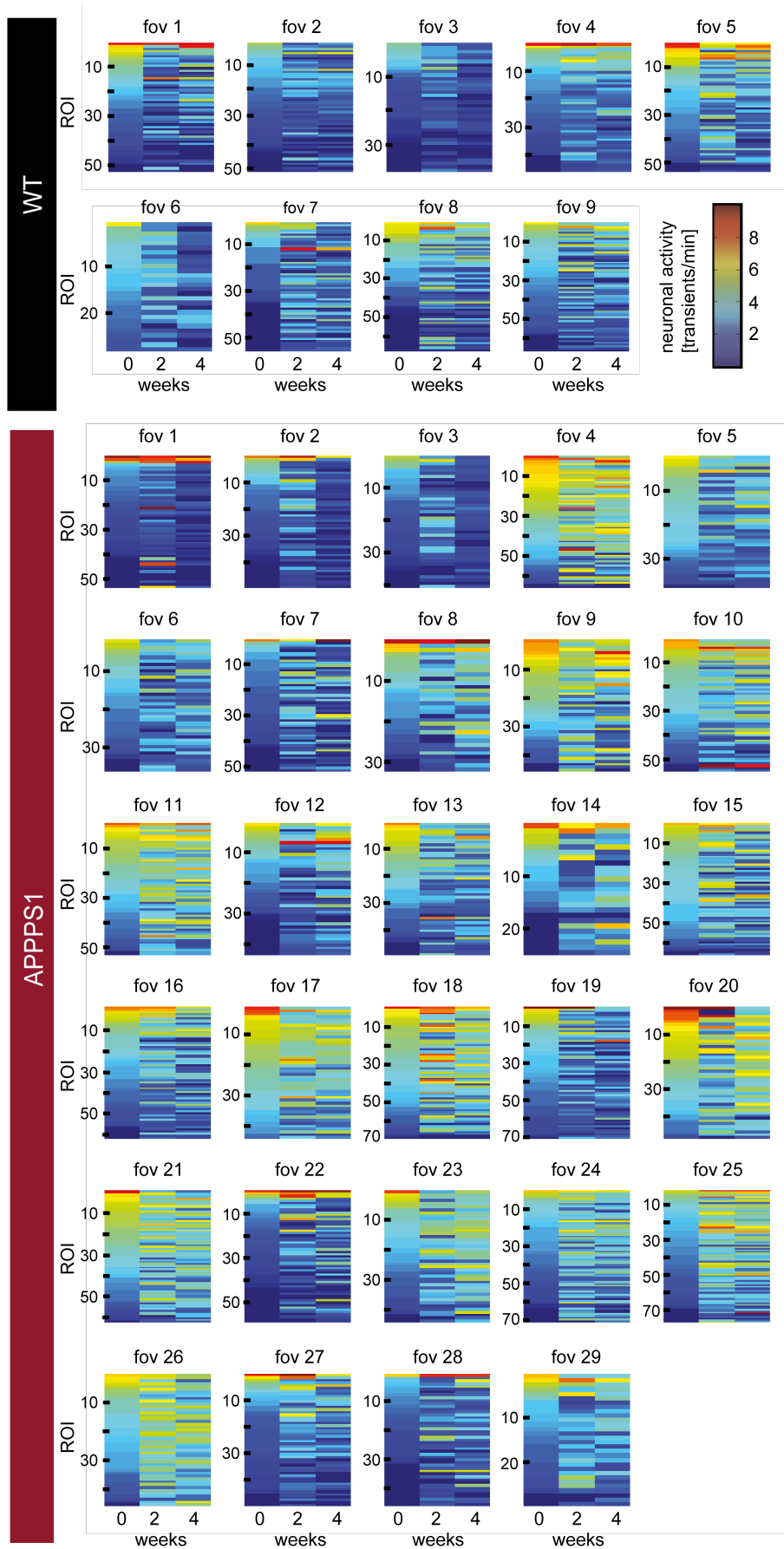
A. There is no correlation between average neuronal activity and fraction of whisking time in the total imaging time.

B. Cumulative distribution of neuronal activity if the whole imaging period is included.

C. Cumulative distribution of neuronal activity if whisking periods are excluded.

In total in the neuronal activity analysis 14 mice were included, 9 transgenic mice of APPPS1 line and 5 of their non-transgenic littermates as a control (WT), with 38 individual experiments (fovs)

and 2253 neurons (APPS1: 29 fofs, 1691 neurons; WT: 9 fofs, 562 neurons) analysed (Figure 21).



---

Figure 21. Color-coded neuronal activity of individual neurons (ROI) over time in each of the individual experiments (fov - field of view).

## 4.2 Identity of the imaged neurons

Neocortex consists of two major populations of neurons, that have very different influence on the overall neuronal circuit dynamics - excitatory and inhibitory neurons. It is thus important to distinguish these two populations when looking at the neuronal activity. It was earlier reported that high titer of AAV2/1 efficiently transduces both cortical excitatory and inhibitory neuronal populations, but the use of lower virus titers leads a strong preference for transduction of cortical inhibitory neurons and layer 5 pyramidal neurons (Nathanson *et al.*, 2009). However, other studies reported equal expression of the virus construct carried by AAV2 (Aschauer, Kreuz and Rumpel, 2013). Thus, it was important for me to determine which neurons are expressing the viral construct in my experimental settings and which neurons – excitatory or inhibitory – were preferentially imaged.

To probe the identity of neurons that were imaged *in vivo*, post-hoc immunochemical stainings against GAD67, inhibitory neurons marker, were performed on the brain slices from the imaged area of frontal cortex. Fluorescence of the Ruby protein was used as a marker of virus-transfected cells, as the respective gene was carried by our virus construct and thus is only expressed in the transfected neurons.

After the staining, the number of GAD67-positive, Ruby-positive and GAD67-Ruby double-positive neurons in the layer 2/3 of the cortex were calculated. In total, 760 Ruby-positive neurons were included in the analysis (n=3 mice). Out of these neurons, expressing Ruby and GCaMP6 in layer 2/3, only 3,57% (SD 1,14) were stained against GAD67. This means that most of the imaged neurons (>95%) are excitatory neurons and the contribution of the inhibitory neurons impact on the resulting neuronal activity can be neglected (Figure 22).

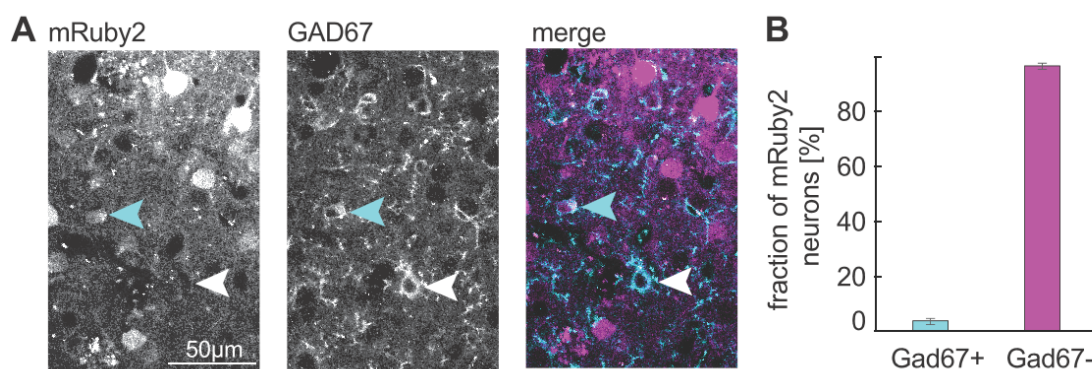


Figure 22. Immunostaining of Ruby-expressing neurons against GAD67 to identify inhibitory neurons.

A. Immunohistochemical analysis of GCaMP6s-mRuby2-expressing neurons. Left, middle and right panels represent confocal images of mRuby2, Gad67 immunohistochemical staining and merged image, respectively. The white arrowhead marks a Gad67 positive neuron, cyan arrowhead points to a mRuby2 positive, Gad67 positive neuron.

B. Quantification of the relative proportion of Gad67 positive, mRuby2-expressing neurons. 3.57% of the mRuby2 expressing neurons (which co-express GCaMP6s) were positive for Gad67 (760 mRuby2-positive neurons, three mice, data are mean  $\pm$  SD).

### 4.3 Frontal cortex neurons in the AD transgenic mice have increased activity

For the assessment of the activity of cortical neurons in APPPS1, we analysed the spontaneous ongoing cortical activity, which is known to be an important determinant of information processing in the brain (Arieli *et al.*, 1996; Anderson *et al.*, 2000; Ferezou, Bolea and Petersen, 2006; Marshall *et al.*, 2006; Ji and Wilson, 2007). Importantly, mice were awake so that no artifacts of anesthesia would hinder the activity. I simultaneously monitored spontaneously occurring somatic  $\text{Ca}^{2+}$  transients in many individual cells. Such  $\text{Ca}^{2+}$  transients directly reflect the firing of action potentials in neurons (Kerr, Greenberg and Helmchen, 2005; Sato *et al.*, 2007). The calcium imaging data was then processed and analyzed with the help of the custom-written MATLAB scripts, kindly provided by Dr. Gotlstein (pre-processing) and Dr. Liebscher (frequency analysis) (for a detailed description see Material and Methods).

APPPS1 mice demonstrated the higher average activity of cortical neurons at all three time points compared to the control. However, there was no significant difference of average activity between the three time points in each of the groups (Figure 23, A). Average neuronal activity of layer 2/3 neurons in the frontal cortex of WT and APPPS1 mice was measured as transients per minute and as the area under the curve per minute. The frequency of transients (effect of group:  $F_{1,72} = 6.07$ ,  $p = 0.02$ ; effect of time:  $F_{2,72} = 2.23$ ,  $p = 0.12$ ; group-by-time interaction effect:  $F_{2,72} = 0.91$ ,  $p = 0.41$ ) increased in APPPS1 mice throughout the experimental period and the same is

true for the area under the curve (effect of group:  $F_{1,72} = 4.58, p = 0.04$ ; effect of time:  $F_{2,72} = 9.72, p = 0.0002$ ; group-by-time interaction effect:  $F_{2,72} = 1.67, p = 0.2$ ) are. These results are in agreement with the previous publications, reporting increased activity of the neurons in AD mice (Busche *et al.*, 2008, 2012, 2015; Keskin *et al.*, 2017).

Previous publications reported that AD mice exhibit increased number of hyperactive neurons (Busche *et al.*, 2008). This finding was based on the division of all the neurons into three groups, according to their activity. So, we next also classified all the imaged neurons into three categories (the same classification as in Busche *et al.*, 2008): silent and hypoactive neurons – less than 0,25 transients per minute, normally active neurons – 0,25-4 transients per minute and hyperactive neurons – more than 4 transients per minute. Both APPPS1 transgenic mice and their non-transgenic littermates had all three types of neurons, but in the transgenic mice the pattern of activity was distinctly different from that in the non-transgenic control animals (Figure 23, B). APPPS1 mice have a significantly higher fraction of hyperactive neurons (week 0: WT 16 +/- 3%, APPPS1 27 +/- 3%, week 2: WT 14 +/- 3%, APPPS1 28 +/- 3%, week 4: WT 11 +/- 2%, APPPS1 28 +/- 3%, data are mean +/- SEM, plotted is only the mean; effect of group:  $F_{1,72} = 7.55, p = 0.009$ , effect of time:  $F_{2,72} = 0.15, p = 0.86$ , group-by-time interaction effect:  $F_{2,72} = 0.84, p = 0.43$ ). The fraction of normoactive neurons is higher in WT mice (week 0: WT 67 +/- 4%, APPPS1 61 +/- 2%, week 2: WT 76 +/- 3%, APPPS1 65 +/- 2%, week 4: WT 74 +/- 3%, APPPS1 63 +/- 2%, effect of group:  $F_{1,72} = 6.08, p = 0.019$ , effect of time:  $F_{2,72} = 3.35, p = 0.041$ , group-by-time interaction effect:  $F_{2,72} = 0.88, p = 0.42$ ). The fraction of silent and hypoactive neurons does not differ between genotypes (week 0: WT 17 +/- 4%, APPPS1 11 +/- 2%, week 2: WT 10 +/- 2%, APPPS1 7 +/- 1%, week 4: WT 14 +/- 3%, APPPS1 8 +/- 2%, effect of group:  $F_{1,72} = 3.71, p = 0.062$ , effect of time:  $F_{2,72} = 5.06, p = 0.009$ , group-by-time interaction effect:  $F_{2,72} = 0.45, p = 0.64$ , WT n = 9, APPPS1 n = 29 experiments, two-way repeated measures ANOVA).

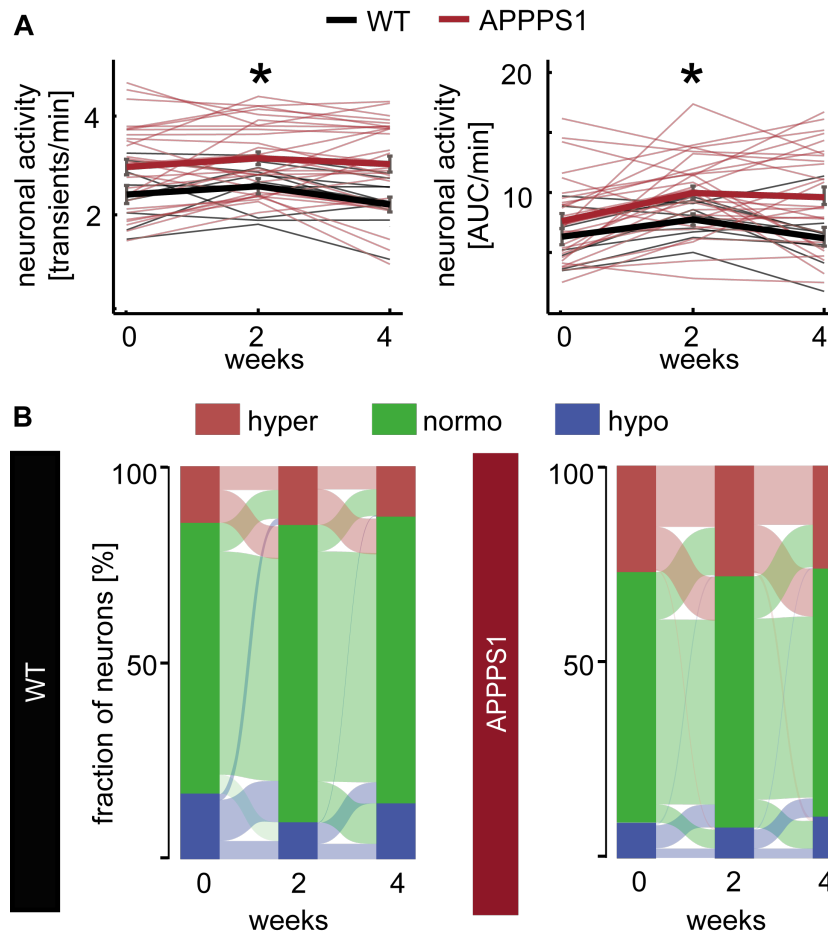


Figure 23. Three neuronal activity types in transgenic and non-transgenic mice.

**A.** Average neuronal activity of layer 2/3 neurons in the frontal cortex of WT and APPPS1 mice, measured as transients per minute (left) and as the area under the curve per minute (right). Thin lines represent the averages of individual FOVs (same set of neurons imaged over three consecutive time points), thick lines represent the mean  $\pm$  SEM for each time point.

**B.** Alluvial plots representing the relative proportion as well as the fractional change of hyperactive ( $>4$  transients/min), normoactive (0.25-4 transients/min) and silent ( $<0.25$  transients/min) neurons in WT (left) and APPPS1 (right) mice.

#### 4.4 Aberrant activity of neurons in the AD mouse model represents a stable pattern

Comparing the activity of neurons over time, we have noticed that while the activity of individual neurons can change between three analyzed time point, the composition of different activities stayed stable (Figure 24). Specifically, similarity index of neuronal activity (Figure 24, A) did not differ between WT and APPPS1 both for week 0-2 and week 0-4 (effect of group:  $F_{1,72} = 0.27$ ,  $p = 0.6$ ; effect of time:  $F_{2,72} = 195.5$ ,  $p < 10^{-9}$ ; group-by-time interaction effect:  $F_{2,72} = 0.27$ ,  $p = 0.8$ ). Moreover, the distribution of activity changes (Figure 24, B) does not differ between week 0 and 2 and slightly increases in APPPS1 mice from week 0 – 4 (week 0 – 2:  $p = 0.08$ , week 0 – 4:  $p = 0.03$ , KS test, WT  $n = 562$  neurons, APPPS1  $n = 1691$  neurons).

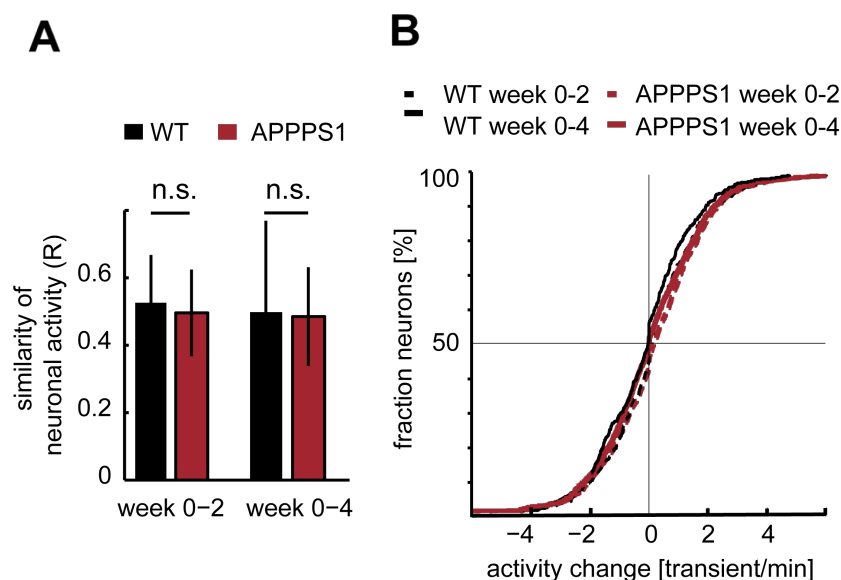


Figure 24. The change of activity of individual neurons over time.

A. Similarity index of neuronal activity. B. The distribution of activity changes.

#### 4.5 Only 5% of neurons stay hypoactive in the AD mouse model

Based on the published data on the activity of neurons in AD mouse models, the hypothesis of the stepwise dysfunction of the neurons in AD cortex was proposed (Busche and Konnerth, 2015, 2016). According to this model, as the first step, cortical neurons increase their activity (possibly, due to dysfunction of inhibitory circuitry). This can happen even before the plaque accumulation as a very early step of the disease progression. As the second step of the pathology, neurons, especially those close to the plaques, “turn off” – lose their activity and become silent, which later can lead to neuronal loss according to this model.

The investigation of the neuronal activity in my project confirms an early increase in the activity of neurons. Is it, however, true that the neurons stay in the same level of activity forever? Do the silent and hypoactive neurons lose their activity once and for all?

To address this question, we analyzed the activity of individual neurons and their development over three time points (Figure 25). Interestingly, results demonstrate that only around 5% of all the neurons both in transgenic and control mice stay in the “hypoactive” category. Less than 20% of the neurons change their activity over time both in WT and APPPS1 mice, going from hyperactive or hypoactive to normal activity and *vice versa*. The fraction of stably hyperactive neurons, i.e., neurons being hyperactive at all three imaging time points, is significantly higher in APPPS1 mice (WT 20% (0 – 21.43 % CI), APPPS1 33.3% (27.3 – 47.2 % CI),  $p = 0.03$ , Mann-Whitney U test). Significantly fewer neurons remain normoactive in APPPS1 mice throughout

the whole imaging period (WT 68.75% (63.89 – 79.1 % CI), APPPS1 57.89 % (48.72 – 67.71% CI),  $p = 0.02$ ). The fraction of continuously silent neurons does not differ between the genotypes (WT 12.5 % (11.35 -18.2% CI), APPPS1 6.67 % (0 – 13.81% CI),  $p = 0.18$ , WT  $n = 9$  experiments, APPPS1  $n = 29$  experiments, data are median +/- the 95 % confidence interval).

Many of the neurons that change their activity probably have the activity very close to the thresholds of 0,25 and 4 transients per minutes, thus easily changing their category. Only 2% of neurons change dramatically from hyperactivity to hypoactive or the other way around (WT: 9 neurons and 5 neurons change from hyperactivity to hypoactive or *vice versa* between week 0 and 2 and 0 and 4, respectively, out of 562 neurons; APPPS1: 17 neurons and 21 neurons change from hyperactivity to hypoactive or *vice versa* between week 0 and 2 and 0 and 4, respectively, out of 1691 neurons).

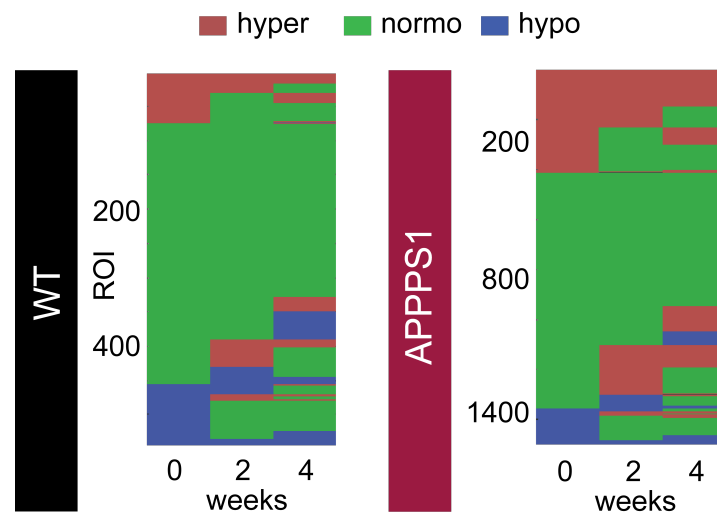


Figure 25. The activity of individual neurons over time according to three activity categories.

These results demonstrate that categorization of the neuronal activity is not a robust approach, as there will always be some borderline values and thus neurons that can easily change the category. This also demonstrates the advantages of the chronic measurements that provide researchers with more robust information compared to single time point snapshots.

Importantly, the proportion of three groups and overall activity distribution stays stable for each genotype and stably different between them for the whole month of observations. The proportion of stably hyperactive neurons is significantly increased in AD transgenic mice compared to WT mice (WT 20% (0 – 21.43 % CI), APPPS1 33.3% (27.3 – 47.2 % CI),  $p = 0.03$ , Mann-Whitney U test). This suggests that however individual neurons can change their activity and even sometimes dramatically, overall circuit composition stays stable.

#### 4.6 Influence of plaque distance on neuronal activity

A $\beta$  plaques are a hallmark of AD and it is well established that the local plaque environment is associated with several pathological features, like dystrophic neurites, synapse loss, and instability, reactive microglia and astrocytes, while the role plaques play in the development of those features is still debated. In some of the previous studies, altered neuronal activity patterns in anesthetized mice were linked to the amyloid plaque proximity (Busche *et al.*, 2008), while in others no dependency of pathological activity alteration from the plaque proximity was found (Liebscher *et al.*, 2016). So, it remains a controversial question whether the direct proximity of the plaque and the factors associated with the plaques can play an important role in the development of the pathological neuronal activity.

We, therefore, analyzed the plaque distance for each neuron and asked if the neuronal activity is different on the different distances to plaques or if neurons close to plaques would present more changes in their activity than neurons further away from plaque.

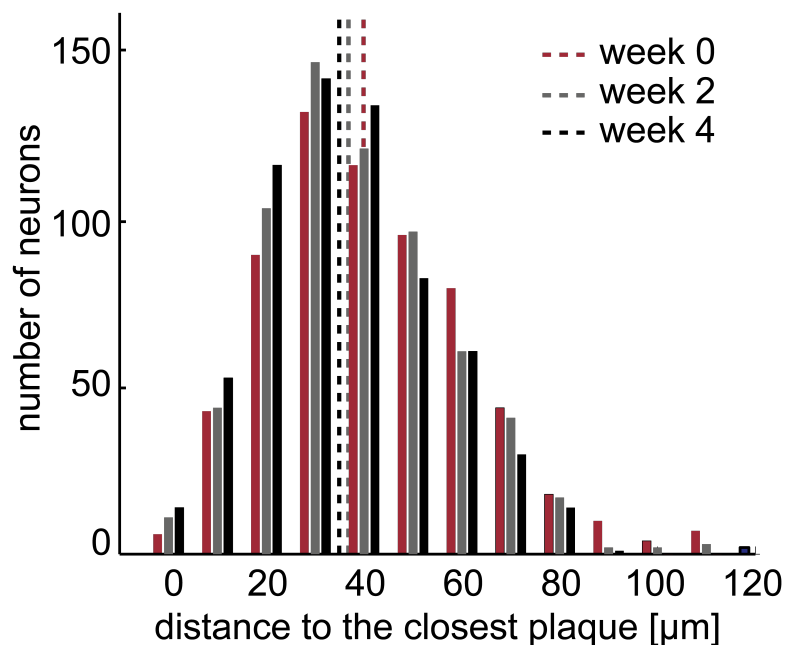


Figure 26. Distribution of plaque to neuron distances at three different imaging time points.

For plaque distance-dependent activity analysis, we used 653 neurons from 6 APPPS1 transgenic mice, which comprise 15 individual experiments (individual neuronal activity imaging areas). To allow for reliable results, only experiments, in which it was possible to track the distance to the

nearest plaque for all neurons at all imaging time points were included. Included neurons were also included in the overall activity analysis discussed in the previous sections. Distance to the closest plaque, visualized by the Methoxy-XO4 staining, was measured in the 3D space, thus providing a real-life estimation of this distance as compared to the 2D space measurements performed in the earlier studies (Busche *et al.*, 2008).

We have observed that most neurons are located within 100 $\mu$ m from the closest plaque with over half of neurons located in the 40 $\mu$ m vicinity to the plaque. Median plaque distance at the first time point (week 0) was 39.9 $\mu$ m, week 2 – 36.8 $\mu$ m, week 4 – 34.9  $\mu$ m. As seen from Figure 26 with time plaque distances get smaller, which is natural as the plaques grow.

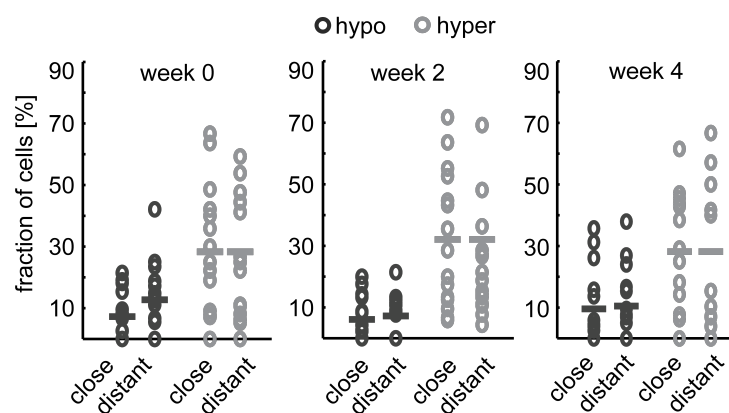


Figure 27. The fraction of hyperactive and hypoactive neurons in APPPS1 mice for close and distant neurons in individual experiments. Horizontal line denotes the mean.

Based on the above stated median neuron-to-plaque distances, we divided neurons into close ( $< 40 \mu\text{m}$  from the plaque border) and distant ( $> 40 \mu\text{m}$  from plaque border) from the nearest plaque, respectively. The fraction of hyperactive or silent neurons did not significantly differ between close and distant neurons at the level of individual experiments (Figure 27; week 0: fraction silent close  $7 \pm 8\%$ , distant  $13 \pm 12\%$ ,  $p = 0.15$ , fraction hyperactive close  $28 \pm 21\%$ , distant  $25 \pm 20\%$ ,  $p = 0.62$ , week 2: fraction silent close  $6 \pm 7\%$ , distant:  $7 \pm 7\%$ , fraction hyperactive close  $32 \pm 22\%$ , distant  $24 \pm 17\%$ , week 4: fraction silent neurons close  $10 \pm 12\%$ , distant  $10 \pm 12\%$ , close  $n = 15$  experiments, distant  $n = 15$  experiments, Students' t-test).

Relative proportions of hyperactive, normoactive and silent neurons in APPPS1 mice were stable for both close and distant neurons (Figure 28, A; fraction silent neurons: effect of group:  $F_{1,56} = 0.68$ ,  $p = 0.41$ , effect of time:  $F_{2,56} = 2.62$ ,  $p = 0.08$ , group-by-time interaction effect:  $F_{2,56} = 1.16$ ,  $p = 0.32$ ; fraction hyperactive neurons: effect of group:  $F_{1,56} = 0.44$ ,  $p = 0.51$ , effect of time:  $F_{2,56} = 0.13$ ,  $p = 0.88$ , group-by-time interaction effect:  $F_{2,56} = 0.78$ ,  $p = 0.46$ , two-way repeated measures

ANOVA, close  $n = 15$ , distant  $n = 15$  experiments; 326 neurons close, 326 neurons distant). However, we also noted that silent or hyperactive neurons were more likely to maintain their activity level from one imaging time point to another if they were close to plaques than if they were further away from plaques (Figure 28, B).

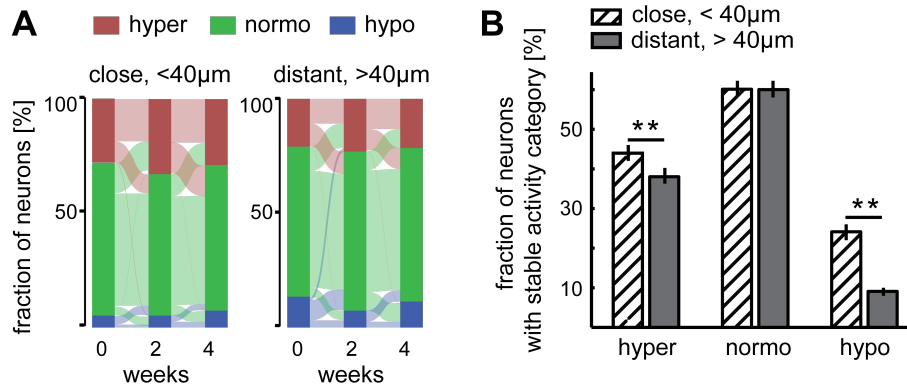


Figure 28. Changes in neuronal activity with respect to plaque proximity.

A. The relative proportion of hyperactive, normoactive and silent neurons and their fractional change over time in *APP/PS1* mice for close (< 40µm, left panel) and distant (> 40 µm, right panel) neurons.

B. The fraction of neurons with stable neuronal activity category over the whole imaging period for each of the three neuronal activity types for neurons close (striped) and distant (filled) from plaques. Bootstrapped median +/- the 95% confidence interval of the median are presented.

We then divided the neuronal population into plaque distance bins: neurons located within 0-20µm, 20-40µm, 40-60µm, 60-80µm to the closest plaque (Figure 29) and analyzed changes of neuronal activity in these bins.

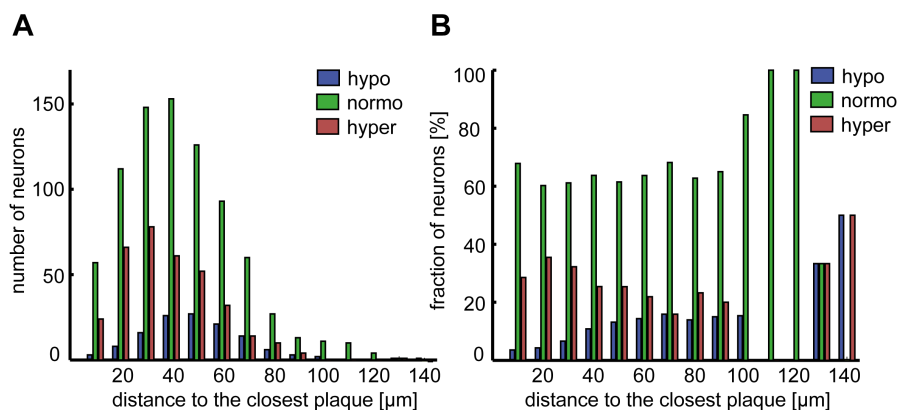


Figure 29. Distribution of plaques distances.

A. Distribution of the absolute number of neurons of the three neuronal activity categories as a function of plaque distance.

B. Distribution of the relative fraction of neurons for the three activity categories as a function of plaque distance (data is based on pooled neurons from 15 experiments). Important to note, beyond 100 µm very few cells were found, which affects the proportional abundance of the three categories.

We have found that the majority of neurons preserve their activity. Most of neurons (week 0 – 2: 79%, 82%, 78%, 80 %; week 0 – 4: 76 %, 81%, 81%, 86%) of the respective bins 0-20, 20-40, 40-60, 60-80 $\mu$ m distance change their activity within a range of  $\pm 2$  transients/min, and this change was independent of the plaque proximity (Figure 30).

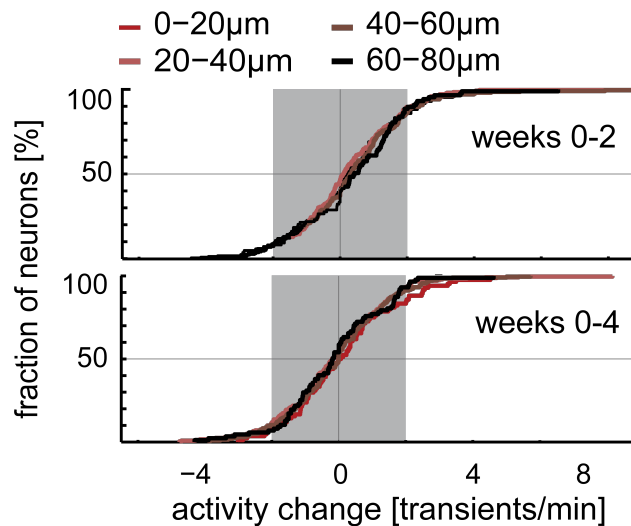


Figure 30. Cumulative distribution of the change in neuronal activity for neurons in different plaque-distance bins.

Activity changes are calculated from the first imaging time point to the second (upper panel) and from the first to the third (lower panel). The vast majority of neurons changes its activity within a range of  $\pm 2$  transients/min (gray box).

# 4

## Discussion

The aim of this thesis was to investigate the activity of the cortical neurons in the Alzheimer's disease model mouse in the early stages of pathology progression with the use of *in vivo* two-photon microscopy. The specific focus of this study was to follow neuronal activity over time: from an early stage of the disease to the stage where amyloid plaque load is high and advanced axonal pathology is present.

Alzheimer's disease is accompanied by a range of synaptic dysfunction signs, from synaptic depression and hyperexcitability to eventual synapse loss. Despite decades of research, the pathological triggers behind these alterations remain poorly understood and thus hinder the development of effective treatment. Moreover, it is unclear what is the sequence of pathological events and their relation to amyloid- $\beta$  ( $A\beta$ ) and amyloid plaque deposition.

Results obtained in various animal models of the disease show  $A\beta$ -mediated inhibition of synaptic currents (Hsia *et al.*, 1999; Kamenetz *et al.*, 2003; Chang *et al.*, 2006), disruption of synaptic plasticity (Walsh *et al.*, 2002; Jacobsen *et al.*, 2006), as well as endocytosis of glutamate receptors (Kamenetz *et al.*, 2003; Oddo *et al.*, 2003; Snyder *et al.*, 2005; Hsieh *et al.*, 2006; Shankar *et al.*, 2007; Nimmrich *et al.*, 2008). These findings are summarized in the synaptic failure hypothesis suggesting that "AD represents, at least initially, an attack on synapses" (Selkoe, 2002). At the same time, different dysfunctional states were observed in different experimental approaches, which makes it difficult to put these events together in one timeline and see their relationship. It is still an open question of how these low-level synaptic changes are connected to overall circuit dysfunction.

The classic view is that the structural damage by amyloid plaques and the loss of neurons underlie cognitive impairment in AD through a reduced cortical activity (synaptic failure hypothesis of AD). However, this hypothesis is challenged by recent findings from animal and human studies showing

that excessive neuronal activity, hypersynchrony and altered brain oscillations are also key features of the disease. However, even though abundant, the data provided by different laboratories does not seem to come to a consensus, some pointing to the direction of hyperexcitability of individual neurons, others seeing the cause in impaired inhibitory networks activity. Most probably, synaptic depression and excessive neuronal activity coexist in an unknown manner in AD transgenic mice as well as in humans with AD, leading to overall functional distortion of the circuits and networks.

Another controversial point in understanding Alzheimer's disease neuronal activity pathology is the relationship between amyloid plaques and neuronal activity alterations. On the one hand, many evidence suggests that the vicinity of the plaque creates the pathological environment, that leads to neuronal activity alterations (Busche and Konnerth, 2015). However, it remains unclear whether these alterations appear due to the presence of the fibrillar  $A\beta$ , direct effect of  $A\beta$  oligomers or other factors such as proinflammatory substances released from activated microglia and astrocytes, that surround the plaque. On the other hand, some other researchers found no correlation between the vicinity of the plaque and neuronal activity (Liebscher *et al.*, 2016).

To better understand the intricate relationship between neuronal activity changes and amyloid aggregate formation, more studies are needed, that will focus on longitudinal measurements of both parameters. Especially important is to move the focus from the late advanced stages of the disease to the early and prodromal stages to catch the first pathological events. Observing the early stages of AD progression was exactly the motivation behind my PhD project, the results of which were presented in the previous chapters.

My results support previously published reports of the increased proportion of hyperactive neurons in the AD mouse model. Importantly, my results also demonstrate that this increased activity is present in an awake state and is stable over a longer period (one month).

Compared to earlier studies the approach of *in vivo* awake calcium imaging used in the current study has many benefits for brain research. The main advantage is that the brain activity can be measured in the intact state without artefacts generated by anesthesia, which can exaggerate or mitigate experimental readouts. Thus, it is very valuable that in my project I could support earlier published anaesthetized data with awake imaging.

My PhD project presented in this thesis is the first ever longitudinal study investigating the activity of individual neurons in AD. This was possible thanks to the implementation of the two-photon *in vivo* microscopy with genetically-encoded calcium indicators, which, despite having certain limitations, presents a robust tool for this kind of studies. The result, briefly commented in this

chapter will be further discussed in the following chapters 4.1-4.45, while specifics of further application of two-photon calcium imaging in awake mice will be discussed in chapter 4.1.

## **5.1 Chronic awake calcium imaging as a tool to further investigate AD pathology**

An additional advantage of the presented study is longitudinal imaging approach for the first time applied to investigate the neuronal activity of frontal cortex neurons in AD. This approach allowed for the investigation of neuronal activity of individual neurons over a period of time. By taking advantage of the two-photon microscopy approach and use of genetically-encoded calcium indicators in this study I imaged a large set of individual neurons over a prolonged period and without artifacts of the anesthesia. This provided me with a robust dataset that allows for making solid conclusions.

Nevertheless, the current approach has some limitation, and certain results should be interpreted with care.

The first limitation that comes with calcium imaging is calcium buffering by the calcium indicators. Since calcium indicator like GCAMP6, that was used in the current study, bind intracellular calcium it can modify calcium concentrations in the cell and thus affect signaling pathways, in which calcium is involved. To mitigate this risk, I have adjusted the titer of GCAMP6-coding virus to still have the required level of GCAMP6 expression but reduce the toxic effects. Further, I have carefully chosen the imaging areas and analyzed neurons. Very bright neurons that did not show fluorescence dynamics were excluded from the dataset. These measures helped to minimize toxic buffering effects of GCAMP6 while providing a stable expression of the indicator.

Another concern that was noted in earlier studies is that the plaque-staining dye Methoxy X-100 can influence and decrease the plaque growth (Cohen, Ikonovic, *et al.*, 2009; Pratim Bose *et al.*, 2010). Even though, complete elimination of this effect is not possible and should be carried in mind, to decrease this effect Methoxy concentration was possibly low, based on the earlier studies in the lab. Moreover, it should be noted that even if slight alterations in plaque dynamics occurred this should not have influenced the main outcomes of the study, as plaque growth was still observed.

Also, *in vivo* brain microscopy is an invasive technique where inflammation occurs after the surgery due to exposure of the brain and virus injections. Inflammation can influence many signaling pathways in the tissue and have diverse effects on cell behavior, including the activity of neurons (Zhang and An, 2007). However, earlier studies have shown (Holtmaat *et al.*, 2009) that after the

recovery period levels of inflammation in the brain tissue goes to normal, and thus I used the recovery period of 1 month before the start of the imaging session.

Moreover, the nature of the animal experiments limits the number of animals that can be taken into study. The number of mice used for the plaque distance measurements limits the interpretation power of this part of the study, suggesting that future research should be done to access this question in more details.

Although my study provides new insights into the characterization of the neuronal activity in the AD-affected brain, further work is needed to pinpoint the exact cause of the activity dysregulations. Do alterations in neuronal activity lead to cognitive impairment or are they merely by-products of disease-induced cellular dysfunction? Do alterations in network synchrony cause the dysfunction of microcircuits, larger distributed networks, or both?

Chronic awake calcium imaging used in this project proved to be an invaluable tool to further investigate these questions. Usage of awake and chronic experiments allows to mitigate anesthesia-related artifacts and ensures a more robust readout due to repetitive measurements of the same neurons. Moreover, it provides a robust readout to investigate possible therapeutic interventions, as network activities can be experimentally or behaviorally manipulated.

Having in mind all the benefits of *in vivo* awake calcium imaging several features of this approach should be taken into account. An important consideration for the usage of *in vivo* awake imaging is that more consistency needs to be gained in the methodology so that different research groups would use the same approach to the imaging, data analysis, and classification of the activity readouts. Since division into separate activity groups is by definition arbitrary, it is very important to use the same thresholds throughout different studies.

Hopefully, in the coming year's researchers will further apply chronic awake *in vivo* calcium imaging as a tool to investigate AD pathology, at the same time paying more attention to consistency and accuracy of the experiments, and through this providing a better understanding of the pathology and possible therapeutic approaches.

## **5.2 AD model mice demonstrate neuronal hyperactivity**

Growing evidence from cellular-level recordings, as well as brain-wide monitoring of activity with blood oxygen level-dependent functional magnetic resonance imaging and electroencephalography, suggest that neuronal hyperactivity is a key pathophysiological feature in AD-like mouse models and humans with early-stage AD, underlying behavior-relevant local and

long-range circuit dysfunctions (for the review see Jorge J Palop and Mucke, 2010; Busche and Konnerth, 2016). In my work I conducted two-photon calcium imaging, employing the genetically encoded calcium indicator GCaMP6 (Chen *et al.*, 2013) in APPPS1 transgenic mice and age-matched transgene negative siblings (WT) during four weeks period (4;5-5,5 months of age) to assess AD-related changes of neuronal activity. APPPS1 mice demonstrated the higher average activity of cortical neurons at all three time points compared to control ( $p=0,03$ ), however, there was no significant difference of average activity between the three time points ( $p=0,23$ ).

These results provide supportive evidence for the hyperactivity in AD mice in the longitudinal study, that was earlier shown only in acute experiments (Busche *et al.*, 2008). This is valuable support since the chronic imaging approach helps to exclude many factors that usually accompany acute 2P *in vivo* imaging, such as inflammatory response, naturally occurring as a result of craniotomy and calcium indicator injection. In chronic studies, several weeks pass after the surgery, thus providing more stable and physiologically relevant result. Moreover, the fact that these results are in accordance with the acute experiments data provide a strong support to the earlier results. This spontaneous activity could reflect the described hyperexcitability in AD transgenic mice, which was suggested to be based on impaired inhibition (Palop *et al.*, 2007; Busche *et al.*, 2008; Garcia-Marin *et al.*, 2009; Jorge J. Palop and Mucke, 2010; Limon, Reyes-Ruiz and Mileli, 2012; Verret *et al.*, 2012).

My results add to the previous observation made mostly in the anesthetized mice. Previous studies in the frontal and visual cortex, demonstrating hyperactivity in AD mice, were only done in anesthetized mice (Busche *et al.*, 2008; Grienberger *et al.*, 2012). Moreover, this is an important finding as studies made in awake mice that overexpress a human mutant form of tau (P301L) and develop cortical NFTs showed no functional changes compared to the healthy neurons (Kuchibhotla *et al.*, 2014).

In that study, researchers used awake *in vivo* two-photon calcium imaging to monitor neuronal function in adult rTg4510 mice. Unexpectedly, NFT-bearing neurons in the visual cortex appeared to be completely functionally intact, to be capable of integrating dendritic inputs and effectively encoding orientation and direction selectivity, and of having a stable baseline resting calcium level (Kuchibhotla *et al.*, 2014).

At the same time, my results agree with another awake study conducted by Liebscher *et al.* (Liebscher *et al.*, 2016), in which researchers observed increased spontaneous activity during quiescent states when neuronal activity is typically strongly reduced.

The discrepancy with some of the earlier studies potentially results from the different experimental conditions, as in these studies researchers conducted their experiments in anesthetized mice, employing the synthetic calcium indicator Oregon Green BAPTA-1 (OGB-1) (Busche *et al.*, 2008; Grienberger *et al.*, 2012). Moreover, experiments using OGB-1 are performed acutely, shortly after the craniotomy and indicator injection. Conversely, experiments employing virus-mediated expression of genetically encoded calcium indicators are performed at least 4 weeks post-injection and window implantation, allowing for complete recovery time from potential tissue damage.

Thus, my results provide strong support for the findings of hyperactivity in AD mice. This also suggests that this line of research should be continued further to identify the underlying cause of the activity changes.

Surprisingly, according to my results, there is no progress in the activity changes throughout these four weeks. One could expect to observe the change from normal activity to hyperactivity and further change from hyperactivity to hypoactivity according to the model proposed by Konnerth and Busche based on the acute experiments data comparing young and old AD mice (Busche and Konnerth, 2016). In the APPPS1 model, the age between two to four months is a time of fast development of the pathology, manifested in increasing plaque load (Radde *et al.*, 2006) and increasing malfunction in behavioral tests (Radde *et al.*, 2006; Serneels *et al.*, 2009). One could expect that neuronal activity changes would follow the development of the pathology; however, this was not observed in my experiments.

This discrepancy with previously published data and proposed hypothesis can be due to several reasons. Firstly, possibly the imaging period was not long enough to see the changes in the activity. Secondly, maybe at this age there are no changes of activity anymore, as the neuronal activity is altered but stabilized by this time point. Thirdly, it is possible that in this mouse line neuronal activity is altered from a very early age due to the transgene expression and this the controversy with published data could be connected to the mouse line differences. Mouse line differences exist both due to the different nature of the transgene (APP or PS mutation, promoter, insertion site) and due to the differences in line background (Võikar *et al.*, 2001).

To summarize, the results of my study do not only provide strong support to the earlier findings of neuronal hyperactivity in AD but also point out to the need of further chronic studies in AD models. One-time snapshots gained with the use of acute experiments do not provide us with extensive data on neuronal activity changes development. There is a clear need in further longitudinal studies that will allow for recording the development of the changes and deciphering

details of how individual cells change their activity. These studies should both approach the early and late stages of AD progression, and presented study provided first hints in this direction.

### **5.3 The altered pattern of neuronal activity is stable**

Earlier studies demonstrated that AD mice exhibit changed proportion of hyperactive and silent neurons compared to healthy mice (for the review see Jorge J Palop and Mucke, 2010; Busche and Konnerth, 2016), however, as earlier studies were done acutely, it was not possible to find out whether this altered activity pattern is transient or a stable.

To address this question, I researched neuronal activity in the early stage of AD over four weeks. My hypothesis was based on the fact that A $\beta$  oligomers were soluble and might spread throughout the brain, thus if they affect neuronal activity, these effects would be transient, and the pattern of neuronal activity would not be stable. However, if some early pathological events influence neuronal circuits, we would observe a stable pattern of altered neuronal activity. To this end, I utilized an approach of *in vivo* two-photon calcium imaging of the cortical neurons in transgenic mouse models of AD. This method allows functional, cellular-resolution imaging of neuronal populations in the cortex over a prolonged period of time.

According to my data, in the transgenic mice a larger proportion of neurons were hyperactive and a smaller proportion – hypoactive, compared to the control non-transgenic mice. In the transgenic mice, hyperactive neurons represent 20% of all the neurons, hypoactive – 10% and normoactive – 70%. These results are comparable to published reports, but are not completely equal (Busche *et al.*, 2008; Greenberg, Houweling and Kerr, 2008). In these earlier studies, in transgenic mice, only 50% of the neurons were active in the normal frequency range, whereas the remaining neurons were at roughly equal proportions, either silent or hyperactive. Busche *et al.* observed a 16-fold increase in the fraction of hyperactive neurons and a threefold increase in the fraction of silent neurons compared to the healthy mouse brain (Busche *et al.*, 2008).

Why the proportion of normally active neurons is higher in my experiments can be explained by the differences between transgenic lines and the age difference. The mice examined by Busche and colleagues were of the age 6-10 months, while my experiment lasted from 4 months to 5 months of age, which means my mice were younger and maybe had less pronounced pathology of the neuronal activity.

My results indicate that there is indeed a bigger proportion of very active neurons which is caused either by the disturbed properties of the neurons or by the disbalance of underlying circuitry. To

address the question of the underlying cause of the activity alterations we analyzed the activity of individual neurons and its development over three time points.

Importantly, the proportion of three groups and overall activity distribution stays stable for each genotype and stably different between them for the whole month of observations, meaning that most of the neurons stay in the same type of activity (hyper-, normo- or silent) throughout this month. If we exclude all the neurons that change between the groups, the proportion of stably hyperactive neurons is still increased in AD transgenic mice compared to control mice (15% in APPPS1 mice and 10% in control mice). This suggests that even though individual neurons can change their activity and sometimes dramatically, overall circuit composition stays stable. This is an important finding as the stability of the altered circuitry in AD mice was not investigated so far in the experimental work since no chronic experiments were done.

While overall circuitry stays stable, almost a quarter of the neurons change their activity over time, going from hyperactive or hypoactive to normal activity and *vice versa*. However, most of these neurons have the activity very close to the thresholds of 0,25 and 4 transients per minutes, thus easily changing their category. Only 2% of neurons change dramatically from hyperactivity to hypoactive or the other way around. This observation demonstrates that categorisation of the neuronal activity is not a robust approach, as there will always be some borderline values and thus neurons that can easily change the category. This also demonstrates the advantages of the chronic measurements that provide researchers with more robust information compared to single time point snapshots.

Overall, my results suggest that early pathological events influence the whole neuronal circuitry rather than individual neurons, and for this reason, we observe a stable pattern of altered neuronal activity.

#### **5.4 Hypoactive neurons might still be functional**

As mentioned in the previous chapter, a prominent proportion of neurons changes their activity between three activity groups, and main changes happen in the hypoactive and silent group, distinguished by the activity level of 0-0,25 transients per minute. Interestingly, my results demonstrate that only around 5% of all the neurons both in transgenic and control mice stay in this hypoactive category. This is an interesting finding that has important implications for how hypoactivity of neurons in AD is interpreted.

According to the earlier reports, based on the acute experiments, researchers suggested that hypoactivity leads to silencing of neurons and is one of the pathological features of AD, that causes neurons to later degenerate. However, my results point out that most of the observed neurons did not stay in hypoactive state for all the 4 weeks of observation. This suggests, that the hypoactivity and silencing of the neurons can be reversed at least at the early stages of the disease.

My observations correspond well to the recent study by Keskin *et al.* in which researchers were able to revert hyperactivity with BACE inhibition (Keskin *et al.*, 2017). Authors mention that this finding was unexpected in regard to previous evidence indicating that at such advanced disease stages, many pathological and cellular processes are chronic and mostly irreversible. On the contrary, they found that most dysfunctional neurons in the amyloid-plaque bearing neocortex are still viable and that their “hyperactive phenotype” can be reversed by reducing A $\beta$  in the brain. Moreover, this correction of excess neuronal activity correlated with both a recovery of long-range circuits and memory functions. My results support the interesting finding of Keskin and colleagues, as my study also shows that indeed most of the silent and hypoactive neurons are still functional, suggesting that also the hyperactive neurons might not be fully dysfunctional. Moreover, if the alterations in neuronal activity are mainly due to the circuit dysfunction and not the alterations of individual neurons as suggested in the section 4.2., one could expect that these changes are more easily reversed.

Discussing the work of Keskin *et al.* it is also worth mentioning that there is a significant inconsistency in how researchers use neuronal activity categories even within the same research group, shifting the threshold for hyperactive neurons from 4 transients per minute in the earlier studies (Busche *et al.*, 2008) to 6 transients per minute in more recent studies (Keskin *et al.*, 2017). In my opinion, it is important to gain more consistency in the experiments and reporting of the neuronal activity changes in AD, that would allow for more precise comparison of the different studies. It also points out the importance of longitudinal studies as they help to gain more reliable results. Acute studies provide a chance for bigger sample groups but are more prone to outside factors that can contribute to the data fluctuations.

To summarize, results of my project together with another recent study by Keskin *et al.* (Keskin *et al.*, 2017) suggest that activity alteration of neurons, both in the direction of hypo- and hyperactivity can be reversed as the neurons are still functional. This finding has important implications for the potential treatment of AD, as it points out that interventions can stabilize and revert activity alterations and even if not cure at least prevent worsening of the cognitive symptoms. Recently, increasing evidence from animal and human studies indicated that along with contributing to

memory impairment, neuronal hyperactivity can worsen A $\beta$  plaque deposition (Bero *et al.*, 2011; Yamamoto *et al.*, 2015; Yuan and Grutzendler, 2016; Leal *et al.*, 2017), and even neurodegeneration (Putcha *et al.*, 2011); thus, the normalization of neuronal activity levels may directly modify disease progression.

## **5.5 Distance to the plaques does not affect aberrant neuronal activity**

Amyloid plaques have been intensively studied over decades, however, as discussed in the chapter 1.1.2. Their role in the pathology is still debated. Several studies reported that direct vicinity to the plaques influences the stability of synapses leading to the elimination of spines (Bittner *et al.*, 2012; Liebscher *et al.*, 2014). However, some other studies suggest that spines loss can occur even before plaque deposition (Hsia *et al.*, 1999; Mucke *et al.*, 2000; Lanz, Carter and Merchant, 2003; Jacobsen *et al.*, 2006) and also in the areas far away from plaques (Bittner *et al.*, 2010).

The results of neuronal activity investigation in relation to plaque distances are also inconclusive. Early study by Busche *et al.* for the first time reported activity changes in the AD mice and also reported that most of the affected neurons are located in the direct vicinity of the amyloid plaques, proposing that pathological conditions around the plaque are the main cause of the activity changes (Busche *et al.*, 2008). Nevertheless, some of the later studies did not find a correlation of neuronal activity changes with the vicinity of the plaque (Liebscher *et al.*, 2016).

The study by Busche *et al.* (Busche *et al.*, 2008) was performed implementing acute calcium imaging, and plaque distances were only calculated within the 2D space of the imaging plane. To perform a more robust measurement of plaque influence on the neuronal activity in my study, I imaged neuronal plaques repeatedly at all three time points along with activity measurements and also imaged tissue in 3D. Surprisingly, my data suggested that distance to the plaque is not a factor impacting activity changes of affected neurons, as the majority of the neurons preserve their activity during 4 weeks of imaging independent of plaque proximity.

One of the possible explanations of the contradiction with previous literature could be the difference in methodological approach. In my study, the distance to the plaque was assessed in the 3D space, while in the earlier publication by Busche, which established the connection between the plaque and the activity changes, distance measurement was done in the 2D plane. According to my experimental experience 3D assessment is indeed crucial, as in many cases the closest plaque was situated right above or below the imaging plane. Simply visually examining the planes above and below the imaging plane as reported by Busche and colleagues (Busche *et al.*, 2008) is not enough for reliable measurements of plaque distances.

However, my results are in agreement with the recent paper by Liebscher et al. (Liebscher *et al.*, 2016), where authors found no indication that neurons close to plaques are affected differently by neurodegenerative processes than those being further away. This finding at first glance seems to contradict other results of the structural alterations (reduced spine density and synaptic instability) tightly linked spatially to amyloid plaques (Liebscher *et al.*, 2014). A neuron's activity can, however, be dysregulated at multiple levels and while structural changes only occur close to the plaque, the consequences of these changes also affect the neuronal soma that is not in the direct vicinity of the plaque.

The earlier studies propose that there is something particularly toxic in the direct vicinity of the plaque, e.g., toxic A $\beta$  species or some mediators of inflammation. However, my results indicate that a more plausible explanation would be the overall circuit dysfunction in the AD mice, as also discussed in the previous sections. In this case, the distance to the closest plaque is not expected to have a big impact on the neuronal activity. This does not mean though that the vicinity of the plaque is not toxic, but rather that it is not adding more to the activity changes. At the same time, this activity can be toxic to the spines or microglia as was pointed out in the earlier studies to find the closest plaque and thus precise measurements in 3D space are required.

## References

- Abramowski, D. *et al.* (2008) 'Dynamics of A $\beta$  Turnover and Deposition in Different  $\beta$ -Amyloid Precursor Protein Transgenic Mouse Models Following  $\beta$ -Secretase Inhibition', *Journal of Pharmacology and Experimental Therapeutics*, 327(2), pp. 411–424. doi: 10.1124/jpet.108.140327.
- Adlard, P. A. and Bush, A. I. (2018) 'Metals and Alzheimer's Disease: How Far Have We Come in the Clinic?', *Journal of Alzheimer's Disease*. Edited by G. Perry, J. Avila, and X. Zhu. IOS Press, 62(3), pp. 1369–1379. doi: 10.3233/JAD-170662.
- Aizenstein, H. J. *et al.* (2008) 'Frequent amyloid deposition without significant cognitive impairment among the elderly', *Archives of Neurology*. American Medical Association, 65(11), pp. 1509–1517. doi: 10.1001/archneur.65.11.1509.
- Albert, M. S. *et al.* (2011) 'The diagnosis of mild cognitive impairment due to Alzheimer's disease: Recommendations from the National Institute on Aging-Alzheimer's Association workgroups on diagnostic guidelines for Alzheimer's disease', *Alzheimer's & Dementia*. Elsevier, 7(3), pp. 270–279. doi: 10.1016/j.jalz.2011.03.008.
- Allen, N. J. (2014) 'Astrocyte Regulation of Synaptic Behavior', *Annual Review of Cell and Developmental Biology*. Annual Reviews, 30(1), pp. 439–463. doi: 10.1146/annurev-cellbio-100913-013053.
- Alzheimer, A. (1907) 'Über eine eigenartige Erkrankung der Hirnrinde. Vortrag in der Versammlung Südwestdeutscher Irrenärzte in Tübingen am 3. November 1906', *Allgemeine Zeitschrift für Psychiatrie und psychisch-gerichtliche Medizin*, 64(November 1906), pp. 146–148. Available at: [https://commons.wikimedia.org/wiki/File:%22Über\\_eine\\_eigenartige\\_Erkrankung\\_der\\_Hirnrinde%22\\_\(Alois\\_Alzheimer,\\_1906\).jpg](https://commons.wikimedia.org/wiki/File:%22Über_eine_eigenartige_Erkrankung_der_Hirnrinde%22_(Alois_Alzheimer,_1906).jpg) (Accessed: 4 September 2017).
- Amatniek, J. C. *et al.* (2006) 'Incidence and Predictors of Seizures in Patients with Alzheimer's Disease', *Epilepsia*. Wiley/Blackwell (10.1111), 47(5), pp. 867–872. doi: 10.1111/j.1528-1167.2006.00554.x.
- Andermann, M. L. (2010) 'Chronic cellular imaging of mouse visual cortex during operant behavior and passive viewing', *Frontiers in Cellular Neuroscience*, 4, p. 3. doi: 10.3389/fncel.2010.00003.
- Andermann, M. L. *et al.* (2011) 'Functional specialization of mouse higher visual cortical areas', *Neuron*, 72(6), pp. 1025–1039. doi: 10.1016/j.neuron.2011.11.013.
- Anderson, J. *et al.* (2000) 'Stimulus dependence of two-state fluctuations of membrane potential in cat visual cortex', *Nature Neuroscience*. Nature Publishing Group, 3(6), pp. 617–621. doi: 10.1038/75797.
- Arieli, A. *et al.* (1996) 'Dynamics of ongoing activity: explanation of the large variability in evoked cortical responses.', *Science (New York, N.Y.)*, 273(5283), pp. 1868–71. Available at:

<http://www.ncbi.nlm.nih.gov/pubmed/8791593> (Accessed: 21 June 2018).

Arispe, N., Rojas, E. and Pollard, H. B. (1993) 'Alzheimer disease amyloid beta protein forms calcium channels in bilayer membranes: blockade by tromethamine and aluminum.', *Proceedings of the National Academy of Sciences*. National Academy of Sciences, 90(2), pp. 567–571. doi: 10.1073/pnas.90.2.567.

Asai, M. *et al.* (2003) 'Putative function of ADAM9, ADAM10, and ADAM17 as APP  $\alpha$ -secretase', *Biochemical and Biophysical Research Communications*, 301(1), pp. 231–235. doi: 10.1016/S0006-291X(02)02999-6.

Aschauer, D. F., Kreuz, S. and Rumpel, S. (2013) 'Analysis of Transduction Efficiency, Tropism and Axonal Transport of AAV Serotypes 1, 2, 5, 6, 8 and 9 in the Mouse Brain', *PLoS ONE*. Edited by J. Qiu. Public Library of Science, 8(9), p. e76310. doi: 10.1371/journal.pone.0076310.

Ashe, K. H. and Zahs, K. R. (2010) 'Probing the Biology of Alzheimer's Disease in Mice', *Neuron*. Cell Press, pp. 631–645. doi: 10.1016/j.neuron.2010.04.031.

Ashley, C. C. and Ridgway, E. B. (1968) 'Simultaneous recording of membrane potential, calcium transient and tension in single muscle fibers', *Nature*, 219(5159), pp. 1168–1169. doi: 10.1038/2191168a0.

Atkin, S. D. *et al.* (2009) 'Transgenic mice expressing aameleon fluorescent Ca<sup>2+</sup> indicator in astrocytes and Schwann cells allow study of glial cell Ca<sup>2+</sup> signals in situ and in vivo', *Journal of Neuroscience Methods*, 181(2), pp. 212–226. doi: 10.1016/j.jneumeth.2009.05.006.

Augustine, G. J. and Neher, E. (1992) 'Calcium requirements for secretion in bovine chromaffin cells', *The Journal of physiology*. Wiley-Blackwell, 450(1), pp. 247–71. doi: 10.1113/jphysiol.1992.sp019126.

Bacsikai, B. J. *et al.* (2001) 'Imaging of amyloid-beta deposits in brains of living mice permits direct observation of clearance of plaques with immunotherapy.', *Nature medicine*. Nature Publishing Group, 7(3), pp. 369–372. doi: 10.1038/85525.

Bacsikai, B. J. *et al.* (2003) 'Four-dimensional multiphoton imaging of brain entry, amyloid binding, and clearance of an amyloid-beta ligand in transgenic mice.', *Proceedings of the National Academy of Sciences of the United States of America*. National Academy of Sciences, 100(21), pp. 12462–7. doi: 10.1073/pnas.2034101100.

Baimbridge, K. G., Celio, M. R. and Rogers, J. H. (1992) 'Calcium-binding proteins in the nervous system', *Trends in Neurosciences*, 15(8), pp. 303–308. doi: 10.1016/0166-2236(92)90081-I.

Bakker, A. *et al.* (2012) 'Reduction of Hippocampal Hyperactivity Improves Cognition in Amnesic Mild Cognitive Impairment', *Neuron*. Cell Press, 74(3), pp. 467–474. doi: 10.1016/J.NEURON.2012.03.023.

Bakker, A. *et al.* (2015) 'Response of the medial temporal lobe network in amnesic mild cognitive impairment to therapeutic intervention assessed by fMRI and memory task performance', *NeuroImage: Clinical*. Elsevier, 7, pp. 688–698. doi: 10.1016/j.nicl.2015.02.009.

Balch, W. E. *et al.* (2008) 'Adapting proteostasis for disease intervention', *Science*, pp. 916–919. doi: 10.1126/science.1141448.

Ball, M. *et al.* (1997) 'Consensus recommendations for the postmortem diagnosis of Alzheimer's disease', *Neurobiology of Aging*, 18(4 SUPPL.), pp. S1-2. doi: 10.1016/S0197-4580(97)00057-2.

Ballatore, C., Lee, V. M.-Y. and Trojanowski, J. Q. (2007) 'Tau-mediated neurodegeneration in Alzheimer's disease and related disorders.', *Nature reviews. Neuroscience*. Nature Publishing Group, 8(9), pp. 663–72. doi: 10.1038/nrn2194.

- Banik, A. *et al.* (2015) ‘Translation of Pre-Clinical Studies into Successful Clinical Trials for Alzheimer’s Disease: What are the Roadblocks and How Can They Be Overcome?’, *Journal of Alzheimer’s disease : JAD*, 47(4), pp. 815–43. doi: 10.3233/JAD-150136.
- Bateman, R. J. *et al.* (2012) ‘Clinical and Biomarker Changes in Dominantly Inherited Alzheimer’s Disease’, *New England Journal of Medicine*. Massachusetts Medical Society, 367(9), pp. 795–804. doi: 10.1056/NEJMoa1202753.
- Bathellier, B., Ushakova, L. and Rumpel, S. (2012) ‘Discrete Neocortical Dynamics Predict Behavioral Categorization of Sounds’, *Neuron*, 76(2), pp. 435–449. doi: 10.1016/j.neuron.2012.07.008.
- Bero, A. W. *et al.* (2011) ‘Neuronal activity regulates the regional vulnerability to amyloid- $\beta$  deposition’, *Nature Neuroscience*. Nature Publishing Group, 14(6), pp. 750–756. doi: 10.1038/nn.2801.
- Bertram, L. and Tanzi, R. E. (2012) ‘The Genetics of Alzheimer’s Disease’, in *Progress in molecular biology and translational science*, pp. 79–100. doi: 10.1016/B978-0-12-385883-2.00008-4.
- Bezzina, C. *et al.* (2015) ‘Early onset of hypersynchronous network activity and expression of a marker of chronic seizures in the Tg2576 mouse model of Alzheimer’s disease’, *PLOS ONE*. Edited by Y. Herault. Public Library of Science, 10(3), p. e0119910. doi: 10.1371/journal.pone.0119910.
- Bhatia, R., Lin, H. and Lal, R. (2000) ‘Fresh and globular amyloid beta protein (1-42) induces rapid cellular degeneration: evidence for AbetaP channel-mediated cellular toxicity.’, *FASEB journal: official publication of the Federation of American Societies for Experimental Biology*, 14(9), pp. 1233–43. Available at: <http://www.ncbi.nlm.nih.gov/pubmed/10834945> (Accessed: 19 April 2018).
- Bielschowsky, M. (1902) ‘Die Silberimprägnation der Achsenylinder’, *Neurologisches Zentralblatt*, 21, pp. 579–584.
- Bittner, T. *et al.* (2010) ‘Multiple events lead to dendritic spine loss in triple transgenic Alzheimer’s disease mice’, *PLoS ONE*. Edited by S. G. Meuth. Public Library of Science, 5(11), p. e15477. doi: 10.1371/journal.pone.0015477.
- Bittner, T. *et al.* (2012) ‘Amyloid plaque formation precedes dendritic spine loss’, *Acta Neuropathologica*. Springer-Verlag, 124(6), pp. 797–807. doi: 10.1007/s00401-012-1047-8.
- Blauvelt, D. G. *et al.* (2013) ‘Distinct spatiotemporal activity in principal neurons of the mouse olfactory bulb in anesthetized and awake states’, *Frontiers in Neural Circuits*. Frontiers, 7(March), p. 46. doi: 10.3389/fncir.2013.00046.
- Blazquez-Llorca, L. *et al.* (2017a) ‘High plasticity of axonal pathology in Alzheimer’s disease mouse models’, *Acta Neuropathologica Communications*. BioMed Central, 5(1), p. 14. doi: 10.1186/s40478-017-0415-y.
- Blazquez-Llorca, L. *et al.* (2017b) ‘High plasticity of axonal pathology in Alzheimer’s disease mouse models’, *Acta neuropathologica communications*. BioMed Central, 5(1), p. 14. doi: 10.1186/s40478-017-0415-y.
- Blennow, K. *et al.* (2012) ‘Effect of immunotherapy with bapineuzumab on cerebrospinal fluid biomarker levels in patients with mild to moderate Alzheimer disease.’, *Archives of neurology*. United States, 69(8), pp. 1002–1010. doi: 10.1001/archneurol.2012.90.
- Blennow, K., de Leon, M. J. and Zetterberg, H. (2006) ‘Alzheimer’s disease’, *Lancet (London, England)*, 368(9533), pp. 387–403. doi: 10.1016/S0140-6736(06)69113-7.

- Blessed, G., Tomlinson, B. E. and Roth, M. (1968) 'The association between quantitative measures of dementia and of senile change in the cerebral grey matter of elderly subjects.', *The British journal of psychiatry: the journal of mental science*. The Royal College of Psychiatrists, 114(512), pp. 797–811. doi: 10.1192/bjp.114.512.797.
- Bolmont, T. *et al.* (2008) 'Dynamics of the microglial/amyloid interaction indicate a role in plaque maintenance.', *The Journal of neuroscience: the official journal of the Society for Neuroscience*, 28(16), pp. 4283–92. doi: 10.1523/JNEUROSCI.4814-07.2008.
- Bookheimer, S. Y. *et al.* (2000) 'Patterns of Brain Activation in People at Risk for Alzheimer's Disease', *New England Journal of Medicine*. Massachusetts Medical Society, 343(7), pp. 450–456. doi: 10.1056/NEJM200008173430701.
- Born, H. A. *et al.* (2014) 'Genetic Suppression of Transgenic APP Rescues Hypersynchronous Network Activity in a Mouse Model of Alzheimer's Disease', *Journal of Neuroscience*, 34(11), pp. 3826–3840. doi: 10.1523/JNEUROSCI.5171-13.2014.
- Bouchard, M. B. *et al.* (2015) 'Swept confocally-aligned planar excitation (SCAPE) microscopy for high speed volumetric imaging of behaving organisms', *Nature photonics*, 9(2), pp. 113–119. doi: 10.1038/nphoton.2014.323.
- Bouleau, S. and Tricoire, H. (2015) 'Drosophila models of Alzheimer's disease: advances, limits, and perspectives', *Journal of Alzheimer's disease: JAD*, 45(4), pp. 1015–38. doi: 10.3233/JAD-142802.
- Boutajangout, A. and Wisniewski, T. (2014) 'Tau-based therapeutic approaches for Alzheimer's disease - a mini-review', *Gerontology*, 60(5), pp. 381–5. doi: 10.1159/000358875.
- Bouwman, F. H. *et al.* (2007) 'CSF biomarkers and medial temporal lobe atrophy predict dementia in mild cognitive impairment', *Neurobiology of Aging*. Elsevier, 28(7), pp. 1070–1074. doi: 10.1016/j.neurobiolaging.2006.05.006.
- Braak, H. and Braak, E. (1991) 'Neuropathological staging of Alzheimer-related changes', *Acta Neuropathologica*. Springer-Verlag, 82(4), pp. 239–259. doi: 10.1007/BF00308809.
- Brendza, R. P. *et al.* (2003) 'PDAPP; YFP double transgenic mice: A tool to study amyloid-?? associated changes in axonal, dendritic, and synaptic structures', *Journal of Comparative Neurology*. Wiley Subscription Services, Inc., A Wiley Company, 456(4), pp. 375–383. doi: 10.1002/cne.10536.
- Brendza, R. P. *et al.* (2005) 'Anti-A $\beta$  antibody treatment promotes the rapid recovery of amyloid-associated neuritic dystrophy in PDAPP transgenic mice', *Journal of Clinical Investigation*. American Society for Clinical Investigation, 115(2), pp. 428–433. doi: 10.1172/JCI200523269.
- Brettschneider, J. *et al.* (2015) 'Spreading of pathology in neurodegenerative diseases: A focus on human studies', *Nature Reviews Neuroscience*. Nature Publishing Group, pp. 109–120. doi: 10.1038/nrn3887.
- Brookmeyer, R. *et al.* (2002) 'Survival following a diagnosis of Alzheimer disease', *Archives of Neurology*. American Medical Association, 59(11), pp. 1764–1767. doi: 10.1001/archneur.59.11.1764.
- Brunden, K. R. *et al.* (2017) 'Altered microtubule dynamics in neurodegenerative disease: Therapeutic potential of microtubule-stabilizing drugs', *Neurobiology of Disease*, 105, pp. 328–335. doi: 10.1016/j.nbd.2016.12.021.
- Buckner, R. L. (2005) 'Molecular, Structural, and Functional Characterization of Alzheimer's Disease: Evidence for a Relationship between Default Activity, Amyloid, and Memory', *Journal of Neuroscience*, 25(34), pp. 7709–7717. doi: 10.1523/JNEUROSCI.2177-05.2005.

- Burgold, S. *et al.* (2014) 'In vivo imaging reveals sigmoidal growth kinetic of  $\beta$ -amyloid plaques', *Acta Neuropathologica Communications*, 2(1), p. 30. doi: 10.1186/2051-5960-2-30.
- Busche, M. A. *et al.* (2008) 'Clusters of hyperactive neurons near amyloid plaques in a mouse model of Alzheimer's disease', *Science (New York, N.Y.)*, 321(5896), pp. 1686–9. doi: 10.1126/science.1162844.
- Busche, M. A. *et al.* (2012) 'Critical role of soluble amyloid- $\beta$  for early hippocampal hyperactivity in a mouse model of Alzheimer's disease', *Proceedings of the National Academy of Sciences of the United States of America*. National Academy of Sciences, 109(22), pp. 8740–5. doi: 10.1073/pnas.1206171109.
- Busche, M. A. *et al.* (2015) 'Rescue of long-range circuit dysfunction in Alzheimer's disease models', *Nature Neuroscience*. Nature Publishing Group, 18(11), pp. 1623–1630. doi: 10.1038/nn.4137.
- Busche, M. A. and Konnerth, A. (2015) 'Neuronal hyperactivity - A key defect in Alzheimer's disease?', *BioEssays*, 37(6), pp. 624–632. doi: 10.1002/bies.201500004.
- Busche, M. A. and Konnerth, A. (2016) 'Impairments of neural circuit function in Alzheimer's disease', *Philosophical transactions of the Royal Society of London. Series B, Biological sciences*, 371(1700), p. 20150429. doi: 10.1098/rstb.2015.0429.
- Bussire, T. *et al.* (2003) 'Stereologic analysis of neurofibrillary tangle formation in prefrontal cortex area 9 in aging and Alzheimer's disease', *Neuroscience*, 117(3), pp. 577–592. doi: 10.1016/S0306-4522(02)00942-9.
- Buxbaum, J. D. *et al.* (1998) 'Evidence that tumor necrosis factor ?? converting enzyme is involved in regulated ??-secretase cleavage of the Alzheimer amyloid protein precursor', *Journal of Biological Chemistry*, 273(43), pp. 27765–27767. doi: 10.1074/jbc.273.43.27765.
- Cabrejo, L. *et al.* (2006) '[Sporadic cerebral amyloidotic angiopathy]', *Rev.Neurol.(Paris)*, 162(0035-3787 (Print)), pp. 1059–1067. doi: 10.1016/S0035-3787(06)75118-9.
- de Calignon, A. *et al.* (2009) 'Tangle-Bearing Neurons Survive Despite Disruption of Membrane Integrity in a Mouse Model of Tauopathy', *Journal of Neuropathology & Experimental Neurology*. Oxford University Press, 68(7), pp. 757–761. doi: 10.1097/NEN.0b013e3181a9fc66.
- De Calignon, A. *et al.* (2010) 'Caspase activation precedes and leads to tangles', *Nature*. Nature Publishing Group, 464(7292), pp. 1201–1204. doi: 10.1038/nature08890.
- Campbell, S. L., Hablitz, J. J. and Olsen, M. L. (2014) 'Functional changes in glutamate transporters and astrocyte biophysical properties in a rodent model of focal cortical dysplasia', *Frontiers in Cellular Neuroscience*. Frontiers, 8, p. 425. doi: 10.3389/fncel.2014.00425.
- Canter, R. G., Penney, J. and Tsai, L.-H. (2016) 'The road to restoring neural circuits for the treatment of Alzheimer's disease', *Nature*, 539(7628), pp. 187–196. doi: 10.1038/nature20412.
- Cao, R. *et al.* (2017) 'Functional and oxygen-metabolic photoacoustic microscopy of the awake mouse brain', *NeuroImage*, 150, pp. 77–87. doi: 10.1016/j.neuroimage.2017.01.049.
- Carey, R. M. *et al.* (2009) 'Temporal structure of receptor neuron input to the olfactory bulb imaged in behaving rats.', *Journal of neurophysiology*, 101(2), pp. 1073–88. doi: 10.1152/jn.90902.2008.
- Caspersen, C. *et al.* (2005) 'Mitochondrial A $\beta$ : a potential focal point for neuronal metabolic dysfunction in Alzheimer's disease', *The FASEB Journal*, 19(14), pp. 2040–2041. doi: 10.1096/fj.05-3735fje.
- Castellani, R. J. and Perry, G. (2012) 'Pathogenesis and Disease-modifying Therapy in Alzheimer's Disease: The Flat Line of Progress', *Archives of Medical Research*. Elsevier, pp. 694–698. doi:

10.1016/j.arcmed.2012.09.009.

Celone, K. A. *et al.* (2006) 'Alterations in memory networks in mild cognitive impairment and Alzheimer's disease: an independent component analysis.', *The Journal of neuroscience : the official journal of the Society for Neuroscience*. Society for Neuroscience, 26(40), pp. 10222–31. doi: 10.1523/JNEUROSCI.2250-06.2006.

Chang, E. H. *et al.* (2006) 'AMPA receptor downscaling at the onset of Alzheimer's disease pathology in double knockin mice', *Proceedings of the National Academy of Sciences*, 103(9), pp. 3410–3415. doi: 10.1073/pnas.0507313103.

Chapman, P. F. *et al.* (1999) 'Impaired synaptic plasticity and learning in aged amyloid precursor protein transgenic mice', *Nature Neuroscience*, 2(3), pp. 271–276. doi: 10.1038/6374.

Chávez-Gutiérrez, L. *et al.* (2012) 'The mechanism of  $\gamma$ -Secretase dysfunction in familial Alzheimer disease', *The EMBO Journal*, 31(10), pp. 2261–2274. doi: 10.1038/emboj.2012.79.

Chen, T.-W. *et al.* (2013) 'Ultrasensitive fluorescent proteins for imaging neuronal activity', *Nature*. Nature Publishing Group, 499(7458), pp. 295–300. doi: 10.1038/nature12354.

Cheng, A. *et al.* (2011) 'Simultaneous two-photon calcium imaging at different depths with spatiotemporal multiplexing', *Nature methods*, 8(2), pp. 139–42. doi: 10.1038/nmeth.1552.

Chin, J. *et al.* (2005) 'Fyn kinase induces synaptic and cognitive impairments in a transgenic mouse model of Alzheimer's disease.', *The Journal of neuroscience : the official journal of the Society for Neuroscience*, 25(42), pp. 9694–703. doi: 10.1523/JNEUROSCI.2980-05.2005.

Chopra, K., Misra, S. and Kuhad, A. (2011) 'Neurobiological aspects of Alzheimer's disease', *Expert Opinion on Therapeutic Targets*. Taylor & Francis, 15(5), pp. 535–555. doi: 10.1517/14728222.2011.557363.

Christie, R. H. *et al.* (2001) 'Growth arrest of individual senile plaques in a model of Alzheimer's disease observed by in vivo multiphoton microscopy.', *The Journal of neuroscience : the official journal of the Society for Neuroscience*. Society for Neuroscience, 21(3), pp. 858–64. doi: 10.1523/jneurosci.4814-07.2008.

Chung, W.-S. *et al.* (2015) 'Do glia drive synaptic and cognitive impairment in disease?', *Nature Neuroscience*. Nature Publishing Group, 18(11), pp. 1539–1545. doi: 10.1038/nn.4142.

Cirrito, J. R. *et al.* (2005) 'Synaptic Activity Regulates Interstitial Fluid Amyloid- $\beta$  Levels In Vivo', *Neuron*. Cell Press, 48(6), pp. 913–922. doi: 10.1016/J.NEURON.2005.10.028.

Cleary, J. P. *et al.* (2005) 'Natural oligomers of the amyloid- $\beta$  protein specifically disrupt cognitive function', *Nature Neuroscience*. Nature Publishing Group, 8(1), pp. 79–84. doi: 10.1038/nn1372.

Cohen, A. D., Ikonomic, M. D., *et al.* (2009) 'Anti-Amyloid Effects of Small Molecule A $\beta$ -Binding Agents in PS1/APP Mice.', *Letters in drug design & discovery*, 6(6), p. 437. doi: 10.2174/157018009789057526.

Cohen, A. D., Price, J. C., *et al.* (2009) 'Basal Cerebral Metabolism May Modulate the Cognitive Effects of A $\beta$  in Mild Cognitive Impairment: An Example of Brain Reserve', *Journal of Neuroscience*, 29(47), pp. 14770–14778. doi: 10.1523/JNEUROSCI.3669-09.2009.

Connor, J. A. (1986) 'Digital imaging of free calcium changes and of spatial gradients in growing processes in single, mammalian central nervous system cells', *Proceedings of the National Academy of Sciences of the United States of America*, 83(16), pp. 6179–83. Available at: <http://www.ncbi.nlm.nih.gov/pubmed/3461482> (Accessed: 10 March 2017).

Constantinople, C. M. and Bruno, R. M. (2011) 'Effects and Mechanisms of Wakefulness on Local

- Cortical Networks', *Neuron*, 69(6), pp. 1061–1068. doi: 10.1016/j.neuron.2011.02.040.
- Cummings, J. L. (2006) 'Challenges to demonstrating disease-modifying effects in Alzheimer's disease clinical trials', *Alzheimer's and Dementia*. Elsevier, 2(4), pp. 263–271. doi: 10.1016/j.jalz.2006.07.001.
- Cummings, J. L., Morstorf, T. and Zhong, K. (2014) 'Alzheimer's disease drug-development pipeline: Few candidates, frequent failures', *Alzheimer's Research and Therapy*. BioMed Central, 6(4), p. 37. doi: 10.1186/alzrt269.
- D'Amore, J. D. *et al.* (2003) 'In vivo multiphoton imaging of a transgenic mouse model of Alzheimer disease reveals marked thioflavine-S-associated alterations in neurite trajectories.', *Journal of neuropathology and experimental neurology*. Oxford University Press, 62(2), pp. 137–145. doi: 10.1093/jnen/62.2.137.
- Dana, H. *et al.* (2014) 'Thy1-GCaMP6 Transgenic Mice for Neuronal Population Imaging In Vivo', *PLoS ONE*. Edited by B. Arenkiel, 9(9), p. e108697. doi: 10.1371/journal.pone.0108697.
- Davalos, D. *et al.* (2005) 'ATP mediates rapid microglial response to local brain injury in vivo', *Nature Neuroscience*. Nature Publishing Group, 8(6), pp. 752–758. doi: 10.1038/nn1472.
- Davis, J. *et al.* (2004) 'Early-onset and robust cerebral microvascular accumulation of amyloid beta-protein in transgenic mice expressing low levels of a vasculotropic Dutch/Iowa mutant form of amyloid beta-protein precursor.', *The Journal of biological chemistry*, 279(19), pp. 20296–306. doi: 10.1074/jbc.M312946200.
- Deane, R. *et al.* (2003) 'RAGE mediates amyloid- $\beta$  peptide transport across the blood-brain barrier and accumulation in brain', *Nature Medicine*, 9(7), pp. 907–913. doi: 10.1038/nm890.
- Deane, R. and Zlokovic, B. V (2007) 'Role of the blood-brain barrier in the pathogenesis of Alzheimer's disease', *Current Alzheimer Research*, 4(2), pp. 191–197. doi: 10.2174/156720507780362245.
- DeKosky, S. T. and Scheff, S. W. (1990) 'Synapse loss in frontal cortex biopsies in Alzheimer's disease: Correlation with cognitive severity', *Annals of Neurology*. Wiley Subscription Services, Inc., A Wiley Company, 27(5), pp. 457–464. doi: 10.1002/ana.410270502.
- Delekate, A. *et al.* (2014) 'Metabotropic P2Y1 receptor signalling mediates astrocytic hyperactivity in vivo in an Alzheimer's disease mouse model', *Nature Communications*. Nature Publishing Group, 5, p. 5422. doi: 10.1038/ncomms6422.
- Denk, W., Strickler, J. H. and Webb, W. W. (1990) 'Two-photon laser scanning fluorescence microscopy', *Science (New York, N.Y.)*, 248(4951), pp. 73–6. doi: 10.1126/science.2321027.
- Denk, W. and Svoboda, K. (1997) 'Photon upmanship: Why multiphoton imaging is more than a gimmick', *Neuron*, pp. 351–357. doi: 10.1016/S0896-6273(00)81237-4.
- Dickerson, B. C. *et al.* (2005) 'Increased hippocampal activation in mild cognitive impairment compared to normal aging and AD', *Neurology*. Lippincott Williams & Wilkins, 65(3), pp. 404–411. doi: 10.1212/01.wnl.0000171450.97464.49.
- Dickson, T. C. and Vickers, J. C. (2001) 'The morphological phenotype of  $\beta$ -amyloid plaques and associated neuritic changes in Alzheimer's disease', *Neuroscience*. Pergamon, 105(1), pp. 99–107. doi: 10.1016/S0306-4522(01)00169-5.
- Díez-García, J. *et al.* (2005) 'Activation of cerebellar parallel fibers monitored in transgenic mice expressing a fluorescent Ca<sup>2+</sup> indicator protein', *European Journal of Neuroscience*, 22(3), pp. 627–635. doi: 10.1111/j.1460-9568.2005.04250.x.

- Ding, J. *et al.* (2014) 'Structural basis of the ultrasensitive calcium indicator GCaMP6', *Science China Life Sciences*. Science China Press, 57(3), pp. 269–274. doi: 10.1007/s11427-013-4599-5.
- Direnberger, S. *et al.* (2012) 'Biocompatibility of a genetically encoded calcium indicator in a transgenic mouse model', *Nature Communications*, 3, p. 1031. doi: 10.1038/ncomms2035.
- Dombeck, D. A. *et al.* (2007) 'Imaging Large-Scale Neural Activity with Cellular Resolution in Awake, Mobile Mice', *Neuron*, 56(1), pp. 43–57. doi: 10.1016/j.neuron.2007.08.003.
- Dombeck, D. A., Graziano, M. S. and Tank, D. W. (2009) 'Functional clustering of neurons in motor cortex determined by cellular resolution imaging in awake behaving mice.', *The Journal of neuroscience: the official journal of the Society for Neuroscience*, 29(44), pp. 13751–60. doi: 10.1523/JNEUROSCI.2985-09.2009.
- Dong Hee, K. *et al.* (2014) 'Genetic markers for diagnosis and pathogenesis of Alzheimer's disease', *Gene*. Elsevier, 545(2), pp. 185–93. doi: 10.1016/j.gene.2014.05.031.
- Doody, R. S. *et al.* (2014) 'Phase 3 Trials of Solanezumab for Mild-to-Moderate Alzheimer's Disease', *New England Journal of Medicine*. Massachusetts Medical Society, 370(4), pp. 311–321. doi: 10.1056/NEJMoa1312889.
- Dujardin, S., Colin, M. and Buée, L. (2015) 'Invited review: Animal models of tauopathies and their implications for research/translation into the clinic', *Neuropathology and Applied Neurobiology*. Wiley/Blackwell (10.1111), 41(1), pp. 59–80. doi: 10.1111/nan.12200.
- Dyrks, T. *et al.* (1988) 'Identification, transmembrane orientation and biogenesis of the amyloid A4 precursor of Alzheimer's disease.', *The EMBO journal*, 7(4), pp. 949–57. doi: 10.1002/j.1460-2075.1988.tb02900.x.
- Ecker, A. S. *et al.* (2014) 'State Dependence of Noise Correlations in Macaque Primary Visual Cortex', *Neuron*, 82(1), pp. 235–248. doi: 10.1016/j.neuron.2014.02.006.
- Eilers, J. *et al.* (1995) 'Calcium signaling in a narrow somatic submembrane shell during synaptic activity in cerebellar Purkinje neurons', *Proceedings of the National Academy of Sciences of the United States of America*, 92(22), pp. 10272–10276. doi: 10.1073/pnas.92.22.10272.
- Fanutza, T. *et al.* (2015) 'APP and APLP2 interact with the synaptic release machinery and facilitate transmitter release at hippocampal synapses', *eLife*. eLife Sciences Publications Limited, 4(NOVEMBER2015), p. e09743. doi: 10.7554/eLife.09743.
- Fellgiebel, A. *et al.* (2004) 'Ultrastructural hippocampal and white matter alterations in mild cognitive impairment: A diffusion tensor imaging study', *Dementia and Geriatric Cognitive Disorders*. Karger Publishers, 18(1), pp. 101–108. doi: 10.1159/000077817.
- Ferezou, I., Bolea, S. and Petersen, C. C. H. (2006) 'Visualizing the Cortical Representation of Whisker Touch: Voltage-Sensitive Dye Imaging in Freely Moving Mice', *Neuron*, 50(4), pp. 617–629. doi: 10.1016/j.neuron.2006.03.043.
- Filippini, N. *et al.* (2009) 'Distinct patterns of brain activity in young carriers of the APOE- 4 allele', *Proceedings of the National Academy of Sciences*. National Academy of Sciences, 106(17), pp. 7209–7214. doi: 10.1073/pnas.0811879106.
- Flusberg, B. A. *et al.* (2008) 'High-speed, miniaturized fluorescence microscopy in freely moving mice', *Nature Methods*. Howard Hughes Medical Institute, 5(11), pp. 935–938. doi: 10.1038/nmeth.1256.
- Fogel, H. *et al.* (2014) 'APP homodimers transduce an amyloid- $\beta$ -mediated increase in release probability at excitatory synapses', *Cell Reports*, 7(5), pp. 1560–1576. doi: 10.1016/j.celrep.2014.04.024.

- Forlenza, O. V, Diniz, B. S. and Gattaz, W. F. (2010) 'Diagnosis and biomarkers of predementia in Alzheimer's disease', *BMC Medicine*. BioMed Central, p. 89. doi: 10.1186/1741-7015-8-89.
- Franks, N. P. (2008) 'General anaesthesia: from molecular targets to neuronal pathways of sleep and arousal.', *Nature reviews. Neuroscience*. Nature Publishing Group, 9(5), pp. 370–86. doi: 10.1038/nrn2372.
- Fu, H. *et al.* (2017) 'Tau Pathology Induces Excitatory Neuron Loss, Grid Cell Dysfunction, and Spatial Memory Deficits Reminiscent of Early Alzheimer's Disease', *Neuron*. Elsevier, 93(3), pp. 533–541.e5. doi: 10.1016/j.neuron.2016.12.023.
- Fuhrmann, M. *et al.* (2007) 'Dendritic pathology in prion disease starts at the synaptic spine.', *The Journal of neuroscience: the official journal of the Society for Neuroscience*, 27(23), pp. 6224–33. doi: 10.1523/JNEUROSCI.5062-06.2007.
- Games, D. *et al.* (1995) 'Alzheimer-type neuropathology in transgenic mice overexpressing V717F beta-amyloid precursor protein', *Nature*, 373(6514), pp. 523–7. doi: 10.1038/373523a0.
- Ganguli, M. *et al.* (2005) 'Alzheimer Disease and Mortality', *Archives of Neurology*. American Medical Association, 62(5), p. 779. doi: 10.1001/archneur.62.5.779.
- Garcia-Alloza, M. *et al.* (2006) 'Characterization of amyloid deposition in the APP<sup>swe</sup>/PS1<sup>dE9</sup> mouse model of Alzheimer disease', *Neurobiology of Disease*, 24(3), pp. 516–524. doi: 10.1016/j.nbd.2006.08.017.
- Garcia-Marin, V. *et al.* (2009) 'Diminished perisomatic GABAergic terminals on cortical neurons adjacent to amyloid plaques', *Frontiers in Neuroanatomy*, 3, p. 28. doi: 10.3389/neuro.05.028.2009.
- Gengler, S., Hamilton, A. and Hölscher, C. (2010) 'Synaptic plasticity in the hippocampus of a APP/PS1 mouse model of Alzheimer's disease is impaired in old but not young mice.', *PloS one*. Edited by S. Gaetani, 5(3), p. e9764. doi: 10.1371/journal.pone.0009764.
- Glabe, C. G. (2006) 'Common mechanisms of amyloid oligomer pathogenesis in degenerative disease', *Neurobiology of Aging*, pp. 570–575. doi: 10.1016/j.neurobiolaging.2005.04.017.
- Glenner, G. G. and Wong, C. W. (1984) 'Alzheimer's disease: Initial report of the purification and characterization of a novel cerebrovascular amyloid protein', *Biochemical and Biophysical Research Communications*. Academic Press, 120(3), pp. 885–890. doi: 10.1016/S0006-291X(84)80190-4.
- Golde, T. E. (2016) 'Alzheimer disease: Host immune defence, amyloid- $\beta$  peptide and Alzheimer disease', *Nature Reviews Neurology*. Nature Publishing Group, 12(8), pp. 433–434. doi: 10.1038/nrneurol.2016.105.
- Golde, T. E., Schneider, L. S. and Koo, E. H. (2011) 'Anti-A $\beta$  Therapeutics in Alzheimer's Disease: The Need for a Paradigm Shift', *Neuron*, 69(2), pp. 203–213. doi: 10.1016/j.neuron.2011.01.002.
- Golshani, P. *et al.* (2009) 'Internally Mediated Developmental Desynchronization of Neocortical Network Activity', *Journal of Neuroscience*, 29(35), pp. 10890–10899. doi: 10.1523/JNEUROSCI.2012-09.2009.
- Goltstein, P. M., Montijn, J. S. and Pennartz, C. M. A. (2015) 'Effects of isoflurane anesthesia on ensemble patterns of Ca<sup>2+</sup> activity in mouse v1: reduced direction selectivity independent of increased correlations in cellular activity.', *PloS one*. Edited by N. S. C. Price. Public Library of Science, 10(2), p. e0118277. doi: 10.1371/journal.pone.0118277.
- Gómez-Isla, T. *et al.* (1997) 'Neuronal loss correlates with but exceeds neurofibrillary tangles in Alzheimer's disease', *Annals of Neurology*, 41(1), pp. 17–24. doi: 10.1002/ana.410410106.
- Gómez-Isla, T. *et al.* (1999) 'The impact of different presenilin 1 and presenilin 2 mutations on

- amyloid deposition, neurofibrillary changes and neuronal loss in the familial Alzheimer's disease brain. Evidence for other phenotype-modifying factors', *Brain*, 122(9), pp. 1709–1719. doi: 10.1093/brain/122.9.1709.
- Gomez-Isla, T. *et al.* (2008) 'Neuropathology of Alzheimer's Disease', *Handbook of Clinical Neurology*. Elsevier, 89, pp. 233–243. doi: 10.1016/S0072-9752(07)01222-5.
- Götz, J. *et al.* (2011) 'Modes of A $\beta$  toxicity in Alzheimer's disease', *Cellular and Molecular Life Sciences*. SP Birkhäuser Verlag Basel, pp. 3359–3375. doi: 10.1007/s00018-011-0750-2.
- Greenberg, D. S., Houweling, A. R. and Kerr, J. N. D. (2008) 'Population imaging of ongoing neuronal activity in the visual cortex of awake rats.', *Nature Neuroscience*. Nature Publishing Group, 11(7), pp. 749–751. doi: 10.1038/nn.2140.
- Greenberg, S. M. (2002) 'Cerebral amyloid angiopathy and vessel dysfunction', *Cerebrovascular Diseases*. Karger Publishers, 13(SUPPL. 2), pp. 42–47. doi: 10.1159/000049149.
- Grienberger, C. *et al.* (2012) 'Staged decline of neuronal function in vivo in an animal model of Alzheimer's disease', *Nature Communications*. Nature Publishing Group, 3(1), p. 774. doi: 10.1038/ncomms1783.
- Grienberger, C. and Konnerth, A. (2012) 'Imaging Calcium in Neurons', *Neuron*. Molecular Probes, Eugene, OR, USA, 73(5), pp. 862–885. doi: 10.1016/j.neuron.2012.02.011.
- Grutzendler, J. *et al.* (2007) 'Various dendritic abnormalities are associated with fibrillar amyloid deposits in Alzheimer's disease.', *Annals of the New York Academy of Sciences*. Blackwell Publishing Inc, 1097(1), pp. 30–9. doi: 10.1196/annals.1379.003.
- Grynkiewicz, G., Poenie, M. and Tsien, R. Y. (1985) 'A new generation of Ca<sup>2+</sup> indicators with greatly improved fluorescence properties', *Journal of Biological Chemistry*, pp. 3440–3450. doi: 3838314.
- Guerreiro, R. and Hardy, J. (2014) 'Genetics of Alzheimer's Disease', *Neurotherapeutics*, 11(4), pp. 732–737. doi: 10.1007/s13311-014-0295-9.
- Guizar-Sicairos, M., Thurman, S. T. and Fienup, J. R. (2008) 'Efficient subpixel image registration algorithms.', *Optics letters*, 33(2), pp. 156–8. Available at: <http://www.ncbi.nlm.nih.gov/pubmed/18197224> (Accessed: 19 June 2018).
- Haass, C. *et al.* (1992) 'Amyloid  $\beta$ -peptide is produced by cultured cells during normal metabolism', *Nature*, 359(6393), pp. 322–325. doi: 10.1038/359322a0.
- Haass, C. and Selkoe, D. J. (2007) 'Soluble protein oligomers in neurodegeneration: Lessons from the Alzheimer's amyloid  $\beta$ -peptide', *Nature Reviews Molecular Cell Biology*, pp. 101–112. doi: 10.1038/nrm2101.
- Haider, B., Häusser, M. and Carandini, M. (2013) 'Inhibition dominates sensory responses in the awake cortex', *Nature*. Nature Publishing Group, 493(7430), pp. 97–102. doi: 10.1038/nature11665.
- Hampel, H. *et al.* (2017) 'Revisiting the cholinergic hypothesis in Alzheimer's disease: Emerging evidence from translational and clinical research', *Alzheimer's and Dementia*. Elsevier Inc., (October). doi: 10.1016/j.jalz.2017.08.016.
- Hannan, S. B. *et al.* (2016) 'Cellular and molecular modifier pathways in tauopathies: the big picture from screening invertebrate models.', *Journal of neurochemistry*, 137(1), pp. 12–25. doi: 10.1111/jnc.13532.
- Hardy, J. (2006a) 'A Hundred Years of Alzheimer's Disease Research', *Neuron*. Elsevier, 52(1), pp.

3–13. doi: 10.1016/j.neuron.2006.09.016.

Hardy, J. (2006b) ‘Alzheimer’s disease: the amyloid cascade hypothesis: an update and reappraisal.’, *Journal of Alzheimer’s disease: JAD*, 9(3 Suppl), pp. 151–153. doi: 10.3233/JAD-2006-9S317.

Hardy, J. and Higgins, G. (1992) ‘Alzheimer’s disease: the amyloid cascade hypothesis’, *Science*, 256(5054), pp. 184–185. doi: 10.1126/science.1566067.

Hardy, J. and Selkoe, D. J. (2002) ‘The amyloid hypothesis of Alzheimer’s disease: Progress and problems on the road to therapeutics’, *Science*, pp. 353–356. doi: 10.1126/science.1072994.

Harris, J. A. *et al.* (2010) ‘Transsynaptic Progression of Amyloid- $\beta$ -Induced Neuronal Dysfunction within the Entorhinal-Hippocampal Network’, *Neuron*. Cell Press, 68(3), pp. 428–441. doi: 10.1016/J.NEURON.2010.10.020.

Hasan, M. T. *et al.* (2004) ‘Functional fluorescent Ca<sup>2+</sup> indicator proteins in transgenic mice under TET control’, *PLoS Biology*. Edited by Lawrence Katz, 2(6), p. e163. doi: 10.1371/journal.pbio.0020163.

Hedden, T. *et al.* (2009) ‘Disruption of functional connectivity in clinically normal older adults harboring amyloid burden’, *J Neurosci*. Society for Neuroscience, 29(40), pp. 12686–12694. doi: 10.1523/JNEUROSCI.3189-09.2009.

Heim, N. *et al.* (2007) ‘Improved calcium imaging in transgenic mice expressing a troponin C-based biosensor’, *Nat Methods*, 4(2), pp. 127–129. doi: 10.1038/nmeth1009.

Helmchen, F. *et al.* (2001) ‘A miniature head-mounted two-photon microscope: High-resolution brain imaging in freely moving animals’, *Neuron*, 31(6), pp. 903–912. doi: 10.1016/S0896-6273(01)00421-4.

Helmchen, F., Borst, J. G. and Sakmann, B. (1997) ‘Calcium dynamics associated with a single action potential in a CNS presynaptic terminal’, *Biophysical Journal*, 72(3), pp. 1458–1471. doi: 10.1016/S0006-3495(97)78792-7.

Helmchen, F. and Denk, W. (2005) ‘Deep tissue two-photon microscopy’, *Nature Methods*, 2(12), pp. 932–940. doi: 10.1038/nmeth818.

Helmchen, F., Imoto, K. and Sakmann, B. (1996) ‘Ca<sup>2+</sup> buffering and action potential-evoked Ca<sup>2+</sup> signaling in dendrites of pyramidal neurons’, *Biophysical Journal*, 70(2), pp. 1069–1081. doi: 10.1016/S0006-3495(96)79653-4.

Helzner, E. P. *et al.* (2008) ‘Survival in Alzheimer disease: A multiethnic, population-based study of incident cases’, *Neurology*. Wolters Kluwer Health, Inc. on behalf of the American Academy of Neurology, 71(19), pp. 1489–1495. doi: 10.1212/01.wnl.0000334278.11022.42.

Heneka, M. T. *et al.* (2012) ‘NLRP3 is activated in Alzheimer’s disease and contributes to pathology in APP/PS1 mice’, *Nature*, 493(7434), pp. 674–678. doi: 10.1038/nature11729.

Heneka, M. T. *et al.* (2015) ‘Neuroinflammation in Alzheimer’s disease’, *The Lancet Neurology*. Elsevier, pp. 388–405. doi: 10.1016/S1474-4422(15)70016-5.

Heppner, F. L., Ransohoff, R. M. and Becher, B. (2015) ‘Immune attack: the role of inflammation in Alzheimer disease.’, *Nature reviews. Neuroscience*. Nature Publishing Group, 16(6), pp. 358–72. doi: 10.1038/nrn3880.

Heys, J. G., Rangarajan, K. V. and Dombeck, D. A. (2014) ‘The functional micro-organization of grid cells revealed by cellular-resolution imaging’, *Neuron*. Elsevier, 84(5), pp. 1079–1090. doi: 10.1016/j.neuron.2014.10.048.

Hick, M. *et al.* (2015) ‘Acute function of secreted amyloid precursor protein fragment APP<sub>s</sub> in

- synaptic plasticity', *Acta Neuropathologica*. Springer Berlin Heidelberg, 129(1), pp. 21–37. doi: 10.1007/s00401-014-1368-x.
- Higley, M. J. and Sabatini, B. L. (2008) 'Calcium Signaling in Dendrites and Spines: Practical and Functional Considerations', *Neuron*, pp. 902–913. doi: 10.1016/j.neuron.2008.08.020.
- Hires, S. A., Tian, L. and Looger, L. L. (2008) 'Reporting neural activity with genetically encoded calcium indicators', *Brain Cell Biol*, 36(1–4), pp. 69–86. doi: 10.1007/s11068-008-9029-4.
- Hof, P. R. *et al.* (2003) 'Stereologic evidence for persistence of viable neurons in layer II of the entorhinal cortex and the CA1 field in Alzheimer disease', *Journal of Neuropathology and Experimental Neurology*, 62(1), pp. 55–67. doi: 10.1093/jnen/62.1.55.
- Holtmaat, A. *et al.* (2009) 'Long-term, high-resolution imaging in the mouse neocortex through a chronic cranial window', *Nature Protocols*, 4(8), pp. 1128–1144. doi: 10.1038/nprot.2009.89.
- Holtmaat, A. *et al.* (2012) 'Imaging neocortical neurons through a chronic cranial window', *Cold Spring Harbor Protocols*, 7(6), pp. 694–701. doi: 10.1101/pdb.prot069617.
- Holtmaat, A. and Svoboda, K. (2009) 'Experience-dependent structural synaptic plasticity in the mammalian brain', *Nature reviews. Neuroscience*, 10(9), pp. 647–58. doi: 10.1038/nrn2699.
- Horikawa, K. *et al.* (2010) 'Spontaneous network activity visualized by ultrasensitive Ca<sup>2+</sup> indicators, yellow Cameleon-Nano', *Nature Methods*. Nature Publishing Group, 7(9), pp. 729–732. doi: 10.1038/nmeth.1488.
- Horton, N. G. *et al.* (2013) 'In vivo three-photon microscopy of subcortical structures within an intact mouse brain.', *Nature photonics*. IEEE, 7(3), pp. 1–1. doi: 10.1038/nphoton.2012.336.
- Hsia, A. Y. *et al.* (1999) 'Plaque-independent disruption of neural circuits in Alzheimer's disease mouse models.', *Proceedings of the National Academy of Sciences of the United States of America*. National Academy of Sciences, 96(6), pp. 3228–33. doi: 10.1073/pnas.96.6.3228.
- Hsiao, K. *et al.* (1996) 'Correlative memory deficits, Aβ elevation, and amyloid plaques in transgenic mice', *Science (New York, N.Y.)*, 274(5284), pp. 99–102. doi: 10.1126/science.274.5284.99.
- Hsieh, H. *et al.* (2006) 'AMPA Removal Underlies Aβ-Induced Synaptic Depression and Dendritic Spine Loss', *Neuron*. Cell Press, 52(5), pp. 831–843. doi: 10.1016/j.neuron.2006.10.035.
- Huang, Y.-W. A. *et al.* (2017) 'ApoE2, ApoE3, and ApoE4 Differentially Stimulate APP Transcription and Aβ Secretion.', *Cell*, 168(3), pp. 427–441.e21. doi: 10.1016/j.cell.2016.12.044.
- Huber, D. *et al.* (2012) 'Multiple dynamic representations in the motor cortex during sensorimotor learning', *Nature*. Nature Publishing Group, 484(7395), pp. 473–478. doi: 10.1038/nature11039.
- Hyman, B. T. *et al.* (2012) 'National Institute on Aging-Alzheimer's Association guidelines for the neuropathologic assessment of Alzheimer's disease.', *Alzheimer's & dementia: the journal of the Alzheimer's Association*. Elsevier, 8(1), pp. 1–13. doi: 10.1016/j.jalz.2011.10.007.
- Hyman, B. T. and Trojanowski, J. Q. (1997) 'Consensus recommendations for the postmortem diagnosis of Alzheimer disease from the National Institute on Aging and the Reagan Institute Working Group on diagnostic criteria for the neuropathological assessment of Alzheimer disease.', *Journal of neuropathology and experimental neurology*. Edited by Intergovernmental Panel on Climate Change. Cambridge: Cambridge University Press, 56(10), pp. 1095–7. doi: 10.1017/CBO9781107415324.004.
- Iaccarino, H. F. *et al.* (2016) 'Gamma frequency entrainment attenuates amyloid load and modifies microglia', *Nature*. Nature Publishing Group, 540(7632), pp. 230–235. doi: 10.1038/nature20587.

- Ingelsson, M. *et al.* (2004) 'Early Abeta accumulation and progressive synaptic loss, gliosis, and tangle formation in AD brain.', *Neurology*. Lippincott Williams & Wilkins, 62(6), pp. 925–931. doi: 10.1212/01.WNL.0000115115.98960.37.
- Iqbal, K. and Grundke-Iqbal, I. (2002) 'Neurofibrillary pathology leads to synaptic loss and not the other way around in Alzheimer disease', *Journal of Alzheimer's Disease*, pp. 235–238. doi: 10.3233/JAD-2002-4313.
- Ittner, A. *et al.* (2014) 'p38 MAP kinase-mediated NMDA receptor-dependent suppression of hypersynchronicity in a mouse model of Alzheimer's disease', *Acta Neuropathol Commun*. BioMed Central, 2(1), p. 149. doi: 10.1186/s40478-014-0149-z.
- Ittner, A. A. *et al.* (2014) 'p38 MAP kinase-mediated NMDA receptor-dependent suppression of hippocampal hypersynchronicity in a mouse model of Alzheimer's disease', *Acta Neuropathologica Communications*. BioMed Central, 2(1), p. 149. doi: 10.1186/s40478-014-0149-z.
- Ittner, L. M. and Götz, J. (2011) 'Amyloid- $\beta$  and tau - A toxic pas de deux in Alzheimer's disease', *Nature Reviews Neuroscience*. Nature Publishing Group, 12(2), pp. 67–72. doi: 10.1038/nrn2967.
- Jack, C. R. *et al.* (2009) 'Serial PIB and MRI in normal, mild cognitive impairment and Alzheimer's disease: Implications for sequence of pathological events in Alzheimer's disease', *Brain*. Oxford University Press, 132(5), pp. 1355–1365. doi: 10.1093/brain/awp062.
- Jacobsen, J. S. *et al.* (2006) 'Early-onset behavioral and synaptic deficits in a mouse model of Alzheimer's disease', *Proceedings of the National Academy of Sciences*, 103(13), pp. 5161–5166. doi: 10.1073/pnas.0600948103.
- Jan, A. *et al.* (2008) 'The ratio of monomeric to aggregated forms of A $\beta$ 40 and A $\beta$ 42 is an important determinant of amyloid- $\beta$  aggregation, fibrillogenesis, and toxicity', *Journal of Biological Chemistry*, 283(42), pp. 28176–28189. doi: 10.1074/jbc.M803159200.
- Jankowsky, J. L. *et al.* (2004) 'Mutant presenilins specifically elevate the levels of the 42 residue  $\beta$ -amyloid peptide in vivo: Evidence for augmentation of a 42-specific  $\gamma$  secretase', *Human Molecular Genetics*, pp. 159–170. doi: 10.1093/hmg/ddh019.
- Jansen, W. J. *et al.* (2015) 'Prevalence of Cerebral Amyloid Pathology in Persons Without Dementia', *JAMA*. American Medical Association, 313(19), p. 1924. doi: 10.1001/jama.2015.4668.
- Ji, D. and Wilson, M. A. (2007) 'Coordinated memory replay in the visual cortex and hippocampus during sleep', *Nature Neuroscience*, 10(1), pp. 100–107. doi: 10.1038/nn1825.
- Johnson, S. C. *et al.* (2014) 'Amyloid burden and neural function in people at risk for Alzheimer's Disease', *Neurobiology of Aging*, 35(3), pp. 576–584. doi: 10.1016/j.neurobiolaging.2013.09.028.
- Jonsson, T. *et al.* (2012) 'A mutation in APP protects against Alzheimer's disease and age-related cognitive decline', *Nature*. Nature Publishing Group, 488(7409), pp. 96–9. doi: 10.1038/nature11283.
- Jung, C. K. E. *et al.* (2015) 'Fibrillar Amyloid Plaque Formation Precedes Microglial Activation', *PLOS ONE*. Edited by J. El Khoury. Public Library of Science, 10(3), p. e0119768. doi: 10.1371/journal.pone.0119768.
- Kalyan-Raman, U. P. and Kalyan-Raman, K. (1984) 'Cerebral amyloid angiopathy causing intracranial hemorrhage', *Annals of Neurology*. Wiley-Blackwell, 16(3), pp. 321–329. doi: 10.1002/ana.410160308.
- Kam, K. *et al.* (2016) 'Interictal spikes during sleep are an early defect in the Tg2576 mouse model of  $\beta$ -amyloid neuropathology', *Scientific Reports*. Nature Publishing Group, 6(1), p. 20119. doi: 10.1038/srep20119.

- Kamenetz, F. *et al.* (2003) 'APP processing and synaptic function', *Neuron*. Cell Press, 37(6), pp. 925–937. doi: 10.1016/S0896-6273(03)00124-7.
- Kang, J.-E. *et al.* (2009) 'Amyloid-beta dynamics are regulated by orexin and the sleep-wake cycle.', *Science (New York, N.Y.)*. American Association for the Advancement of Science, 326(5955), pp. 1005–7. doi: 10.1126/science.1180962.
- Karch, C. M., Cruchaga, C. and Goate, A. M. (2014) 'Alzheimer's Disease Genetics: From the Bench to the Clinic', *Neuron*. NIH Public Access, 83(1), pp. 11–26. doi: 10.1016/j.neuron.2014.05.041.
- Karch, C. M. and Goate, A. M. (2015) 'Alzheimer's disease risk genes and mechanisms of disease pathogenesis', *Biological Psychiatry*, 77(1), pp. 43–51. doi: 10.1016/j.biopsych.2014.05.006.
- Karran, E. and Hardy, J. (2014) 'A critique of the drug discovery and phase 3 clinical programs targeting the amyloid hypothesis for Alzheimer disease', *Annals of Neurology*. Wiley-Blackwell, pp. 185–205. doi: 10.1002/ana.24188.
- Karran, E., Mercken, M. and Strooper, B. De (2011) 'The amyloid cascade hypothesis for Alzheimer's disease: An appraisal for the development of therapeutics', *Nature Reviews Drug Discovery*, pp. 698–712. doi: 10.1038/nrd3505.
- Kastanenka, K. V. *et al.* (2017) 'Optogenetic restoration of disrupted slow oscillations halts amyloid deposition and restores calcium homeostasis in an animal model of Alzheimer's disease', *PLoS ONE*. Edited by S. D. Ginsberg, 12(1), p. e0170275. doi: 10.1371/journal.pone.0170275.
- Kato, H. K. *et al.* (2012) 'Dynamic Sensory Representations in the Olfactory Bulb: Modulation by Wakefulness and Experience', *Neuron*. NIH Public Access, 76(5), pp. 962–975. doi: 10.1016/j.neuron.2012.09.037.
- Kayed, R. *et al.* (2003) 'Common Structure of Soluble Amyloid Oligomers Implies Common Mechanism of Pathogenesis', *Science*. American Association for the Advancement of Science, 300(5618), pp. 486–489. doi: 10.1126/science.1079469.
- Kayed, R. and Lasagna-Reeves, C. A. (2012) 'Molecular Mechanisms of Amyloid Oligomers Toxicity', *Journal of Alzheimer's Disease*. Edited by G. Perry et al. IOS Press, 33(s1), pp. S67–S78. doi: 10.3233/JAD-2012-129001.
- Kepp, K. P. (2016) 'Alzheimer's disease due to loss of function: A new synthesis of the available data.', *Progress in neurobiology*. Elsevier Ltd, 143, pp. 36–60. doi: 10.1016/j.pneurobio.2016.06.004.
- Kerr, J. N. D. and Denk, W. (2008) 'Imaging in vivo: watching the brain in action', *Nature reviews. Neuroscience*, 9(3), pp. 195–205. doi: 10.1038/nrn2338.
- Kerr, J. N. D., Greenberg, D. and Helmchen, F. (2005) 'From The Cover: Imaging input and output of neocortical networks in vivo', *Proceedings of the National Academy of Sciences*, 102(39), pp. 14063–14068. doi: 10.1073/pnas.0506029102.
- Keskin, A. D. *et al.* (2017) 'BACE inhibition-dependent repair of Alzheimer's pathophysiology', *Proceedings of the National Academy of Sciences*, 114(32), pp. 8631–8636. doi: 10.1073/pnas.1708106114.
- Kim, J. H. *et al.* (2001) 'Use-dependent effects of amyloidogenic fragments of (beta)-amyloid precursor protein on synaptic plasticity in rat hippocampus in vivo', *Journal of Neuroscience*, 21(4), pp. 1327–1333. Available at: <http://www.jneurosci.org/content/21/4/1327.short> (Accessed: 29 March 2017).
- Klein, W. L. (2006) 'Synaptic targeting by A $\beta$  oligomers (ADDLS) as a basis for memory loss in early Alzheimer's disease', *Alzheimer's and Dementia*, pp. 43–55. doi: 10.1016/j.jalz.2005.11.003.

- Klunk, W. E. *et al.* (2002) 'Imaging A-beta plaques in living transgenic mice with multiphoton microscopy and methoxy-X04, a systemically administered Congo red derivative.', *Journal of neuropathology and experimental neurology*. Oxford University Press, 61(9), pp. 797–805. doi: 10.1093/jnen/61.9.797.
- Klyubin, I. *et al.* (2014) 'Peripheral administration of a humanized anti-PrP antibody blocks Alzheimer's disease A $\beta$  synaptotoxicity.', *The Journal of neuroscience: the official journal of the Society for Neuroscience*, 34(18), pp. 6140–5. doi: 10.1523/JNEUROSCI.3526-13.2014.
- De Kock, C. P. J. and Sakmann, B. (2008) 'High frequency action potential bursts ( $\geq 100$  Hz) in L2/3 and L5B thick tufted neurons in anaesthetized and awake rat primary somatosensory cortex', *The Journal of Physiology*. Blackwell Publishing Ltd, 586(14), pp. 3353–3364. doi: 10.1113/jphysiol.2008.155580.
- Koenigsknecht-Talboo, J. *et al.* (2008) 'Rapid Microglial Response Around Amyloid Pathology after Systemic Anti-A Antibody Administration in PDAPP Mice', *Journal of Neuroscience*, 28(52), pp. 14156–14164. doi: 10.1523/JNEUROSCI.4147-08.2008.
- Koffie, R. M. *et al.* (2009) 'Oligomeric amyloid associates with postsynaptic densities and correlates with excitatory synapse loss near senile plaques', *Proceedings of the National Academy of Sciences*, 106(10), pp. 4012–4017. doi: 10.1073/pnas.0811698106.
- Koh, M. T. *et al.* (2010) 'Treatment strategies targeting excess hippocampal activity benefit aged rats with cognitive impairment', *Neuropsychopharmacology*. Nature Publishing Group, 35(4), pp. 1016–1025. doi: 10.1038/npp.2009.207.
- Koistinaho, M. *et al.* (2001) 'Specific spatial learning deficits become severe with age in -amyloid precursor protein transgenic mice that harbor diffuse -amyloid deposits but do not form plaques', *Proceedings of the National Academy of Sciences*, 98(25), pp. 14675–14680. doi: 10.1073/pnas.261562998.
- Komiyama, T. *et al.* (2010) 'Learning-related fine-scale specificity imaged in motor cortex circuits of behaving mice', *Nature*. Nature Publishing Group, 464(7292), pp. 1182–1186. doi: 10.1038/nature08897.
- Kraepelin, E. (1910) 'Das senile und prasenile Irresein', in *Psychiatrie, ein Lehrbuch für Studierende und Ärzte*, pp. 593–632.
- Kreuzer, M. *et al.* (2010) 'Cross-approximate entropy of cortical local field potentials quantifies effects of anesthesia--a pilot study in rats.', *BMC neuroscience*. BioMed Central, 11(1), p. 122. doi: 10.1186/1471-2202-11-122.
- Krstic, D. and Knuesel, I. (2013) 'Deciphering the mechanism underlying late-onset Alzheimer disease.', *Nature reviews. Neurology*. Nature Publishing Group, 9(1), pp. 25–34. doi: 10.1038/nrneurol.2012.236.
- Kuchibhotla, K. V. *et al.* (2008) 'A $\beta$  plaques lead to aberrant regulation of calcium homeostasis in vivo resulting in structural and functional disruption of neuronal networks', *Neuron*, 59(2), pp. 214–25. doi: 10.1016/j.neuron.2008.06.008.
- Kuchibhotla, K. V. *et al.* (2009) 'Synchronous hyperactivity and intercellular calcium waves in astrocytes in Alzheimer mice', *Science*, 323(5918), pp. 1211–1215. doi: 10.1126/science.1169096.
- Kuchibhotla, K. V. *et al.* (2014) 'Neurofibrillary tangle-bearing neurons are functionally integrated in cortical circuits in vivo', *Proceedings of the National Academy of Sciences*. National Academy of Sciences, 111(1), pp. 510–514. doi: 10.1073/pnas.1318807111.
- Kumar, D. K. V. *et al.* (2016) 'Amyloid- peptide protects against microbial infection in mouse and worm models of Alzheimers disease', *Science Translational Medicine*. American Association for the

- Advancement of Science, 8(340), pp. 340ra72-340ra72. doi: 10.1126/scitranslmed.aaf1059.
- Kunz, L. *et al.* (2015) 'Reduced grid-cell-like representations in adults at genetic risk for Alzheimer's disease.', *Science (New York, N.Y.)*. American Association for the Advancement of Science, 350(6259), pp. 430–3. doi: 10.1126/science.aac8128.
- Kurudenkandy, F. R. *et al.* (2014) 'Amyloid- $\beta$ -induced action potential desynchronization and degradation of hippocampal gamma oscillations is prevented by interference with peptide conformation change and aggregation.', *The Journal of neuroscience: the official journal of the Society for Neuroscience*, 34(34), pp. 11416–25. doi: 10.1523/JNEUROSCI.1195-14.2014.
- Kurz, A. and Perneczky, R. (2011) 'Novel insights for the treatment of Alzheimer's disease', *Progress in Neuro-Psychopharmacology and Biological Psychiatry*, 35(2), pp. 373–379. doi: 10.1016/j.pnpbp.2010.07.018.
- Lalonde, R. *et al.* (2005) 'Neurobehavioral characterization of APP23 transgenic mice with the SHIRPA primary screen', *Behavioural Brain Research*. Elsevier, 157(1), pp. 91–98. doi: 10.1016/J.BBR.2004.06.020.
- Lambert, M. P. *et al.* (1998) 'Diffusible, nonfibrillar ligands derived from A $\beta$ 1-42 are potent central nervous system neurotoxins.', *Proceedings of the National Academy of Sciences of the United States of America*. National Academy of Sciences, 95(11), pp. 6448–53. doi: 10.1073/pnas.95.11.6448.
- Lanz, T. A., Carter, D. B. and Merchant, K. M. (2003) 'Dendritic spine loss in the hippocampus of young PDAPP and Tg2576 mice and its prevention by the ApoE2 genotype.', *Neurobiology of disease*, 13(3), pp. 246–53. Available at: <http://www.ncbi.nlm.nih.gov/pubmed/12901839> (Accessed: 30 August 2018).
- Larner, A. J. and Doran, M. (2006) 'Clinical phenotypic heterogeneity of Alzheimer's disease associated with mutations of the presenilin-1 gene', *Journal of Neurology*. Steinkopff-Verlag, 253(2), pp. 139–158. doi: 10.1007/s00415-005-0019-5.
- Larson, E. B. *et al.* (2004) 'Survival after Initial Diagnosis of Alzheimer Disease', *Annals of Internal Medicine*. American College of Physicians, 140(7), p. 501. doi: 10.7326/0003-4819-140-7-200404060-00008.
- Lasser-Ross, N. *et al.* (1991) 'High time resolution fluorescence imaging with a CCD camera', *Journal of neuroscience methods*, 36(2–3), pp. 253–261. Available at: <http://www.ncbi.nlm.nih.gov/pubmed/2062120> (Accessed: 10 March 2017).
- Le, R. *et al.* (2001) 'Plaque-induced abnormalities in neurite geometry in transgenic models of Alzheimer disease: Implications for neural system disruption', *Journal of Neuropathology and Experimental Neurology*. Oxford University Press, 60(8), pp. 753–758. doi: 10.1093/jnen/60.8.753.
- Leal, S. L. *et al.* (2017) 'Hippocampal activation is associated with longitudinal amyloid accumulation and cognitive decline', *eLife*, 6. doi: 10.7554/eLife.22978.
- Lecanu, L., Greeson, J. and Papadopoulos, V. (2005) 'Beta-amyloid and oxidative stress jointly induce neuronal death, amyloid deposits, gliosis, and memory impairment in the rat brain', *Pharmacology*, 76(1), pp. 19–33. doi: 10.1159/000088929.
- Lecoq, J. *et al.* (2014) 'Visualizing mammalian brain area interactions by dual-axis two-photon calcium imaging', *Nature neuroscience*, 17(12), pp. 1825–1829. doi: 10.1038/nn.3867.
- Lehman, E. J. H. *et al.* (2003) 'Genetic background regulates beta-amyloid precursor protein processing and beta-amyloid deposition in the mouse', *Human molecular genetics*, 12(22), pp. 2949–56. doi: 10.1093/hmg/ddg322.
- Lesné, S. *et al.* (2006) 'A specific amyloid- $\beta$  protein assembly in the brain impairs memory', *Nature*,

440(7082), pp. 352–357. doi: 10.1038/nature04533.

Li, S. *et al.* (2009) ‘Soluble oligomers of amyloid-beta protein facilitate hippocampal long-term depression by disrupting neuronal glutamate uptake.’, *Neuron*. Cell Press, 62(6), pp. 788–801. doi: 10.1016/j.neuron.2009.05.012.

Lichtman, J. W. and Denk, W. (2011) ‘The Big and the Small: Challenges of Imaging the Brain’s Circuits’, *Science*, 334(6056), pp. 618–623. doi: 10.1126/science.1209168.

Liebscher, S. *et al.* (2014) ‘Chronic gamma-secretase inhibition reduces amyloid plaque-associated instability of pre- and postsynaptic structures.’, *Molecular psychiatry*. Nature Publishing Group, 19(8), pp. 937–946. doi: 10.1038/mp.2013.122.

Liebscher, S. *et al.* (2016) ‘Selective Persistence of Sensorimotor Mismatch Signals in Visual Cortex of Behaving Alzheimer’s Disease Mice’, *Current biology: CB*, 26(7), pp. 956–64. doi: 10.1016/j.cub.2016.01.070.

Liebscher, S. and Meyer-Luehmann, M. (2012) ‘A Peephole into the Brain: Neuropathological Features of Alzheimer’s Disease Revealed by in vivo Two-Photon Imaging’, *Frontiers in psychiatry*. Frontiers Media SA, 3(APR), p. 26. doi: 10.3389/fpsyt.2012.00026.

Limon, A., Reyes-Ruiz, J. M. and Milei, R. (2012) ‘Loss of functional GABAA receptors in the Alzheimer diseased brain’, *Proceedings of the National Academy of Sciences*. National Academy of Sciences, 109(25), pp. 10071–10076. doi: 10.1073/pnas.1204606109.

Linden, D. E. J. (2012) ‘The challenges and promise of neuroimaging in psychiatry’, *Neuron*, 73(1), pp. 8–22. doi: 10.1016/j.neuron.2011.12.014.

Lippa, C. F. and Morris, J. C. (2006) ‘Alzheimer neuropathology in nondemented aging: Keeping mind over matter’, *Neurology*, 27 June, pp. 1801–1802. doi: 10.1212/01.wnl.0000234879.82633.f3.

Liu, L. *et al.* (2004) ‘Role of NMDA Receptor Subtypes in Governing the Direction of Hippocampal Synaptic Plasticity’, *Science*, 304(5673), pp. 1021–1024. doi: 10.1126/science.1096615.

Low, R. J., Gu, Y. and Tank, D. W. (2014) ‘Cellular resolution optical access to brain regions in fissures: imaging medial prefrontal cortex and grid cells in entorhinal cortex.’, *Proceedings of the National Academy of Sciences of the United States of America*. National Academy of Sciences, 111(52), pp. 18739–44. doi: 10.1073/pnas.1421753111.

Ludewig, S. and Korte, M. (2016) ‘Novel Insights into the Physiological Function of the APP (Gene) Family and Its Proteolytic Fragments in Synaptic Plasticity.’, *Frontiers in molecular neuroscience*. Frontiers Media SA, 9, p. 161. doi: 10.3389/fnmol.2016.00161.

Lue, L. F. *et al.* (1996) ‘Inflammation, A beta deposition, and neurofibrillary tangle formation as correlates of Alzheimer’s disease neurodegeneration.’, *Journal of neuropathology and experimental neurology*, 55(10), pp. 1083–8. Available at: <http://www.ncbi.nlm.nih.gov/pubmed/8858005> (Accessed: 30 August 2018).

Lustbader, J. W. *et al.* (2004) ‘ABAD Directly Links A $\beta$  to Mitochondrial Toxicity in Alzheimer’s Disease’, *Science*, 304(5669), pp. 448–452. doi: 10.1126/science.1091230.

Lütcke, H. (2010) ‘Optical recording of neuronal activity with a genetically-encoded calcium indicator in anesthetized and freely moving mice’, *Frontiers in Neural Circuits*. Frontiers, 4(April), p. 9. doi: 10.3389/fncir.2010.00009.

Mably, A. J. *et al.* (2017) ‘Impairments in spatial representations and rhythmic coordination of place cells in the 3xTg mouse model of Alzheimer’s disease’, *Hippocampus*. Wiley-Blackwell, 27(4), pp. 378–392. doi: 10.1002/hipo.22697.

- Machulda, M. M. *et al.* (2011) 'Effect of APOE epsilon4 status on intrinsic network connectivity in cognitively normal elderly subjects.', *Archives of neurology*. United States, 68(9), pp. 1131–1136. doi: 10.1001/archneurol.2011.108.
- Maia, L. F. *et al.* (2013) 'Changes in amyloid- $\beta$  and Tau in the cerebrospinal fluid of transgenic mice overexpressing amyloid precursor protein', *Science translational medicine*, 5(194), p. 194re2. doi: 10.1126/scitranslmed.3006446.
- Maloney, J. A. *et al.* (2014) 'Molecular mechanisms of Alzheimer disease protection by the A673T allele of amyloid precursor protein', *Journal of Biological Chemistry*, 289(45), pp. 30990–31000. doi: 10.1074/jbc.M114.589069.
- Manczak, M. *et al.* (2006) 'Mitochondria are a direct site of A $\beta$  accumulation in Alzheimer's disease neurons: Implications for free radical generation and oxidative damage in disease progression', *Human Molecular Genetics*, 15(9), pp. 1437–1449. doi: 10.1093/hmg/ddl066.
- Mandybur, T. I. (1975) 'The incidence of cerebral amyloid angiopathy in Alzheimer's disease', *Neurology*. Wolters Kluwer Health, Inc. on behalf of the American Academy of Neurology, 25(2), pp. 120–126. doi: 10.1212/WNL.25.2.120.
- Mank, M. *et al.* (2008) 'A genetically encoded calcium indicator for chronic in vivo two-photon imaging', *Nature methods*. Nature Publishing Group, 5(9), pp. 805–811. doi: 10.1038/nmeth.1243.
- Mank, M. and Griesbeck, O. (2008) 'Genetically encoded calcium indicators', *Chemical Reviews*, pp. 1550–1564. doi: 10.1021/cr078213v.
- Marshall, L. *et al.* (2006) 'Boosting slow oscillations during sleep potentiates memory', *Nature*, 444(7119), pp. 610–613. doi: 10.1038/nature05278.
- Martinez-Losa, M. *et al.* (2018) 'Nav1.1-Overexpressing Interneuron Transplants Restore Brain Rhythms and Cognition in a Mouse Model of Alzheimer's Disease', *Neuron*. Cell Press, 98(1), pp. 75–89.e5. doi: 10.1016/j.neuron.2018.02.029.
- Masters, C. L. *et al.* (2015) 'Alzheimer's disease.', *Nature reviews. Disease primers*. Macmillan Publishers Limited, 1, p. 15056. doi: 10.1038/nrdp.2015.56.
- Masters, C. L. and Selkoe, D. J. (2012) 'Biochemistry of amyloid  $\beta$ -protein and amyloid deposits in Alzheimer disease', *Cold Spring Harbor Perspectives in Medicine*. Cold Spring Harbor Laboratory Press, p. a006262. doi: 10.1101/cshperspect.a006262.
- Mathys, Z. K. and White, A. R. (2017) 'Copper and Alzheimer's Disease', in *Advances in Neurobiology*. Springer, Cham, pp. 199–216. doi: 10.1007/978-3-319-60189-2\_10.
- Mattson, M. P. (1997) 'Cellular actions of beta-amyloid precursor protein and its soluble and fibrillogenic derivatives', *Physiological Reviews*, 77(4), pp. 1081–1132. doi: 10.1152/physrev.1997.77.4.1081.
- Mattsson, N. *et al.* (2009) 'CSF Biomarkers and Incipient Alzheimer Disease in Patients With Mild Cognitive Impairment', *JAMA*. American Medical Association, 302(4), p. 385. doi: 10.1001/jama.2009.1064.
- Mawuenyega, K. G. *et al.* (2010) 'Decreased clearance of CNS  $\beta$ -amyloid in Alzheimer's disease', *Science*, 330(6012), p. 1774. doi: 10.1126/science.1197623.
- Mayeux, R. and Stern, Y. (2012) 'Epidemiology of Alzheimer disease', *Cold Spring Harbor Perspectives in Medicine*, 2(8), pp. a006239–a006239. doi: 10.1101/cshperspect.a006239.
- Mc Donald, J. M. *et al.* (2010) 'The presence of sodium dodecyl sulphate-stable A $\beta$  dimers is strongly associated with Alzheimer-type dementia', *Brain*. Oxford University Press, 133(5), pp.

1328–1341. doi: 10.1093/brain/awq065.

McKhann, G. M. *et al.* (2011) ‘The diagnosis of dementia due to Alzheimer’s disease: Recommendations from the National Institute on Aging-Alzheimer’s Association workgroups on diagnostic guidelines for Alzheimer’s disease’, *Alzheimer’s & Dementia*. Elsevier, 7(3), pp. 263–269. doi: 10.1016/j.jalz.2011.03.005.

McLellan, M. E. *et al.* (2003) ‘In vivo imaging of reactive oxygen species specifically associated with thioflavine S-positive amyloid plaques by multiphoton microscopy.’, *The Journal of neuroscience: the official journal of the Society for Neuroscience*. Society for Neuroscience, 23(6), pp. 2212–2217. doi: 10.1523/JNEUROSCI.23-06.2003

Meyer-Luehmann, M. *et al.* (2008) ‘Rapid appearance and local toxicity of amyloid-beta plaques in a mouse model of Alzheimer’s disease.’, *Nature*. Nature Publishing Group, 451(7179), pp. 720–724. doi: 10.1038/nature06616.

Miller, J.-E. K. *et al.* (2014) ‘Visual stimuli recruit intrinsically generated cortical ensembles’, *Proceedings of the National Academy of Sciences of the United States of America*, 111(38), pp. E4053–61. doi: 10.1073/pnas.1406077111.

Minkeviciene, R. *et al.* (2009) ‘Amyloid -Induced Neuronal Hyperexcitability Triggers Progressive Epilepsy’, *Journal of Neuroscience*, 29(11), pp. 3453–3462. doi: 10.1523/JNEUROSCI.5215-08.2009.

Miyawaki, A. *et al.* (1997) ‘Fluorescent indicators for Ca<sup>2+</sup> based on green fluorescent proteins and calmodulin’, *Nature*. Nature Publishing Group, 388(August), pp. 882–887. doi: 10.1038/42264.

Moechars, D. *et al.* (1999) ‘Early phenotypic changes in transgenic mice that overexpress different mutants of amyloid precursor protein in brain.’, *The Journal of biological chemistry*. American Society for Biochemistry and Molecular Biology, 274(10), pp. 6483–92. doi: 10.1074/JBC.274.10.6483.

Montagna, E., Dorostkar, M. M. and Herms, J. (2017) ‘The Role of APP in Structural Spine Plasticity’, *Frontiers in Molecular Neuroscience*. Frontiers, 10, p. 136. doi: 10.3389/fnmol.2017.00136.

Morgan, D. *et al.* (2000) ‘A $\beta$  peptide vaccination prevents memory loss in an animal model of Alzheimer’s disease’, *Nature*, 408(6815), pp. 982–985. doi: 10.1038/35050116.

Morris, M. *et al.* (2011) ‘The Many Faces of Tau’, *Neuron*. Cell Press, pp. 410–426. doi: 10.1016/j.neuron.2011.04.009.

Mott, R. T. and Hulette, C. M. (2005) ‘Neuropathology of Alzheimer’s Disease’, *Neuroimaging clinics of North America*. Elsevier, 15(4), pp. 755–765. doi: 10.1016/j.nic.2005.09.003.

Mucke, L. *et al.* (2000) ‘High-level neuronal expression of abeta 1-42 in wild-type human amyloid protein precursor transgenic mice: synaptotoxicity without plaque formation.’, *The Journal of neuroscience: the official journal of the Society for Neuroscience*. Society for Neuroscience, 20(11), pp. 4050–8. doi: 10.1523/JNEUROSCI.20-11-04050.2000.

Mukamel, E. A., Nimmerjahn, A. and Schnitzer, M. J. (2009) ‘Automated Analysis of Cellular Signals from Large-Scale Calcium Imaging Data’, *Neuron*, 63(6), pp. 747–760. doi: 10.1016/j.neuron.2009.08.009.

Nagai, T. *et al.* (2004) ‘Expanded dynamic range of fluorescent indicators for Ca<sup>2+</sup> by circularly permuted yellow fluorescent proteins’, *Proceedings of the National Academy of Sciences*. National Academy of Sciences, 101(29), pp. 10554–10559. doi: 10.1073/pnas.0400417101.

Nakai, J., Ohkura, M. and Imoto, K. (2001) ‘A high signal-to-noise Ca(2+) probe composed of a single green fluorescent protein’, *Nature biotechnology*. Nature Publishing Group, 19(2), pp. 137–41. doi: 10.1038/84397.

- Nathanson, J. L. *et al.* (2009) 'Preferential labeling of inhibitory and excitatory cortical neurons by endogenous tropism of adeno-associated virus and lentivirus vectors', *Neuroscience*. NIH Public Access, 161(2), pp. 441–450. doi: 10.1016/j.neuroscience.2009.03.032.
- Neher, E. (1995) 'The use of fura-2 for estimating ca buffers and ca fluxes', *Neuropharmacology*, 34(11), pp. 1423–1442. doi: 10.1016/0028-3908(95)00144-U.
- Newman, M., Ebrahimie, E. and Lardelli, M. (2014) 'Using the zebrafish model for Alzheimer's disease research.', *Frontiers in genetics*, 5(JUN), p. 189. doi: 10.3389/fgene.2014.00189.
- Nilsberth, C. *et al.* (2001) 'The "Arctic" APP mutation (E693G) causes Alzheimer's disease by enhanced A $\beta$  protofibril formation', *Nature Neuroscience*, 4(9), pp. 887–893. doi: 10.1038/nn0901-887.
- Nimmerjahn, A., Mukamel, E. A. and Schnitzer, M. J. (2009) 'Motor Behavior Activates Bergmann Glial Networks', *Neuron*, 62(3), pp. 400–412. doi: 10.1016/j.neuron.2009.03.019.
- Nimmrich, V. *et al.* (2008) 'Amyloid Oligomers (A 1-42 Globulomer) Suppress Spontaneous Synaptic Activity by Inhibition of P/Q-Type Calcium Currents', *Journal of Neuroscience*, 28(4), pp. 788–797. doi: 10.1523/JNEUROSCI.4771-07.2008.
- O'Brien, J. L. *et al.* (2010) 'Longitudinal fMRI in elderly reveals loss of hippocampal activation with clinical decline', *Neurology*. Lippincott Williams & Wilkins, 74(24), pp. 1969–1976. doi: 10.1212/WNL.0b013e3181e3966e.
- Oddo, S. *et al.* (2003) 'Triple-Transgenic Model of Alzheimer's Disease with Plaques and Tangles: Intracellular A $\beta$  and Synaptic Dysfunction', *Neuron*. Cell Press, 39(3), pp. 409–421. doi: 10.1016/S0896-6273(03)00434-3.
- Oh, H. *et al.* (2014) 'Covarying alterations in A $\beta$  deposition, glucose metabolism, and gray matter volume in cognitively normal elderly', *Human Brain Mapping*, 35(1), pp. 297–308. doi: 10.1002/hbm.22173.
- Ohki, K. *et al.* (2005) 'Functional imaging with cellular resolution reveals precise micro-architecture in visual cortex', *Nature*, 433(7026), pp. 597–603. doi: 10.1038/nature03274.
- Ono, K. (2017) 'Alzheimer's disease as oligomeropathy', *Neurochemistry International*. doi: 10.1016/j.neuint.2017.08.010.
- Ossenkoppele, R. *et al.* (2015) 'Prevalence of Amyloid PET Positivity in Dementia Syndromes', *JAMA*. American Medical Association, 313(19), p. 1939. doi: 10.1001/jama.2015.4669.
- Packer, A. M. *et al.* (2012) 'Two-photon optogenetics of dendritic spines and neural circuits.', *Nature methods*, 9(12), pp. 1202–5. doi: 10.1038/nmeth.2249.
- Packer, A. M. *et al.* (2015) 'Simultaneous all-optical manipulation and recording of neural circuit activity with cellular resolution in vivo.', *Nature methods*, 12(2), pp. 140–6. doi: 10.1038/nmeth.3217.
- Palmer, A. E. *et al.* (2006) 'Ca<sup>2+</sup> Indicators Based on Computationally Redesigned Calmodulin-Peptide Pairs', *Chemistry & Biology*, 13(5), pp. 521–530. doi: 10.1016/j.chembiol.2006.03.007.
- Palop, J. J. *et al.* (2007) 'Aberrant Excitatory Neuronal Activity and Compensatory Remodeling of Inhibitory Hippocampal Circuits in Mouse Models of Alzheimer's Disease', *Neuron*. Cell Press, 55(5), pp. 697–711. doi: 10.1016/j.neuron.2007.07.025.
- Palop, J. J. and Mucke, L. (2009) 'Epilepsy and Cognitive Impairments in Alzheimer Disease', *Archives of Neurology*. American Medical Association, 66(4), p. 435. doi: 10.1001/archneurol.2009.15.
- Palop, Jorge J and Mucke, L. (2010) 'Amyloid- $\beta$ -induced neuronal dysfunction in Alzheimer's disease: from synapses toward neural networks', *Nature Neuroscience*. Nature Publishing Group,

13(7), pp. 812–818. doi: 10.1038/nn.2583.

Palop, Jorge J. and Mucke, L. (2010) ‘Synaptic depression and aberrant excitatory network activity in Alzheimer’s disease: Two faces of the same coin?’, *NeuroMolecular Medicine*. Humana Press Inc, pp. 48–55. doi: 10.1007/s12017-009-8097-7.

Paredes, R. M. *et al.* (2008) ‘Chemical calcium indicators’, *Methods*, 46(3), pp. 143–151. doi: 10.1016/j.ymeth.2008.09.025.

Patterson, M. A., Lagier, S. and Carleton, A. (2013) ‘Odor representations in the olfactory bulb evolve after the first breath and persist as an odor afterimage.’, *Proceedings of the National Academy of Sciences of the United States of America*, 110(35), pp. E3340–9. doi: 10.1073/pnas.1303873110.

Pekny, M. *et al.* (2016) ‘Astrocytes: a central element in neurological diseases’, *Acta Neuropathologica*. Springer Berlin Heidelberg, pp. 323–345. doi: 10.1007/s00401-015-1513-1.

Penzes, P. *et al.* (2011) ‘Dendritic spine pathology in neuropsychiatric disorders.’, *Nature neuroscience*. Nature Publishing Group, 14(3), pp. 285–93. doi: 10.1038/nn.2741.

Persson, J. *et al.* (2008) ‘Altered deactivation in individuals with genetic risk for Alzheimer’s disease’, *Neuropsychologia*. Pergamon, 46(6), pp. 1679–1687. doi: 10.1016/j.neuropsychologia.2008.01.026.

Perusini, G. (1991) ‘The nosographic value of some characteristic histopathologic findings in senility’, *Rivista italiana di Neuropathologia, Psichiatria ed Elettroterapia*, 4, pp. 193–213.

Peters, A. J., Chen, S. X. and Komiyama, T. (2014) ‘Emergence of reproducible spatiotemporal activity during motor learning.’, *Nature*. Nature Publishing Group, 510(7504), pp. 263–7. doi: 10.1038/nature13235.

Peters, F. *et al.* (2018) ‘BACE1 inhibition more effectively suppresses initiation than progression of  $\beta$ -amyloid pathology’, *Acta Neuropathologica*. Springer Berlin Heidelberg, 135(5), pp. 695–710. doi: 10.1007/s00401-017-1804-9.

Petersen, R. C. *et al.* (2009) ‘Mild cognitive impairment: Ten years later’, *Archives of Neurology*. American Medical Association, pp. 1447–1455. doi: 10.1001/archneurol.2009.266.

Piston, D. W. (2005) ‘When Two Is Better Than One: Elements of Intravital Microscopy’, *PLoS Biology*. Public Library of Science, 3(6), p. e207. doi: 10.1371/journal.pbio.0030207.

Poisnel, G. *et al.* (2012) ‘Increased regional cerebral glucose uptake in an APP/PS1 model of Alzheimer’s disease.’, *Neurobiology of aging*, 33(9), pp. 1995–2005. doi: 10.1016/j.neurobiolaging.2011.09.026.

Pooler, A. M. *et al.* (2013) ‘Propagation of tau pathology in Alzheimer’s disease: identification of novel therapeutic targets’, *Alzheimer’s Research & Therapy*. BioMed Central, 5(5), p. 49. doi: 10.1186/alzrt214.

Pratim Bose, P. *et al.* (2010) ‘Effects of Congo Red on A $\beta$  1–40 Fibril Formation Process and Morphology’, *ACS Chemical Neuroscience*. American Chemical Society, 1(4), pp. 315–324. doi: 10.1021/cn900041x.

Prince, M. *et al.* (2013) ‘The global prevalence of dementia: a systematic review and metaanalysis’, *Alzheimer’s & dementia: the journal of the Alzheimer’s Association*, 9(1), pp. 63–75.e2. doi: 10.1016/j.jalz.2012.11.007.

Prvulovic, D. *et al.* (2005) ‘Functional activation imaging in aging and dementia’, *Psychiatry Research - Neuroimaging*, pp. 97–113. doi: 10.1016/j.psychresns.2005.06.006.

Putch, D. *et al.* (2011) ‘Hippocampal Hyperactivation Associated with Cortical Thinning in Alzheimer’s Disease Signature Regions in Non-Demented Elderly Adults’, *Journal of Neuroscience*.

- Society for Neuroscience, 31(48), pp. 17680–17688. doi: 10.1523/JNEUROSCI.4740-11.2011.
- Puzzo, D. *et al.* (2015a) ‘Rodent models for Alzheimer’s disease drug discovery’, *Expert Opinion on Drug Discovery*. Informa Healthcare, 10(7), pp. 703–711. doi: 10.1517/17460441.2015.1041913.
- Puzzo, D. *et al.* (2015b) ‘Rodent models for Alzheimer’s disease drug discovery’, *Expert opinion on drug discovery*, 10(7), pp. 703–11. doi: 10.1517/17460441.2015.1041913.
- Quirin, S. *et al.* (2014) ‘Simultaneous imaging of neural activity in three dimensions.’, *Frontiers in neural circuits*. Frontiers, 8(April), p. 29. doi: 10.3389/fncir.2014.00029.
- Quiroz, Y. T. *et al.* (2010) ‘Hippocampal hyperactivation in presymptomatic familial Alzheimer’s disease’, *Annals of Neurology*. Wiley-Blackwell, 68(6), pp. 865–875. doi: 10.1002/ana.22105.
- Quist, A. *et al.* (2005) ‘Amyloid ion channels: A common structural link for protein-misfolding disease’, *Proceedings of the National Academy of Sciences*, 102(30), pp. 10427–10432. doi: 10.1073/pnas.0502066102.
- Radde, R. *et al.* (2006) ‘Abeta42-driven cerebral amyloidosis in transgenic mice reveals early and robust pathology’, *EMBO reports*, 7(9), pp. 940–6. doi: 10.1038/sj.embor.7400784.
- Radde, R. *et al.* (2008) ‘The value of incomplete mouse models of Alzheimer’s disease’, *European Journal of Nuclear Medicine and Molecular Imaging*, 35(S1), pp. 70–74. doi: 10.1007/s00259-007-0704-y.
- Rak, M. *et al.* (2007) ‘Dense-core and diffuse A $\beta$  plaques in TgCRND8 mice studied with synchrotron FTIR microspectroscopy’, *Biopolymers*, 87(4), pp. 207–217. doi: 10.1002/bip.20820.
- Redlich E. (1898) ‘Uber miliare Sklerose der hirnrinde bei seniler Atrophie’, *Jahrb Psychiatry Neurol*, 17, pp. 208–216. Available at: <https://ci.nii.ac.jp/naid/10024160802/> (Accessed: 15 January 2018).
- Rentz, D. M. *et al.* (2010) ‘Cognition, reserve, and amyloid deposition in normal aging’, *Annals of Neurology*. Wiley-Blackwell, 67(3), pp. 353–364. doi: 10.1002/ana.21904.
- Rickgauer, J. P., Deisseroth, K. and Tank, D. W. (2014) ‘Simultaneous cellular-resolution optical perturbation and imaging of place cell firing fields’, *Nature neuroscience*, 17(12), pp. 1816–24. doi: 10.1038/nn.3866.
- Robakis, N. K. *et al.* (1987) ‘Molecular Cloning and Characterization of a cDNA Encoding the Cerebrovascular and the Neuritic Plaque Amyloid Peptides’, *Proceedings of the National Academy of Sciences*, 84(12), pp. 4190–4194. Available at: <http://www.ncbi.nlm.nih.gov/pubmed/3035574> (Accessed: 19 April 2018).
- Robbins, E. M. *et al.* (2006) ‘Kinetics of cerebral amyloid angiopathy progression in a transgenic mouse model of Alzheimer disease.’, *The Journal of neuroscience: the official journal of the Society for Neuroscience*, 26(2), pp. 365–71. doi: 10.1523/JNEUROSCI.3854-05.2006.
- Roberson, E. D. *et al.* (2011) ‘Amyloid- /Fyn-Induced Synaptic, Network, and Cognitive Impairments Depend on Tau Levels in Multiple Mouse Models of Alzheimer’s Disease’, *Journal of Neuroscience*. Society for Neuroscience, 31(2), pp. 700–11. doi: 10.1523/JNEUROSCI.4152-10.2011.
- Rose, T. *et al.* (2016) ‘Cell-specific restoration of stimulus preference after monocular deprivation in the visual cortex.’, *Science (New York, N.Y.)*, 352(6291), pp. 1319–22. doi: 10.1126/science.aad3358.
- Rosenblum, W. I. (2014) ‘Why Alzheimer trials fail: Removing soluble oligomeric beta amyloid is essential, inconsistent, and difficult’, *Neurobiology of Aging*. Elsevier, pp. 969–974. doi: 10.1016/j.neurobiolaging.2013.10.085.
- Rozkalne, A. *et al.* (2009) ‘A single dose of passive immunotherapy has extended benefits on

- synapses and neurites in an Alzheimer's disease mouse model', *Brain Research*. Elsevier, 1280, pp. 178–185. doi: 10.1016/j.brainres.2009.05.045.
- Rozkalne, A., Hyman, B. T. and Spires-Jones, T. L. (2011) 'Calcineurin inhibition with FK506 ameliorates dendritic spine density deficits in plaque-bearing Alzheimer model mice', *Neurobiology of Disease*, 41(3), pp. 650–654. doi: 10.1016/j.nbd.2010.11.014.
- Rudinskiy, N. *et al.* (2012) 'Orchestrated experience-driven Arc responses are disrupted in a mouse model of Alzheimer's disease', *Nature Neuroscience*. Nature Publishing Group, 15(10), pp. 1422–1429. doi: 10.1038/nn.3199.
- Rudolph, U. and Antkowiak, B. (2004) 'Molecular and neuronal substrates for general anaesthetics', *Nature Reviews Neuroscience*. Nature Publishing Group, 5(9), pp. 709–720. doi: 10.1038/nrn1496.
- Salloway, S. *et al.* (2014) 'Two Phase 3 Trials of Bapineuzumab in Mild-to-Moderate Alzheimer's Disease', *New England Journal of Medicine*. Massachusetts Medical Society, 370(4), pp. 322–333. doi: 10.1056/NEJMoa1304839.
- Sanchez-Mejia, R. O. *et al.* (2008) 'Phospholipase A2 reduction ameliorates cognitive deficits in a mouse model of Alzheimer's disease', *Nature Neuroscience*. Nature Publishing Group, 11(11), pp. 1311–1318. doi: 10.1038/nn.2213.
- Sanchez, P. E. *et al.* (2012) 'Levetiracetam suppresses neuronal network dysfunction and reverses synaptic and cognitive deficits in an Alzheimer's disease model.', *Proceedings of the National Academy of Sciences of the United States of America*. National Academy of Sciences, 109(42), pp. E2895-903. doi: 10.1073/pnas.1121081109.
- Sato, T. R. *et al.* (2007) 'The Functional Microarchitecture of the Mouse Barrel Cortex', *PLoS Biology*. Edited by D. Feldman. Public Library of Science, 5(7), p. e189. doi: 10.1371/journal.pbio.0050189.
- Scheff, S. W. *et al.* (2007) 'Synaptic alterations in CA1 in mild Alzheimer disease and mild cognitive impairment', *Neurology*. Lippincott Williams & Wilkins, 68(18), pp. 1501–1508. doi: 10.1212/01.wnl.0000260698.46517.8f.
- Scheff, S. W., DeKosky, S. T. and Price, D. A. (1990) 'Quantitative assessment of cortical synaptic density in Alzheimer's disease', *Neurobiology of Aging*, 11(1), pp. 29–37. doi: 10.1016/0197-4580(90)90059-9.
- Scheff, S. W. and Price, D. A. (1993) 'Synapse loss in the temporal lobe in Alzheimer's disease', *Annals of Neurology*. Wiley Subscription Services, Inc., A Wiley Company, 33(2), pp. 190–199. doi: 10.1002/ana.410330209.
- Schenk, D. *et al.* (1999) 'Immunization with amyloid- $\beta$  attenuates Alzheimer disease-like pathology in the PDAPP mouse', *Nature*, 400(6740), pp. 173–177. doi: 10.1038/22124.
- Schneider, L. S. *et al.* (2014) 'Clinical trials and late-stage drug development for Alzheimer's disease: An appraisal from 1984 to 2014', *Journal of Internal Medicine*, 275(3), pp. 251–283. doi: 10.1111/joim.12191.
- Sciacca, M. F. M. *et al.* (2012) 'Two-step mechanism of membrane disruption by A $\beta$  through membrane fragmentation and pore formation', *Biophysical Journal*, 103(4), pp. 702–710. doi: 10.1016/j.bpj.2012.06.045.
- Selkoe, D. J. (2002) 'Alzheimer's disease is a synaptic failure', *Science*. American Association for the Advancement of Science, 298(5594), pp. 789–791. doi: 10.1126/science.1074069.
- Selkoe, D. J. and Hardy, J. (2016) 'The amyloid hypothesis of Alzheimer's disease at 25 years', *EMBO Molecular Medicine*. EMBO Press, 8(6), pp. 595–608. doi: 10.15252/emmm.201606210.

- Selkoe, D. J. and Schenk, D. (2003) 'ALZHEIMER'S DISEASE: Molecular Understanding Predicts Amyloid-Based Therapeutics', *Annual Review of Pharmacology and Toxicology*, 43(1), pp. 545–584. doi: 10.1146/annurev.pharmtox.43.100901.140248.
- Sepulveda-Falla, D., Glatzel, M. and Lopera, F. (2012) 'Phenotypic profile of early-onset familial Alzheimer's disease caused by presenilin-1 E280A mutation', *Journal of Alzheimer's Disease*. IOS Press, pp. 1–12. doi: 10.3233/JAD-2012-120907.
- Serneels, L. *et al.* (2009) 'gamma-Secretase heterogeneity in the Aph1 subunit: relevance for Alzheimer's disease', *Science (New York, N.Y.)*, 324(5927), pp. 639–42. doi: 10.1126/science.1171176.
- Serrano-Pozo, A., Frosch, M. P., *et al.* (2011) 'Neuropathological alterations in Alzheimer disease', *Cold Spring Harbor perspectives in medicine*. Cold Spring Harbor Laboratory Press, 1(1), p. a006189. doi: 10.1101/cshperspect.a006189.
- Serrano-Pozo, A., Mielke, M. L., *et al.* (2011) 'Reactive glia not only associates with plaques but also parallels tangles in Alzheimer's disease', *American Journal of Pathology*. Elsevier, 179(3), pp. 1373–1384. doi: 10.1016/j.ajpath.2011.05.047.
- Seubert, P. *et al.* (1992) 'Isolation and quantification of soluble Alzheimer's  $\beta$ -peptide from biological fluids', *Nature*, 359(6393), pp. 325–327. doi: 10.1038/359325a0.
- Sevigny, J. *et al.* (2015) 'Aducanumab (BIIB037), an anti-amyloid beta monoclonal antibody, in patients with prodromal or mild Alzheimer's disease: Interim results of a randomized, double-blind, placebo controlled, phase 1b study', *Alzheimer's and Dementia*. Elsevier, 11(7 SUPPL. 1), p. P277. doi: 10.1016/j.jalz.2015.07.367.
- Shah, R. S. *et al.* (2008) 'Current approaches in the treatment of Alzheimer's disease', *Biomedicine & Pharmacotherapy*. Elsevier Masson, 62(4), pp. 199–207. doi: 10.1016/J.BIOPHA.2008.02.005.
- Shankar, G. M. *et al.* (2007) 'Natural oligomers of the Alzheimer amyloid-beta protein induce reversible synapse loss by modulating an NMDA-type glutamate receptor-dependent signaling pathway.', *The Journal of neuroscience: the official journal of the Society for Neuroscience*, 27(11), pp. 2866–75. doi: 10.1523/JNEUROSCI.4970-06.2007.
- Shankar, G. M. *et al.* (2008) 'Amyloid- $\beta$  protein dimers isolated directly from Alzheimer's brains impair synaptic plasticity and memory', *Nature Medicine*. Nature Publishing Group, 14(8), pp. 837–842. doi: 10.1038/nm1782.
- Sheline, Y. I. *et al.* (2010) 'Amyloid Plaques Disrupt Resting State Default Mode Network Connectivity in Cognitively Normal Elderly', *Biological Psychiatry*. Elsevier, 67(6), pp. 584–587. doi: 10.1016/j.biopsych.2009.08.024.
- Shibata, M. *et al.* (2000) 'Clearance of Alzheimer's amyloid- $\beta$ 1-40peptide from brain by LDL receptor-related protein-1 at the blood-brain barrier', *Journal of Clinical Investigation*, 106(12), pp. 1489–1499. doi: 10.1172/JCI10498.
- Shimada, H. *et al.* (2011) 'Clinical course of patients with familial early-onset Alzheimer's disease potentially lacking senile plaques bearing the E693 $\Delta$  mutation in amyloid precursor protein', *Dementia and Geriatric Cognitive Disorders*, 32(1), pp. 45–54. doi: 10.1159/000330017.
- Shimomura, O., H. Johnson, F. and Saiga, Y. (1962) 'Extraction, Purification and Properties of Aequorin, a Bioluminescent Protein from the Luminous Hydromedusan, Aequorea', *J. Cell. and Comp. Physiol.*, 1353(165), pp. 223–239. doi: 10.1002/jcp.1030590302.
- Shoji, M. *et al.* (1992) 'Production of the Alzheimer amyloid beta protein by normal proteolytic processing', *Science*, 258(5079), pp. 126–129. doi: 10.1126/science.1439760.

- Silverman, D. H. *et al.* (2001) 'Positron emission tomography in evaluation of dementia: Regional brain metabolism and long-term outcome.', *JAMA: the journal of the American Medical Association*. American Medical Association, 286(17), pp. 2120–2127. doi: 10.1001/jama.286.17.2120.
- Šišková, Z. *et al.* (2014) 'Dendritic Structural Degeneration Is Functionally Linked to Cellular Hyperexcitability in a Mouse Model of Alzheimer's Disease', *Neuron*. Cell Press, 84(5), pp. 1023–1033. doi: 10.1016/j.neuron.2014.10.024.
- Smith, S. J. and Augustine, G. J. (1988) 'Calcium ions, active zones and synaptic transmitter release', *Trends in Neurosciences*, pp. 458–464. doi: 10.1016/0166-2236(88)90199-3.
- Snider, B. J. *et al.* (2005) 'Novel Presenilin 1 Mutation (S170F) Causing Alzheimer Disease With Lewy Bodies in the Third Decade of Life', *Archives of Neurology*. American Medical Association, 62(12), p. 1821. doi: 10.1001/archneur.62.12.1821.
- Snyder, E. M. *et al.* (2005) 'Regulation of NMDA receptor trafficking by amyloid- $\beta$ ', *Nature Neuroscience*. Nature Publishing Group, 8(8), pp. 1051–1058. doi: 10.1038/nn1503.
- Somavarapu, A. K. and Kepp, K. P. (2015) 'Direct Correlation of Cell Toxicity to Conformational Ensembles of Genetic A $\beta$  Variants', *ACS Chemical Neuroscience*. American Chemical Society, 6(12), pp. 1990–1996. doi: 10.1021/acscchemneuro.5b00238.
- Sorg, C. *et al.* (2007) 'Selective changes of resting-state networks in individuals at risk for Alzheimer's disease.', *Proceedings of the National Academy of Sciences of the United States of America*. United States, 104(47), pp. 18760–18765. doi: 10.1073/pnas.0708803104.
- Sorrentino, P. *et al.* (2014) 'The dark sides of amyloid in Alzheimer's disease pathogenesis', *FEBS Letters*, pp. 641–652. doi: 10.1016/j.febslet.2013.12.038.
- Sperling, R. A. *et al.* (2009) 'Amyloid Deposition Is Associated with Impaired Default Network Function in Older Persons without Dementia', *Neuron*. Cell Press, 63(2), pp. 178–188. doi: 10.1016/j.neuron.2009.07.003.
- Sperling, R. A. *et al.* (2011) 'Toward defining the preclinical stages of Alzheimer's disease: Recommendations from the National Institute on Aging-Alzheimer's Association workgroups on diagnostic guidelines for Alzheimer's disease', *Alzheimer's & Dementia*. Elsevier, 7(3), pp. 280–292. doi: 10.1016/j.jalz.2011.03.003.
- Spielmeyer, W. (1922) *Histopathologie des Nervensystems*.
- Spires-Jones, T. L. *et al.* (2009) 'Passive immunotherapy rapidly increases structural plasticity in a mouse model of Alzheimer disease', *Neurobiology of Disease*. Academic Press, 33(2), pp. 213–220. doi: 10.1016/j.nbd.2008.10.011.
- Spires-Jones, T. L. *et al.* (2011) 'Calcineurin inhibition with systemic FK506 treatment increases dendritic branching and dendritic spine density in healthy adult mouse brain', *Neuroscience Letters*, 487(3), pp. 260–263. doi: 10.1016/j.neulet.2010.10.033.
- Spires, T. L. (2005) 'Dendritic Spine Abnormalities in Amyloid Precursor Protein Transgenic Mice Demonstrated by Gene Transfer and Intravital Multiphoton Microscopy', *Journal of Neuroscience*, 25(31), pp. 7278–7287. doi: 10.1523/JNEUROSCI.1879-05.2005.
- Spires, T. L. and Hyman, B. T. (2004) 'Neuronal structure is altered by amyloid plaques', *Reviews in the Neurosciences*. De Gruyter, pp. 267–278. doi: 10.1515/REVNEURO.2004.15.4.267.
- Steiner, H. and Haass, C. (2000) 'Intramembrane proteolysis by presenilins [Review]', *Nature Reviews Molecular Cell Biology*. Nature Publishing Group, 1(December), pp. 217–224. doi: 10.1038/35043065.

- Steriade, M., Nuñez, A. and Amzica, F. (1993) 'A novel slow (< 1 Hz) oscillation of neocortical neurons in vivo: depolarizing and hyperpolarizing components.', *The Journal of neuroscience : the official journal of the Society for Neuroscience*. Society for Neuroscience, 13(8), pp. 3252–65. doi: 3252-3265.
- Stirman, J. N. *et al.* (2014) *Wide field-of-view, twin-region two-photon imaging across extended cortical networks*, *bioRxiv*. doi: 10.1101/011320.
- Stosiek, C. *et al.* (2003) 'In vivo two-photon calcium imaging of neuronal networks', *Proceedings of the National Academy of Sciences of the United States of America*, 100(12), pp. 7319–24. doi: 10.1073/pnas.1232232100.
- De Strooper, B. *et al.* (1998) 'Deficiency of presenilin-1 inhibits the normal cleavage of amyloid precursor protein', *Nature*, 391(6665), pp. 387–390. doi: 10.1038/34910.
- De Strooper, B. and Chávez Gutiérrez, L. (2015) 'Learning by Failing: Ideas and Concepts to Tackle  $\gamma$ -Secretases in Alzheimer's Disease and Beyond', *Annual Review of Pharmacology and Toxicology*. Annual Reviews, 55(1), pp. 419–437. doi: 10.1146/annurev-pharmtox-010814-124309.
- De Strooper, B. and Karran, E. (2016) 'The Cellular Phase of Alzheimer's Disease', *Cell*. Cell Press, pp. 603–615. doi: 10.1016/j.cell.2015.12.056.
- De Strooper, B., Vassar, R. and Golde, T. (2010) 'The secretases: Enzymes with therapeutic potential in Alzheimer disease', *Nature Reviews Neurology*, pp. 99–107. doi: 10.1038/nrneurol.2009.218.
- Svoboda, K. and Yasuda, R. (2006) 'Principles of two-photon excitation microscopy and its applications to neuroscience', *Neuron*, 50(6), pp. 823–39. doi: 10.1016/j.neuron.2006.05.019.
- Swandulla, D. *et al.* (1991) 'Role of residual calcium in synaptic depression and posttetanic potentiation: fast and slow calcium signaling in nerve terminals', *Neuron*, 7(6), pp. 915–26. doi: 10.1016/0896-6273(91)90337-Y.
- Tallini, Y. N. *et al.* (2006) 'Imaging cellular signals in the heart in vivo: Cardiac expression of the high-signal Ca<sup>2+</sup> indicator GCaMP2', *Proceedings of the National Academy of Sciences of the United States of America*, 103(12), pp. 4753–4758. doi: 10.1073/pnas.0509378103.
- Tallini, Y. N. *et al.* (2007) 'Propagated endothelial Ca<sup>2+</sup> waves and arteriolar dilation in vivo: Measurements in Cx40BAC-GCaMP2 transgenic mice', *Circulation Research*, 101(12), pp. 1300–1309. doi: 10.1161/CIRCRESAHA.107.149484.
- Tampellini, D. (2015) 'Synaptic activity and Alzheimer's disease: A critical update', *Frontiers in Neuroscience*. Frontiers Media SA, 9(NOV), p. 423. doi: 10.3389/fnins.2015.00423.
- Teich, A. F. and Arancio, O. (2012) 'Is the Amyloid Hypothesis of Alzheimer's disease therapeutically relevant?', *Biochemical Journal*, 446(2), pp. 165–177. doi: 10.1042/BJ20120653.
- Terry, R. D. *et al.* (1991) 'Physical basis of cognitive alterations in alzheimer's disease: Synapse loss is the major correlate of cognitive impairment', *Annals of Neurology*. Wiley Subscription Services, Inc., A Wiley Company, 30(4), pp. 572–580. doi: 10.1002/ana.410300410.
- Thal, D. R. *et al.* (2002) 'Phases of A beta-deposition in the human brain and its relevance for the development of AD.', *Neurology*. Wolters Kluwer Health, Inc. on behalf of the American Academy of Neurology, 58(12), pp. 1791–800. doi: 10.1212/WNL.58.12.1791.
- Thal, D. R. *et al.* (2006) 'The Development of Amyloid beta Protein Deposits in the Aged Brain', *Science of Aging Knowledge Environment*, 2006(6), pp. re1–re1. doi: 10.1126/sageke.2006.6.re1.
- Tian, L. *et al.* (2009) 'Imaging neural activity in worms, flies and mice with improved GCaMP calcium indicators', *Nature Methods*. Nature Publishing Group, 6(12), pp. 875–881. doi:

10.1038/nmeth.1398.

Tiwari, M. K. and Kepp, K. P. (2016) ' $\beta$ -Amyloid pathogenesis: Chemical properties versus cellular levels', *Alzheimer's and Dementia*. Elsevier, pp. 184–194. doi: 10.1016/j.jalz.2015.06.1895.

Tönnies, E. and Trushina, E. (2017) 'Oxidative Stress, Synaptic Dysfunction, and Alzheimer's Disease', *Journal of Alzheimer's Disease*. IOS Press, pp. 1105–1121. doi: 10.3233/JAD-161088.

Tramutola, A. *et al.* (2017) 'Oxidative stress, protein modification and Alzheimer disease', *Brain Research Bulletin*. Elsevier, pp. 88–96. doi: 10.1016/j.brainresbull.2016.06.005.

Tsai, J. *et al.* (2004) 'Fibrillar amyloid deposition leads to local synaptic abnormalities and breakage of neuronal branches.', *Nature neuroscience*. Nature Publishing Group, 7(11), pp. 1181–3. doi: 10.1038/nn1335.

Tsien, R. Y. (1980) 'New calcium indicators and buffers with high selectivity against magnesium and protons: design, synthesis, and properties of prototype structures', *Biochemistry*, 19(11), pp. 2396–404. doi: 6770893.

Tsien, R. Y. (1981) 'A non-disruptive technique for loading calcium buffers and indicators into cells', *Nature*, 290(5806), pp. 527–8. doi: 10.1038/290527a0.

Tsubuki, S., Takaki, Y. and Saido, T. C. (2003) 'Dutch, Flemish, Italian, and Arctic mutations of APP and resistance of A $\beta$  to physiologically relevant proteolytic degradation', *Lancet*, 361(9373), pp. 1957–1958. doi: 10.1016/S0140-6736(03)13555-6.

Um, J. W. *et al.* (2012) 'Alzheimer amyloid- $\beta$  oligomer bound to postsynaptic prion protein activates Fyn to impair neurons', *Nature Neuroscience*. Nature Publishing Group, 15(9), pp. 1227–1235. doi: 10.1038/nn.3178.

Urbanc, B. *et al.* (2002) 'Neurotoxic effects of thioflavin S-positive amyloid deposits in transgenic mice and Alzheimer's disease', *Proceedings of the National Academy of Sciences of the United States of America*. National Academy of Sciences, 99(22), pp. 13990–5. doi: 10.1073/pnas.222433299.

Vahle-Hinz, C. *et al.* (2001) 'Local GABAA Receptor Blockade Reverses Isoflurane's Suppressive Effects on Thalamic Neurons In Vivo', *Anesthesia and Analgesia*, 92(6), pp. 1578–1584. doi: 10.1097/0000539-200106000-00046.

Vahle-Hinz, C. *et al.* (2006) 'Contributions of GABAergic and glutamatergic mechanisms to isoflurane-induced suppression of thalamic somatosensory information transfer', *Experimental Brain Research*. Springer-Verlag, 176(1), pp. 159–172. doi: 10.1007/s00221-006-0604-6.

Vassar, R. *et al.* (1999) ' $\beta$ -Secretase cleavage of Alzheimer's amyloid precursor protein by the transmembrane aspartic protease BACE', *Science*, 286(5440), pp. 735–741. doi: 10.1126/science.286.5440.735.

Verhagen, J. V *et al.* (2007) 'Sniffing controls an adaptive filter of sensory input to the olfactory bulb', *Nature neuroscience*, 10(5), pp. 631–639. doi: 10.1038/nn1892.

Verret, L. *et al.* (2012) 'Inhibitory interneuron deficit links altered network activity and cognitive dysfunction in alzheimer model', *Cell*. Elsevier, 149(3), pp. 708–721. doi: 10.1016/j.cell.2012.02.046.

Vinters, H. V (1987) 'Cerebral amyloid angiopathy. A critical review.', *Stroke; a journal of cerebral circulation*, 18(2), pp. 311–24. doi: 10.1161/01.STR.18.2.311.

Vogelstein, J. T. *et al.* (2010) 'Fast Nonnegative Deconvolution for Spike Train Inference From Population Calcium Imaging', *Journal of Neurophysiology*, 104(6), pp. 3691–3704. doi: 10.1152/jn.01073.2009.

- Vogt, D. L. *et al.* (2011) ‘Abnormal neuronal networks and seizure susceptibility in mice overexpressing the APP intracellular domain.’, *Neurobiology of aging*. Elsevier, 32(9), pp. 1725–9. doi: 10.1016/j.neurobiolaging.2009.09.002.
- Võikar, V. *et al.* (2001) ‘Strain and gender differences in the behavior of mouse lines commonly used in transgenic studies’, *Physiology and Behavior*, 72(1–2), pp. 271–281. doi: 10.1016/S0031-9384(00)00405-4.
- Volicer, L., Smith, S. and Volicer, B. J. (1995) ‘Effect of Seizures on Progression of Dementia of the Alzheimer Type’, *Dementia and Geriatric Cognitive Disorders*. Karger Publishers, 6(5), pp. 258–263. doi: 10.1159/000106956.
- Vossel, K. A. *et al.* (2013) ‘Seizures and epileptiform activity in the early stages of Alzheimer disease’, *JAMA Neurology*. American Medical Association, 70(9), pp. 1158–1166. doi: 10.1001/jamaneurol.2013.136.
- Walsh, D. M. *et al.* (2002) ‘Naturally secreted oligomers of amyloid  $\beta$  protein potently inhibit hippocampal long-term potentiation in vivo’, *Nature*. Nature Publishing Group, 416(6880), pp. 535–539. doi: 10.1038/416535a.
- Walsh, D. M. (2005) ‘Certain Inhibitors of Synthetic Amyloid -Peptide (A ) Fibrillogenesis Block Oligomerization of Natural A and Thereby Rescue Long-Term Potentiation’, *Journal of Neuroscience*. Society for Neuroscience, 25(10), pp. 2455–2462. doi: 10.1523/JNEUROSCI.4391-04.2005.
- Wei, W. *et al.* (2010) ‘Amyloid beta from axons and dendrites reduces local spine number and plasticity’, *Nature Neuroscience*, 13(2), pp. 190–196. doi: 10.1038/nn.2476.
- Willem, M. *et al.* (2015) ‘ $\eta$ -Secretase processing of APP inhibits neuronal activity in the hippocampus.’, *Nature*, 526(7573), pp. 443–7. doi: 10.1038/nature14864.
- Wilson, I. A. *et al.* (2005) ‘Age-Associated Alterations of Hippocampal Place Cells Are Subregion Specific’, *Journal of Neuroscience*, 25(29), pp. 6877–6886. doi: 10.1523/JNEUROSCI.1744-05.2005.
- Wisniewski, K. E. *et al.* (1985) ‘Alzheimer’s disease in Down’s syndrome: Clinicopathologic studies’, *Neurology*, 35(7), pp. 957–957. doi: 10.1212/WNL.35.7.957.
- Wisniewski, T. and Sigurdsson, E. M. (2010) ‘Murine models of Alzheimer’s disease and their use in developing immunotherapies’, *Biochimica et biophysica acta*. Elsevier, 1802(10), pp. 847–859. doi: 10.1016/j.bbadis.2010.05.004.
- Wolfe, M. S. (2012) ‘Processive proteolysis by  $\gamma$ -secretase and the mechanism of Alzheimer’s disease’, in *Biological Chemistry*, pp. 899–905. doi: 10.1515/hsz-2012-0140.
- Woodhouse, A. *et al.* (2005) ‘Does  $\beta$ -amyloid plaque formation cause structural injury to neuronal processes?’, *Neurotoxicity Research*. Springer-Verlag, 7(1–2), pp. 5–15. doi: 10.1007/BF03033772.
- Xie, L. *et al.* (2013) ‘Sleep drives metabolite clearance from the adult brain’, *Science*, 342(6156), pp. 373–377. doi: 10.1126/science.1241224.
- Xie, Z. *et al.* (2013) ‘Interaction of anesthetics with neurotransmitter release machinery proteins’, *Journal of Neurophysiology*, 109(3), pp. 758–767. doi: 10.1152/jn.00666.2012.
- Yamada, Y. and Mikoshiba, K. (2012) ‘Quantitative comparison of novel GCaMP-type genetically encoded Ca<sup>2+</sup> indicators in mammalian neurons’, *Frontiers in Cellular Neuroscience*. Frontiers, 6(41), pp. 1–9. doi: 10.3389/fncel.2012.00041.
- Yamamoto, K. *et al.* (2015) ‘Chronic Optogenetic Activation Augments A $\beta$  Pathology in a Mouse Model of Alzheimer Disease’, *Cell Reports*. Cell Press, 11(6), pp. 859–865. doi: 10.1016/j.celrep.2015.04.017.

- Yang, G. *et al.* (2010) 'Thinned-skull cranial window technique for long-term imaging of the cortex in live mice', *Nature Protocols*. NIH Public Access, 5(2), pp. 201–208. doi: 10.1038/nprot.2009.222.
- Yankner, B. A. *et al.* (1989) 'Neurotoxicity of a fragment of the amyloid precursor associated with Alzheimer's disease.', *Science (New York, N.Y.)*, 245(4916), pp. 417–20. doi: 10.1126/science.2474201.
- Yankner, B. A., Lu, T. and Loerch, P. (2008) 'The Aging Brain', *Annual Review of Pathology: Mechanisms of Disease*. Annual Reviews, 3(1), pp. 41–66. doi: 10.1146/annurev.pathmechdis.2.010506.092044.
- Yankner, B., Duffy, L. and Kirschner, D. (1990) 'Neurotrophic and neurotoxic effects of amyloid beta protein: reversal by tachykinin neuropeptides', *Science*, 250(4978), pp. 279–282. doi: 10.1126/science.2218531.
- Yoshikai, S. *et al.* (1990) 'Genomic organization of the human amyloid beta-protein precursor gene', *Gene*, 87(2), pp. 257–263. doi: 10.1016/0378-1119(90)90310-N.
- Yoshiyama, Y. *et al.* (2007) 'Synapse Loss and Microglial Activation Precede Tangles in a P301S Tauopathy Mouse Model', *Neuron*, 53(3), pp. 337–351. doi: 10.1016/j.neuron.2007.01.010.
- You, H. *et al.* (2012) 'A neurotoxicity depends on interactions between copper ions, prion protein, and N-methyl-D-aspartate receptors', *Proceedings of the National Academy of Sciences*, 109(5), pp. 1737–1742. doi: 10.1073/pnas.1110789109.
- Yuan, P. and Grutzendler, J. (2016) 'Attenuation of  $\beta$ -Amyloid Deposition and Neurotoxicity by Chemogenetic Modulation of Neural Activity', *Journal of Neuroscience*, 36(2), pp. 632–641. doi: 10.1523/JNEUROSCI.2531-15.2016.
- Yuste, R. and Denk, W. (1995) 'Dendritic spines as basic functional units of neuronal integration', *Nature*, pp. 682–684. doi: 10.1038/375682a0.
- Zariwala, H. A. *et al.* (2012) 'A Cre-dependent GCaMP3 reporter mouse for neuronal imaging in vivo', *The Journal of neuroscience : the official journal of the Society for Neuroscience*, 32(9), pp. 3131–41. doi: 10.1523/JNEUROSCI.4469-11.2012.
- Zhang, J.-M. and An, J. (2007) 'Cytokines, inflammation, and pain.', *International anesthesiology clinics*. NIH Public Access, 45(2), pp. 27–37. doi: 10.1097/AIA.0b013e318034194e.
- Ziv, Y. *et al.* (2013) 'Long-term dynamics of CA1 hippocampal place codes.', *Nature neuroscience*, 16(3), pp. 264–6. doi: 10.1038/nn.3329.
- Zou, C. *et al.* (2016) 'Amyloid precursor protein maintains constitutive and adaptive plasticity of dendritic spines in adult brain by regulating D-serine homeostasis', *The EMBO Journal*. Wiley-Blackwell, 35(20), pp. 2213–2222. doi: 10.15252/embj.201694085.

# Acknowledgment

I would like to express my sincerest gratitude to the people who supported me in the completion of this PhD thesis.

I would like to thank my supervisor, Prof. Dr. Jochen Herms, for offering me the opportunity to carry out my PhD research in his lab, providing funding, equipment and other resources and members of my TAC, Dr. Dr. Sabine Liebscher, Prof. Dr. Armin Giese, Prof. Dr. Stefan Lichtenthaler, for their time and advice for my project.

I am grateful to all the lab members of Herms working group who helped me through my experimental work in the laboratory as well as while writing of this thesis. I am especially thankful to Dr. Petar Marinković for teaching me everything I know about the two-photon microscopy, for his support and encouragement and the suggestions and corrections of this thesis. I am thankful to Dr. Sonja Blumenstock, Dr. Mario Dorostkar, Dr. Severin Filser and Dr. Lidia Blazquez-Llorca for helping me learn cranial window implantations and other experimental techniques and Dr. Finn Peters for the support with MatLab, their advice and support. I would also like to thank peer PhD students Elena Montagna, Hazal Salihoglu, and Sophie Crux for their engagement, advice, and friendship that immensely helped me through hard times. I also thank Eric Griebinger, Sarah Hanselka, and Nadine Lachner for excellent technical support.

I am very grateful to the GSN for providing guidance and training, and for a chance to be part of a thriving, enthusiastic, and talented group of PhD students and faculty. Many of the fellow students who I met through GSN became dear friends, whose passion and dedication inspired me and served as an example. And I am especially grateful to Dian Anggraini (now Dr. Dian

Anggraini) for being there for me in difficult times, for seeing the best in me in my times of doubt and for literally contributing to the realization of this thesis through our writing sessions.

Moreover, I owe to GSN a prominent role in bringing this PhD project to life, as through GSN, I met two collaborators who immensely helped me with data processing and analysis. In this regard, I am thankful to Dr. Pieter Goltstein, who shared and adapted his MatLab scripts for my calcium data processing. And I am deeply grateful to Dr. Sabine Liebscher for her crucial help with data analysis, for fruitful discussions of the project's results, advice and her immense support and patience that helped me to finalize the project and this thesis.

Additionally, I want to express my gratitude to the people in my personal life for their unconditional support and love. I am incredibly grateful to my parents Liudmila and Valery and my sister Yana for always being on my side and supporting my decisions in life. I am thankful to the students I have the luxury to meet through coaching and to the English-speaking science communication community of Munich (and especially to 15x4 Munich) for a feeling of self-worth I gained through my extracurricular activities. I thank Daniil Pokrovsky, Anastasia Andrushenko, Ivan Timofeev, Evgeny Resnik and Russian Lunch group for making my time in Munich such a great experience and for their understanding and manifold support. And I am immensely grateful to Evgeny Labzin who every day inspires me to be myself and always strive for bringing my dreams to life.

And last but not least, I want to thank my colleagues at the IMPRS-LS coordination office, Dr. Hans-Joerg Schaeffer, Dr. Ingrid Wolf, and Maxi Reif, for their help, advice, support in finishing of this thesis and their patience for my German skills. It was a great pleasure to be a part of IMPRS-LS team and to get to know so many talented people during my time in the coordination office.

My road to this point was longer than I anticipated, and during the last six years, many more people, directly and indirectly, contributed to this PhD thesis. They helped me to find a new home in Munich, but at the same time to stay in touch with my native land and language, to find my strengths and grow points, to stay sane even in the hardest times and enjoy the little things. And I am sincerely grateful for this support!

# Curriculum Vitae

## Viktoria Korzhova

+49-157-3271-0898;  
[viktoria.korzhova@gmail.com](mailto:viktoria.korzhova@gmail.com)  
 Leonrodstr. 27 80636 Munich, Germany  
 Nationality: Russian  
 Date of birth: 20.11.1988

### Education

**PhD student, Ludwig Maximilian University**  
 Graduate school of Systemic Neuroscience

**Nov 2013 – Dec 2019**  
 Munich, Germany

**MSc, St. Petersburg State University**  
 Major – Physiology. *Diploma summa cum laude*

**Sep 2011 – Jul 2013**  
 St.Petersburg, Russia

**BSc, St. Petersburg State University**  
 Major – Genetics. *Diploma summa cum laude*

**Sep 2007 – Aug 2011**  
 St.Petersburg, Russia

### Research experience

**PhD student, German Center for Neurodegenerative Diseases (DZNE)**

**Nov 2013 – Oct 2017**  
 Munich, Germany

Supervisor – Prof. Jochen Herms

*PhD research project:* Investigation of neuronal activity in a murine model of Alzheimer's disease using *in vivo* two-photon calcium imaging

**Weizmann Institute of Science, Department of Biochemistry**

**Jul – Aug 2013**  
 Rehovot, Israel

Supervisor – Prof. Tony Futerman

*Summer research project:* cerebellar involvement in pathology of neuropathic Gaucher disease

**University of Texas, Southwestern Medical Center**

**Sep 2012 – Dec 2012**  
 Dallas, USA

Supervisor – Prof. Ilya Bezprozvanny

*Master research project:* synaptic dysfunction in a mouse model of Huntington's disease

**Lausanne University (UNIL)**

**Jul 2012 – Aug 2012**  
 Lausanne, Switzerland

Supervisor – Prof. Luc Pellerin

*Summer research project:* localization of monocarboxylate transporter MCT2 in lipid rafts

**Sechenov Institute of Evolutionary Physiology and Biochemistry**

**Sep 2011 – Jun 2012**  
 St. Petersburg, Russia

Supervisor – Dr. Yury Pastukhov

*Research project:* protective effects of heat shock protein Hsp70 in rat model of Parkinson's disease

**St. Petersburg State University, Department of Genetics**

**Sep 2008 – Jun 2011**  
 St. Petersburg, Russia

Supervisor – Dr. Alexander Rubel

*Bachelor research project:* development of experimental system to investigate the direct interactions of A $\beta$  peptide and Prion Protein using fluorescent microscopy

## Professional and volunteer experience

### Neurotar Oy Ltd

Application Specialist

Jun 2019 – current

Munich, Germany

- Sales and interaction with prospective clients
- Client support
- Social media and website management

### IMPRS-LS Coordination Office, Max Planck Institute for Biochemistry

scientific coordinator

Nov 2017 – Jun 2019

Munich, Germany

- Organization and management of soft skill courses for PhD students
- Evaluating the application of incoming PhD students and organizing the recruitment and selection of PhD students during the interview week
- Designing the career development program for the PhD students

### Science communication and public outreach activities

Organizer, speaker

2012 – current

Germany and Russia

- Organizer of the [15x4](#), science communication lectures, since 2017
- Director and organizer at the German chapter of the annual science festivals [Pint of Science](#) and [Soapbox Science](#) in Munich, since 2016
- Speaker at the Bavaria finals of science communication competition [FameLab](#), Regensburg, 2016
- Organizing team of [Kids Brain Day](#) at Ludwig-Maximilians University, Munich, 2016
- Author and editor of the Russian science communication website [Biomolecula.ru](#), since 2012

## Languages

**English** (fluent), **Russian** (native), **German** (conversational, B2), **French** (beginner)

# List of Publications

P Marinković, S Blumenstock, PM Goltstein, V Korzhova, F Peters, A Knebl, J Herms. In vivo imaging reveals reduced activity of neuronal circuits in a mouse tauopathy model. *Brain* 142 (4), 1051-1062

M Brendel, F Probst, A Jaworska, F Overhoff, V Korzhova, NL Albert, R Beck, S Lindner, F-J Gildehaus, K Baumann, P Bartenstein, G Kleinberger, C Haass, J Herms, A Rominger. Glial activation and glucose metabolism in a transgenic amyloid mouse model: a triple-tracer PET study. *Journal of Nuclear Medicine* 57 (6), 954-960

M Brendel, A Jaworska, F Probst, F Overhoff, V Korzhova, S Lindner, J Carlsen, P Bartenstein, R Harada, Y Kudo, C Haass, F Van Leuven, N Okamura, J Herms, A Rominger. Small-animal PET imaging of tau pathology with 18F-THK5117 in 2 transgenic mouse models. *Journal of Nuclear Medicine* 57 (5), 792-798

F Overhoff, M Brendel, A Jaworska, V Korzhova, A Delker, F Probst, C Focke, F-J Gildehaus, J Carlsen, K Baumann, C Haass, P Bartenstein, J Herms, A Rominger. Automated spatial brain normalization and hindbrain white matter reference tissue give improved [18F]-florbetaben PET quantitation in Alzheimer's model mice. *Frontiers in neuroscience* 10, 45

DN Artamonov, VV Korzhova, J Wu, PD Rybalchenko, K Im, VA Krasnoborova, OL Vlasova, IB Bezprozvanny. Characterization of synaptic dysfunction in an in vitro corticostriatal model system of Huntington's disease. *Biochemistry (Moscow) Supplement Series A: Membrane and Cell Biology* 7 (3), 192-202

# Eidesstattliche Versicherung Affidavit

Hiermit versichere ich an Eides statt, dass ich die vorliegende Dissertation:

**„Investigation of neuronal activity in a murine model of Alzheimer’s disease using *in vivo* two-photon calcium imaging“**

selbständig angefertigt habe, mich außer der angegebenen keiner weiteren Hilfsmittel bedient und alle Erkenntnisse, die aus dem Schrifttum ganz oder annähernd übernommen sind, als solches kenntlich gemacht und nach ihrer Herkunft unter Bezeichnung der Fundstelle einzeln nachgewiesen habe.

I hereby confirm that the dissertation “**Investigation of neuronal activity in a murine model of Alzheimer’s disease using *in vivo* two-photon calcium imaging**” is the result of my own work and that I have only used sources or materials listed and specified in the dissertation.

Munich, 04.06.2019

Viktorija Korzhova, M.Sc.

# Declaration of Author Contributions

Viktoria Korzhova and Petar Marinković conceived and planned the project, Viktoria Korzhova performed *in vivo* two-photon experiments and analyzed the data. Petar Marinković helped with in cranial window implantation surgeries and imaging. Sabine Liebscher and Pieter Goltstein wrote data analysis scripts. Viktoria Korzhova and Sabine Liebscher performed data analysis and interpreted the data. Viktoria Korzhova wrote the manuscript. Jochen Herms designed the study and supervised the research.

I hereby confirm the specified contributions for the preparation of the manuscripts.

Munich, 04.06.2019

Viktoria Korzhova, M.Sc.

Prof. Dr. Jochen Herms